Aus dem Institut für Arbeits-, Sozial- und Umweltmedizin

der Heinrich-Heine-Universität Düsseldorf

Direktor: Prof. Dr. med. Peter Angerer

Investigation on innate immune responses after the exposure towards fine and ultrafine particles from indoor sources

Dissertation

zur Erlangung des Grades eines Doktors der Medizin

der Medizinischen Fakultät der Heinrich-Heine-Universität Düsseldorf

vorgelegt von

Boris Ludwig

2022

Als Inauguraldissertation gedruckt mit der Genehmigung der

Medizinischen Fakultät der Heinrich-Heine-Universität Düsseldorf

gez.:

Dekan: Prof. Dr. med. Nikolaj Klöcker

Erstgutachterin: Prof. Dr. med. Barbara Hoffmann MPH

Zweitgutachter: Prof. Dr. sc. hum. Oliver Kuss

Für Charlotte, Emilia und Yaron

Zusammenfassung

Luftverschmutzung ist eine häufige Ursache für Krankheit und vorzeitigen Tod und damit ein bedeutendes globales Gesundheitsrisiko. Feinstaub ist eine der bekanntesten Untergruppen der Luftverschmutzung. Feinstaub ist eine Mischung aus Feststoffen und Flüssigkeiten, die durch Atmung sowie passiven und aktiven Transport in den Körper aufgenommen wird. Ein Großteil des Feinstaubs ist anthropogen, er entsteht durch Verkehrsströme, Energieerzeugung oder Landwirtschaft und wird meist in der Umgebungsluft gemessen. Er entsteht auch in Innenräumen durch Alltagshandlungen, kann dort aber schlechter systematisch erfasst werden.

Diese Arbeit beschäftigt sich mit Feinstaubquellen aus Innenräumen und mit gesundheitlichen Folgen nach kontrollierter Exposition. In der zugrunde liegenden EPIA-Studie wurden 41 Probanden randomisiert und kontrolliert durch Braten, Toasten und Kerzenabbrand mit Innenraum-Stäuben belastet. Die Stäube wurden in ihrer Zusammensetzung und Größenverteilung mit verschiedenen Messmethoden charakterisiert.

In Blutproben und Nasallavagen wurden mittels *enzyme-linked immunosorbent assay* (ELISA) die Konzentrationen der Entzündungsparameter *C-reactive Protein* (CRP), *Interleukin 8* (IL-8) und *soluble intercellular adhesion molecule-1* (sICAM) vor und nach entsprechenden Expositionen getestet. Es wurden Änderungen der Absolutwerte berechnet und verschiedene Regressionsanalysen durchgeführt. Berechnet wurden die Biomarker-Änderungen pro festem Inkrement der einzelnen Partikelexpositionen, sowie pro Interquartilsabstand.

Es zeigte sich, dass Partikelquellen aus Innenräumen binnen kurzer Zeit zu einer relevanten Partikelbelastung in Nahbereich führen. Bei gesunden Probanden waren Expositionen mit Veränderungen von Biomarkern im Blut und in den Sekreten der oberen Atemwege assoziiert.

Im Vergleich der Partikelquellen untereinander war Kerzenabbrand mit einem Anstieg des IL-8 in Nasallavage binnen 24 Stunden assoziiert. Ebenfalls zeigten sich im Verlauf von 24 Stunden positive Assoziationen zwischen Stäuben aus Bratvorgängen und dem CRP-Gehalt im Blut.

In einer Analyse pro Interquartilsabstand wurden die Stäube hinsichtlich der relevantesten Partikel-Subgruppe untersucht. Hier waren ultrafeine Partikel (UFP) mit einer Größe von weniger als 100 nm mit den deutlichsten Änderungen von Biomarkern assoziiert.

Die Arbeit verdeutlicht den Einfluss von Partikelbelastungen in Innenräumen durch Handlungen des alltäglichen Lebens. Es zeigen sich rasche biologische Reaktionen nach kurzer und intensiver Exposition. Darüber hinaus unterstreicht die Arbeit die Relevanz der bisher selten beachteten und spärlich regulierten Fraktion der ultrafeinen Staubpartikel in der Umgebungsluft.

Summary

Air pollution is a common cause of disease and premature death and hence a global major health risk. Particulate matter is one subgroup of air pollution. Particulate matter is a mixture of solids and liquids that is incorporated into the body through respiration and passive and active transport. The major part of particulate matter is produced by humans, mainly through traffic and transport, energy production or agriculture and is measured in outdoor air. However, particulate matter is also produced in indoor environments as a result of everyday human activities, where it is more difficult to quantify the extend of exposure.

This work deals with sources of particulate matter from indoor sources and with health consequences after controlled exposure. In the underlying EPIA study, 41 subjects were randomized and exposed under controlled conditions to indoor particulate matter through frying meat, toasting bread and burning candles. The emerging particulate matter was characterized in terms of its composition and size distribution using various measuring methods.

Concentrations of the inflammatory parameters *C-reactive Protein* (CRP), *Interleukin-8* (IL-8) and *soluble interecellular adhesion molecule-1* (sICAM) were tested in blood samples and nasal lavage fluids using an *enzyme-linked immunosorbent assay* (ELISA) before and after the respective exposures. Changes in absolute values were calculated and various regression analyses were performed. Biomarker changes were calculated per fixed increment of particle exposures and per interquartile range.

It was shown that indoor particle sources lead to relevant particle exposure in the immediate vicinity within a short period of time. In healthy volunteers, exposures were associated with changes in biomarkers in blood and upper respiratory tract secretions.

When comparing the particle sources with each other, candle burning was associated with an increase in IL-8 in nasal lavage within 24 hours. Positive associations between particles from frying processes and the CRP content in blood were also found over the course of 24 hours.

In an analysis per interquartile range, particles were examined with regard to the most relevant particle subgroup. Here, ultrafine particles (UFP) with a size of less than 100 nm were associated with the most significant changes in biomarkers.

The work emphasizes the influence of indoor particle pollution through activities of everyday life. There are rapid biological reactions after short and intensive exposure. In addition, the work underlines the relevance of the previously seldom considered and sparsely regulated fraction of ultrafine particles in indoor air.

Abbreviations

BMI	body mass index
C1q	complement component 1q
CAM	cellular adhesion molecule
CB	candle burning
Chl	chloride
CO	carbon monoxide
CRP	C-reactive protein
EDTA	ethylenediaminetetraacetic acid
ELISA	enzyme-linked immunosorbent assay
EU	European Union
FeNO	fraction of exhaled nitric oxide
FMPS	Fast Mobility Particle Sizer Spectrometer
FS	frying sausages
HRV	heart rate variability
ICAM	intercellular adhesion molecule
IL-6	Interleukin-6
IL-8	Interleukin-8
IQR	interquartile range
IUF	Leibniz-Institut für umweltmedizinische Forschung, Düsseldorf
IUTA	Institut für Energie- und Umwelttechnik Duisburg
LANUV	Landesamt für Natur, Umwelt u. Verbraucherschutz
LFA-1	Lymphocyte function-associated Antigen
LVS	Low Volume Sampler
MAPK	mitogen-activated protein kinase
ml	millilitre
MMP	matrix metalloprotease
mRNA	messanger ribonucleic acid
µg	microgram
NAL	nasal lavage
NAS	Nanometer Aerosol Sampler
nfκB	nuclear factor kappa B
ng	nanogram
NH_4	ammonium
NO_2	nitrogen
NO_3	nitrate
NPF	new particle formation
O_3	ozone
OHC	organic hydrocarbon
pg	picogram
PILS	Particle-Into-Liquid-Sampler
PM	Particulate Matter
PM_1	Particulate Matter with aerodynamic diameter smaller 1 µm
$PM_{2.5}$	Particulate Matter with aerodynamic diameter smaller 2.5 µm

PM_{10}	Particulate Matter with aerodynamic diameter smaller 10 µm
PN	particle number
PNC	particle number concentration
PSC	particle surface area concentration
PWA	pulse wave analysis
PWV	pulse wave variability
RA	room air
ROS	reactive oxygen species
Rpm	rounds per minute
RR	blood pressure
SD	standard deviation
SEM	Scanning Electron Microscopy
sICAM	soluble intercellular adhesion molecule
SMPS	Scanning Mobility Particle Sizer
SO_2	sulfur
SO_4	sulfate
SOP	standard operating procedure
t0	timepoint 0
t3	timepoint 2 hours post exposure
t5	timepoint 24 hours post exposure
TB	toasting bread
TNF-α	tumor necrosis factor alpha
TXRF	Reflection-X-Ray-Fluorescence Spectrometry
UBA	Umweltbundesamt
UFP	ultrafine particles
VOC	volatile organic compounds
WHO	World Health Organisation
Δ	delta

Table of Contents

List of Figures

List of Tables

1 Introduction

Half a billion times – that is how often we breathe in a lifetime. A constant flow of air stream, in and out for 12 to 14 times a minute, subconsciously and inevitably. Breathing is our first and probably most important connection to the world. It is the biologic principle that connects us with almost every complex form of life.

Yet this simple and important process is often overseen. Unlike soil or water that can be devided or shared, air seems intangible. It was probably a rather long way in the history of humankind to understand that this invisible life elixir is in reality a mixture of gases and of solid and liquid particles with different chemical properties and various important functions in our organisms.

It was an even longer way to understand that air can be of different qualities, that its mixture can contain traces of our environment, invisible to our senses. Therefore, considering air quality as an important good for the well-being of a society, is a relatively young thought. First systematic scientific explorations of air quality date back to the beginning of the last century, when industrialized manufacturing processes and a fossil carbon fuelled economy reshaped cities and landscapes. By the time, the term "smog" was invented for events of smoke and fog. First scientific findings of adverse health outcomes through "smog" were for example reported in the 1930s in the Meuse valley in Belgium or after a smog episode in London in 1952. During and after these events, death rates and hospital admissions were reported to rise to an unprecedented extend. In the following years and decades, environmental protection - and clean air as a part of it - became a goal of national and international concern for many countries.

Analysing air and air pollution, a great quantity of different pollutants was discovered. Today a solid body of scientific evidence has helped to understand what we breathe. Even more, we can now tell exactly how air can lead to health or disease. Significant knowledge was gained on adverse health outcomes through ambient air pollution. Thus, on a population based level, significant advances could be made in air quality standards and outdoor air quality could be improved.

The individual level of pollutant exposure instead is still poorly understood. None of us knows precisely what they breathe on a daily basis and air pollution is still present, as we spend the majority of the day in houses and closed environments. The puzzle is not complete, yet.

This work will try to elucidate the connection between changes in indoor air and biomarker signals as preclinical signs for health impairments through air contaminants. It might thus contribute to answer the question how we can protect what we breathe.

2 Background

2.1 Air pollution

Air pollution is a regional and source specific mixture of gaseous and particulate pollutants, ranging from solid particulate matter (PM) like soot and other airborne particles to gaseous precursors like oxides of nitrogen, sulphur, carbon or volatile organic compounds (VOC). Depending on the source of emission, the mixture of pollutants can also contain metals, trace elements and anorganic compounds. Immediately after getting airborne from their source of emission, these components of air pollution are called primary pollutants. Being suspended in the atmosphere and given certain physical, chemical and meteorological conditions, these primary pollutants form a medium that can create new particles and substances. (European Environmental Agency, 2016)

Under the impact of solar radiation, ionization, thermal changes or resuspension through wind, substances can undergo chemical reactions. They react or accumulate through condensing processes into so-called secondary pollutants. Among these are ozone, nitrates, sulphates and many others.

Air pollution originates from heterogenous sources which can be anthropogenic or natural. In the Anthropocene it primarily derives from combustion processes and from degradation of organic compounds. Hence major sources in developed societies are the burning of fossil fuels in vehicles, industrial manufacturing processes and power generation. Household activities play a role in the generation of air pollution through residential heating or open fireplaces. Transportation and mobility contribute to ambient air pollution through combustion of fossil fuels, through abradation of tires and breaks, and also through secondary resuspension via physical movement and airstream. Further anthropogenic pollution sources are construction and demolition work and agricultural activities like animal husbandry or biological waste application. Wildfires or volcanic activity are typical examples of natural occurrence of air pollution. (European Environmental Agency, 2016), (Franklin et al., 2015)

Resuspension and distribution of air pollution can be facilitated by meteorological preconditions, via wind and thermal shifting. Thus, air pollution can expand over enormous distances and affect regions far away from the source of emission (Mannucci et al., 2015).

2.1.1 Particulate Matter air pollution

Particulate matter (PM) is the solid or fluid constituent of air pollution. It is a complex mixture of organic and inorganic substances and represents a large and harmful fraction of air pollutants (Brook et al., 2010). Depending on the source, PM consists of a very heterogenous range of particles or droplets that can contain metals (alkali metals, heavy metals, transition metals), sulphates, nitrates, minerals, ammonia or acids, black carbon, organic aerosols and water (Chan, 2006).

In industrialized countries, primary PM originates from anthropogenic combustion sources like power generation and fuel use or waste incineration. Other sources are mechanical abrasion of tires or breaks, construction and agricultural works. Natural sources like sea salt, pollen or volcanic ash seasonally and regionally contribute a significant amount, too. Even bacterial and fungal detritus contribute a fraction to PM (Nemmar, Holme et al., 2013).

Secondary formation of PM can occur through accumulation of extremely small pollutants and air contaminants like SO_2, NO_x or VOCs. These precursors can converse from the gas phase to a solid particle. This process is called New Particle Formation (NPF), and it is more likely to happen under strong solar irradiation or after (mostly anthropogenic) bursts of volatile precursors (Morawska et al., 2019). Apart from NPF, pollutants can condensate on pre-existing PM, which is more likely to happen in areas of dense PM concentrations. Accumulation and condensation both contribute an important fraction of total PM. (European Environmental Agency, 2016)

PM can be quantified in multiple ways, and is commonly categorized by size and weight into various subclasses:

- PM_{10} is a mass unit per cubic meter [$\mu g/m^3$] and contains particles with an aerodynamic diameter smaller than 10 μm. The larger particles in this fraction mainly consist of metal oxides, silicates and minerals, with particles formed artificially through mechanical abradiation. (Nemmar et al., 2013)

- $PM_{2.5}$ is a mass unit per cubic meter [$\mu g/m^3$] and contains particles with an aerodynamic diameter smaller than 2.5 μm. This particle size mainly consists of combustion-derived carbon and other combustion products or organic aerosols. This fraction tends to enlarge with a temporal delay, due to secondary agglomeration and NPF from gas phase pollutants (Nemmar et al., 2013).

- Ultra fine particles (UFP) are nanoparticles in the range of a few nanometres. Often the cut off value for UFP is a diameter of less than 100 nm, whereas other authors count particles smaller than 1000 nm in. UFP have a low mass and are therefore preferably quantified in number concentrations per cubic centimetre [#/cm³] rather than weight measurements. UFP sources are ubiquitous. The most important anthropogenic sources of UFPs are road and non-road transport via combustion of fossil fuels, residential and commercial heating and industrial processes. (HEI Review Panel on Ultrafine Particles, 2013) (Morawska et al., 2008)

In analogy to PM, UFP can be divided into primary and secondary particles. Combustion of fossil fuels or organic material often produces primary UFP with a diameter ranging around 50 nm, but gas-particle exchanges transform these particles quickly, either through dissolvement or accumulation. These now called secondary UFP show a large variety of sizes and shapes. UFP of less than 10 nm are often the result of a nucleation from low-volatile compounds and gas-to-particle reactions (NPF) while UFP around 100 nm are mostly a product of accumulation by condensation or coagulation to existing particles. Larger UFP as a result of this process can grow up to 200 nm in diameter and tend to be less volatile. The agglomeration process can be supported by photochemical reactions with sulphuric or nitrogenic oxides under certain atmospheric preconditions. The resulting fraction of this enlargement is called quasi-ultrafine particles (quasi-UFPs) and sometimes referred to as PM0.25, for particles smaller than 250 nm. (HEI Review Panel on Ultrafine Particles, 2013) or PM1 for particles smaller than 1000 nm (Morawska et al, 2017).

Particles smaller than 10 nm are often referred to as ultrasmall nanoparticles. They can be formed as unforeseen by-products or intentionally as industrial nanoparticles (Morawska et al., 2008).

Another subdivision to quantify only large particles is the so-called coarse PM, a mass unit for particles with a diameter usually ranging between 10 µm and 2.5 µm. This fraction seems to shrink rapidly in industrialized countries, probably on behalf of newly applied filter technologies in industry and vehicles following legislative constraints. (European Environmental Agency, 2016)

2.1.2 Indoor Particulate Matter air pollution

Modern working and living habits lead people to spend almost 90 % of their time indoors (Klepeis et al., 2001). Particles however, although often measured outside buildings in street canyons or public spaces, follow airstream and infiltrate indoor air from outside. If no filter

technique is applied, buildings allow a significant amount of outdoor air pollution and outdoor PM to enter closed rooms. An equilibrium of pollutants is reached by mechanical and natural ventilation, or by infiltration through cracks in the building envelope (Chen et al., 2012).

Particles can also be emitted into indoor air from indoor sources. Indoor particle sources are ubiquitous but differ greatly comparing between countries or socioeconomic milieus. For example, indoor use of solid fuel generates a high particle exposure and is practiced by 2.8 billion people worldwide, overwhelmingly often in developing countries (World Health Organisation, 2015).

Typical developed world indoor particle sources can be hot combustion processes like food processing, burning candles or smoking. Other sources can be household gadgets with moving components or heated surfaces, such as hairdryers or heating devices; each with a characteristic distribution of emitted particles. In office surroundings, printers with colour pigments can release significant amounts of particles, too. (Wallace und Ott, 2011; Morawska et al., 2017).

Secondary particle formation indoors is also possible. Fine and ultrafine particles are produced for example on heated surfaces, where volatile substances are first absorbed and then resuspended and changed in size and shape by thermal energy (Wallace et al. 2015). Another secondary indoor source of UFP are household chemicals like cleansing agents or air fresheners, which can contain reactive agents like terpenes or ozone. These substances propel the formation of particles through a nucleation process (Wallace, 2006) similar to outdoor NPF from solar irradiation. (Waring, 2014)

Furthermore, particle resuspension plays an important role in closed environments with few ventilation. Thus, walking carpets can already create a significant amount of particles in indoor air. (Kim et al., 2015)

Indoor particle sources cause a rapid augmentation of particle number due to the limited volume of air they are emitted into. Indoor particle exposure in general is difficult to quantify. Depending on the accuracy of the measurement technique, particle amount indoors can reach 1200*10^6 /cm³ through normal living and working habits (Isaxon et al., 2015). But different living habits create an uncountable number of microenvironments that must be assessed individually regarding particle sources, particle number, particle properties and possible health impairment. However, it can be stated that indoor PM exposure contributes substantially to the total PM uptake during a day. (Polidori et al., 2006; Isaxon et al., 2015)

An overview of typical household PM sources, their size distribution and emission rate are shown in Table 1.

UFP Source	Particle Size Range (nm)	Emission Rate (number/min)
Candle Burning	20-1000	8.8*10^10
Stove (Gas fuelled)	20-1000	1.3*10^11
Stove (Electric)	20-1000	6.8*10^11
Frying Meat	20-1000	8.3*10^11
Electric Frying Pan	10-400	Up to 2.7*10^10
Cigarette Smoke	20-1000	3.8*10^11
Laser Printer	6-3000	Up to 3.3*10^12

Table 1: ***Indoor UFP sources and emission rates in homes.*** *Particle Size Range in nanometers (nm), Emission Rate in number per minute (number/min). (according to Afshari et al., 2005)*

Table 1 also illustrates that many daily activities produce particles in the UFP size range. UFP contribute most to the total particle number (PN) that is inhaled by an individual throughout a day. Thus, under normal living conditions, PN exposure from indoor sources can exceed PN exposure from outdoor sources. This can even be the case if activities in highly polluted outdoor areas, like biking on a busy street are carried out, because particles outdoors are often bigger in size and smaller in number concentration. Outdoor UFP disperse quicker due to changing meteorological circumstances whereas indoor UFP in closed rooms with reduced ventilation can be stable for a longer period of time (Vinzents et al., 2005). The residential exposure to UFP attributable to indoor activities could thus exceed 60% of the total UFP daily uptake (Bekö et al., 2013).

2.1.3 Measuring Particulate Matter

PM_{10} and $PM_{2.5}$ are frequently measured via filter-sampling techniques which are conducted over a certain period. The filtered particles can be measured gravimetrically and reported as particle mass in a dried, standardized amount in microgram per cubic meter of ambient air. Filter techniques show a low temporal and spatial resolution and usually reflect average particle amounts on a local exposure level. To avoid inaccuracy, real-time samplings can be calculated through mass surrogates like light absorption or beta-attenuation combined with upstream filters to separate the different metrics from one another. Furthermore, particle mass can be calculated indirectly from particle size distribution and particle number counts, assuming a certain particle

weight, as described further in chapter 3.4. Ambient outdoor PM_{10} and $PM_{2.5}$ ranges from 5 to 50 µg/m³ in most anthropogenic environments, with large spatial and temporal differences. (Engel-Cox et al., 2013)

UFP are commonly measured as particle number concentrations (PNC), because in a fraction of very small particles, gravimetric measurements do not adequately reflect the dimension of particle pollution. Background UFP levels in urban environments can exceed numbers of 50.000 per cubic centimetre (cm³) while contributing only 0.5–2 µg/m³ to particle mass (Oberdörster et al., 2005). Thus, the number of particles in the so-called nucleation and accumulation mode is high, while the number of particles in the coarse mode is comparatively negligible as can be seen in Figure 1. (HEI Review Panel on Ultrafine Particles, 2013)
Techniques to count PNC (e.g. electrostatic classification, enlargement in vapor) are described in detail in chapter 3.5.

Another way to measure UFP is via Particle Surface Area Concentration (PSC). This approach accounts for the finding that UFP have a high surface area to mass-ratio. It is assumed, that the size of the particle surface predicts its ability to interact with biological systems by carrying a large amount of adsorbed toxic by-products or by supplying a surface on which chemical reactions can take place (Delfino et al., 2005). However, measuring surface area is difficult to perform and produces estimations only. Consecutively it has not yet been implemented as an international standard. (HEI Review Panel on Ultrafine Particles, 2013)

The above-mentioned sampling methods are stationary and therefore produce data that is prone to reflect only microenvironments. To measure background exposure and spacial distribution, regional grids of sensors are in use in many developed countries. To quantify background concentrations in larger areas, these measurement grids can be used for epidemiological exposure calculation via mathematical models. Another approach to monitor pollution in larger coherent areas is via satellites, measuring optical density in the earth atmosphere as a surrogate for $PM_{2.5}$ levels, for example. (Engel-Cox et al., 2013)

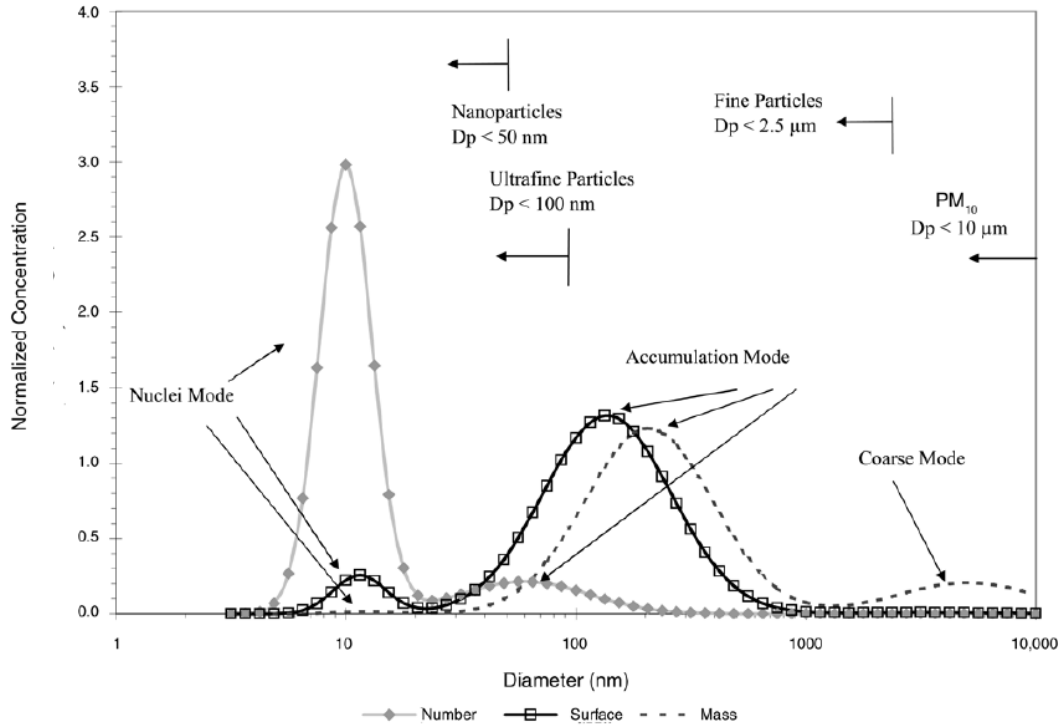

Figure 1: ***Connection between distribution of particle size fractions and particle concentrations.*** *Log-normalized particle size (x-axis) and log-normalized particle concentration (y-axis). Particle Number in grey, Particle Surface Area in black and Particle Mass as spotted black line. UFPs and quasi-UFPs show the highest number concentration and surface area among all particle fractions. Dp: Diameter of particles. Reprinted with permission from (HEI Panel on the Health Effects of Traffic-Related Air Pollution, 2010)*

2.2 Particulate Matter and Health

2.2.1. Incorporation of Particulate Matter

PM of every size category can be inhaled and to a certain extend be deposited along the whole respiratory tract and alveolar airspace during in- and exhalation. The rate of deposition primarily depends on the size of particles. As PM_{10} is mainly adsorbed and removed from the airstream in the upper respiratory tract, $PM_{2.5}$ evades deposition in the upper airways and proceeds to the bronchis and bronchioles. UFP show a heterogenous deposition pattern. The greatest amount of particles from 5 to 100 nm proceed to the alveoles, whereas smaller particles seem to be less influenced by airstream. Due to their extremely small size, particles smaller than 5 nm rather follow a Brownian molecular motion as they get deposited mainly in the upper airways as can be seen in Figure 2. (Oberdörster et al., 2005)

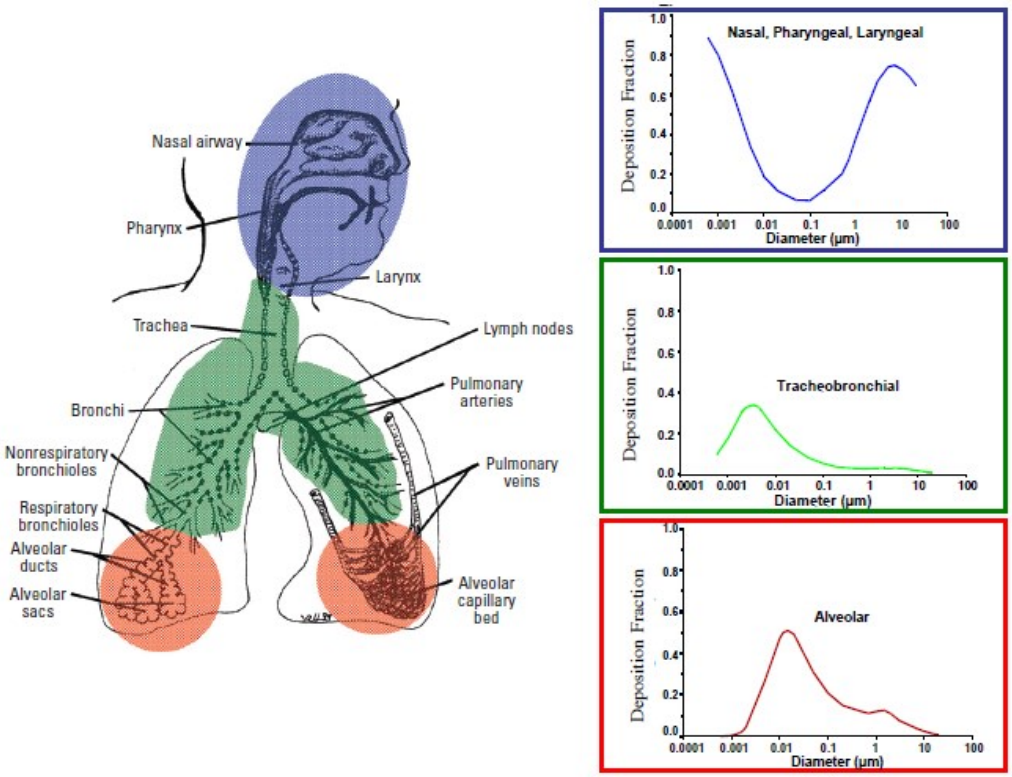

Figure 2: ***Deposition rates of PM in the respiratory tract.*** *Large particles and nanoparticles are mainly deposited in the upper airways (blue). The majority of UFP proceed to the bronchis (green) and the alveolar airspace (red). Reprinted from (Oberdörster et al., 2005) with permission from the author.*

Larger particles are removed from the airways by the mucociliary escalator, where particles are bound to mucus along the respiratory epithelium and transported towards the pharynx with a directed movement of ciliar cells. In the pharynx, the mucous is either swallowed or expectorated. But a considerable fraction of fine particles and a large part of ultrafine particles behave differently. Due to small size, their volatility resembles gases. Thus, particles are transported deeper into the lung where phagocytosis by alveolar macrophages, transgression into blood circulation and lymphatic drainage, uptake in interstitium and neurons could be observed (Oberdörster et al., 2005; Kim et al., 2015). Diminished size could even help to evade immune defence mechanisms like phagocytosis and lead to direct transcellular migration. Nano-sized radiolabelled particles appeared in the liver only minutes after inhalation (Nemmar et al., 2013).

It is therefore probable that ultrafine particles are accessible to compartments that usually possess a very strictly regulated immune defence as can be seen in Figure 3. The biological consequences of this accessibility are the topic of a large field of research. (Oberdörster et al., 2005)

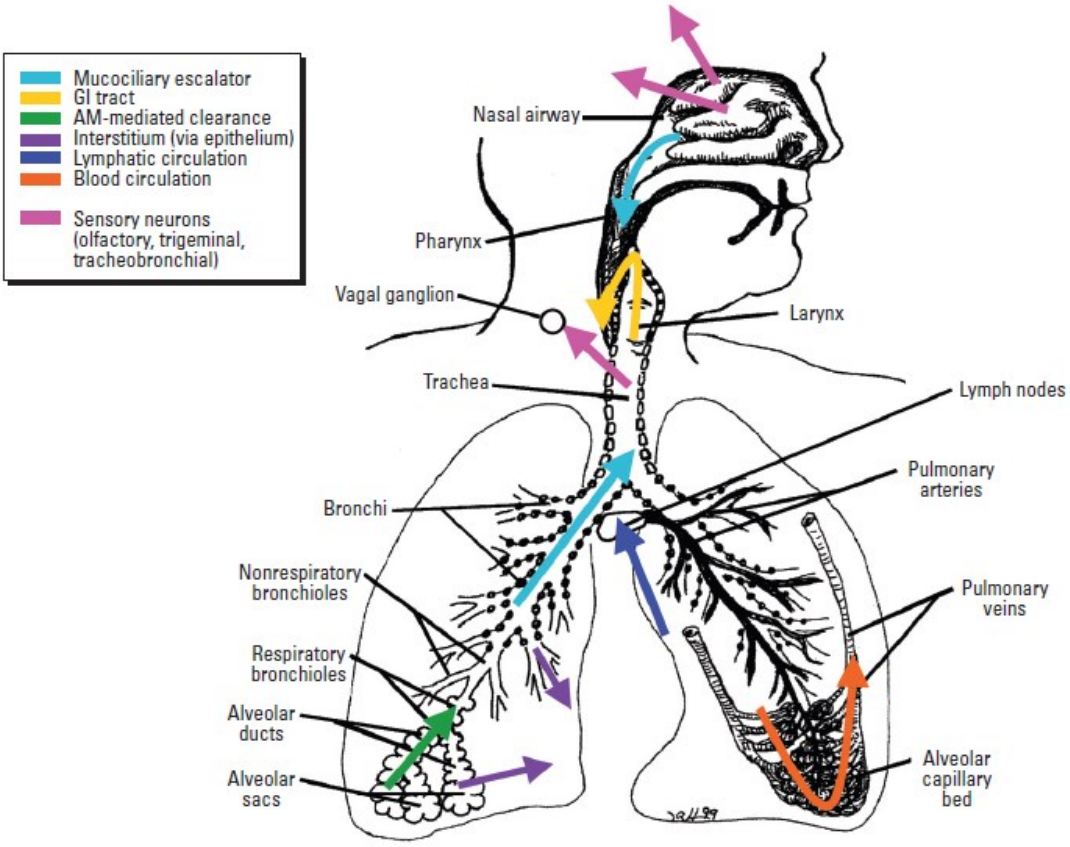

Figure 3: ***Pathways of particle clearance from the respiratory tract.*** *UFP can be removed by all depicted cleansing mechanisms. Each coloured arrow stands for a possible uptake mechanism. AM: Alveolar macrophages; GI: gastro intestinal. Reprinted from (Oberdörster et al., 2005) with permission from the author.*

2.2.2 Health effects of Particulate Matter

It is well established that short- and long-term exposure towards PM leads to the development of impaired health conditions (Franklin et al., 2015) (Brook et al., 2010).

Toxicological, clinical and epidemiological research has for decades given conclusive evidence of PM being accountable for death or chronic disease in millions of cases on a global scale (Rückerl et al., 2011). Air pollution delivers a significant contribution to the global burden of disease and is currently regarded as the fourth most important risk factor to death and disease following elevated systolic blood pressure, smoking and high plasma glucose and cholesterol levels (World Health Organisation, 2015; Cohen et al., 2017). Even in Europe, the attributable burden of disease ranks among the top ten risks for death and disease. It is seen as the largest single environmental health risk, with PM_{10} and $PM_{2.5}$ being the driving forces among all pollutants. (González Ortiz et al., 2020)

A solid body of evidence makes long term exposure to PM accountable for increasing all cause- and cause-specific mortality, although exact figures differ due to the statistical method that is used (Orellano et al., 2020; Chen und Hoek, 2020). The European Environment Agency for example holds long term exposure to outdoor $PM_{2.5}$ accountable for up to 400.000 preterm deaths annually (European Environmental Agency, 2016). The reduced life expectancy was calculated as 2.2 years in Europe (Lelieveld et al., 2019). Every long term elevation of 10µg/m³ $PM_{2.5}$ was reported to increase all-cause mortality by 10% (Brook et al., 2010).

PM exposure is associated with reduced life expectancy primarily by increasing cardiovascular morbidity and mortality (Brook et al., 2010). The causality between this cause-specific mortality and long term PM exposure has proven to be robust even after adjusting for poverty, race or insurance status (Yitshak-Sade et al., 2019).

Long term exposure towards PM also severely effects the respiratory system and evokes considerable changes of respiratory function. Reviewed evidence indicates associations with impaired lung function and asthma development in children and development and deterioration of obstructive airway diseases in adults. Deterioration of respiratory function was seen in diseased subgroups, but also in healthy populations and in individuals likely to perform vigorous physical activity on a daily basis, like children. (Rückerl et al., 2011)

Furthermore, chronic exposure to PM was described as carcinogenic (Pope et al., 2002). It is listed as an independent risk factor for lung cancer by the *International Agency for Research on Cancer* since 2013. It was shown to remain a risk factor for lung cancer even under the current WHO limit values (Hvidtfeldt et al., 2021).

Transmigration of particles into blood stream is thought to cause other systemic long term effects. Large epidemiological studies found an association between $PM_{2.5}$ and prevalence and incidence of diabetes mellitus (Liu et al., 2019b; Yang et al., 2020) or a prediabetic metabolic status (Balti et al., 2014). There is also growing evidence that long term PM exposure affects prenatal development and reproduction outcomes. Exposure towards $PM_{2.5}$ was associated with low birth weight, preterm birth and growth retardation (Shah and Balkhair, 2011). Chronic exposure towards PM could have a negative effect regarding neuronal and cognitive development, as seen in cohorts of school children (Forns et al., 2017). Even end stage renal disease is associated with the magnitude of PM exposure (Xie et al., 2018).

Short term changes of PM levels also seem to play an important role in health endpoints. An association between PM level changes and acute adverse health events was reported multiple times. The relative risk increase for daily cardiovascular mortality due to PM exposure was calculated as 0,4 to 1,0 % for every 10 µg/m³ increase in $PM_{2.5}$ (Pope and Dockery, 2006; Liu et

al., 2019a; Pope et al., 2020). Repeated findings indicate that acute events like myocardial infarction and stroke are the most critical endpoints deriving from short term elevation of PM exposure, being followed by arrhythmia and heart failure exacerbation (Brook et al., 2010; Shah et al., 2015).

Unlike critical endpoints like death and disease, short term PM alterations seem to play a causative role in subclinical health effects, too. In the cardiovascular system, blood pressure elevation, systemic inflammation, blood coagulation and altered heart rate variability was seen in short-term studies (Brook et al., 2010). Short term exposure is also strongly associated with a decline in lung function and an increase in hospital admission due to symptoms of obstructive airway disease. (Franklin et al., 2015)

Interestingly the exposure response concerning lung and cardiovascular outcomes seems to be supralinear. The curve is steep at low PM levels and flattens at higher doses (Brook et al., 2010). If linearity is not applicable to a dose-response curve, then thresholds for $PM_{2.5}$ as implemented by the EU would only have limited implications on public health if not drastically lowered. Generally, older adults, people of chronically reduced health state and children are much more endangered by exposure to PM and therefore should be specially aware of measured ambient $PM_{2.5}$ levels (WHO Regional Office for Europe, 2013; Kim et al., 2015).

2.2.3 Health effects of UFP

Compared to the extensive amount of studies and regulations concerning larger particles like $PM_{2.5}$, there is a considerable knowledge gap to assess health effects of UFP. Higher deposition rates in the lung and a large surface area could make UFP more harmful than larger PM sizes (Li et al., 2016). Various studies tried to model exposures in animals and found evidence of particles in the ultrafine fraction responsible for inflammatory changes in the lung and the cardiovascular system (Nemmar et al., 2013).

Epidemiological and controlled exposure studies that tried to quantify an effect of UFP exposure, show short term signals of health impairment similar to those of $PM_{2.5}$. Exposure could be associated with short term effects like asthma-related hospital admissions, a general worsening of respiratory symptoms, or elevation of blood pressure. (Ohlwein et al., 2019). There is also a large amount of pre- and subclinical findings for short-term changes. Associations could be shown between UFP and short term elevation of oxidative stress markers or systemic inflammatory markers and increase of white blood cells. Short term UFP level

changes were also shown to have vasoactive and procoagulatory properties by activating platelets and elevating fibrinogen activity. (Stone et al., 2017; Díaz-Robles et al., 2014)

When it comes to long term health effects by UFP exposure, evidence is still inconsistent. Both epidemiological and controlled exposure trials face a systemic difficulty when trying to quantify health effects in real life settings: UFP are only one scarcely measured ingredient in a broad range of pollutants and UFP sources rarely occur alone. More than research on larger PM fractions, UFP research highly depends on spatially inclusive and comprehensive data and precise measuring methods with standardized modelling of co-pollutants. None of these preconditions is currently fulfilled to a satisfiable degree. (Magalhaes et al., 2018; Ohlwein et al., 2019; Habre et al., 2018)

2.2.4 Biological pathways

Incorporation of PM can lead to the development of respiratory, cardiovascular and other health endpoints. Three possible pathways explain the linkage between PM exposure and clinical effects.

1) Systemic spill over of local proinflammatory mediators: Particles and their adjunctive molecules or elements interact with tissue, forming reactive oxygen species (ROS). ROS activate an innate immune response via the initiation of NFkB responsive pathways. This triggers an increase of mediators of oxidative stress and inflammation. Chemokines or acute phase proteins eventually form a self-amplifying immune response. (Brook et al., 2010)

2) Lung receptors and nerve endings sense proinflammatory milieus or redox-active agents. Consecutive stimuli of the autonomous nervous system lead to an autonomic imbalance, favouring sympathetic nervous system hyperactivity with all its deleterious effects on the cardiorespiratory system. (Brook et al., 2010)

3) Direct entry via cellular barriers is also possible. This pathway is foremost characteristic for UFP and nano-size particles as they were shown to be able to translocate barriers because of their small size (Oberdörster et al., 2005). This effect could create a direct entry for soluble particles into systemic circulation and hence provoke an inflammatory reaction similar to that described under pathway number 1 in any part of the body. The main area of cellular transmigration is primarily thought to be the alveole (Brook et al., 2010) but other surfaces like mucous membranes on the body surface could facilitate an entry of particles, too (Morawska et

al., 2008). Even hair follicles seem to provide a route for transmigration, as they interrupt skin architecture and limit its sealing function (Kim et al., 2016).

The pathways are depicted in Figure 4, whereas overlaps between pathways are possible. The pathway for an adverse outcomes is likely to depend on the source of exposure, time of exposure, individual health preconditions (Franklin et al., 2015) and environmental factors that are able to transform particles into more or less harmful fractions. (Morawska et al., 2008).

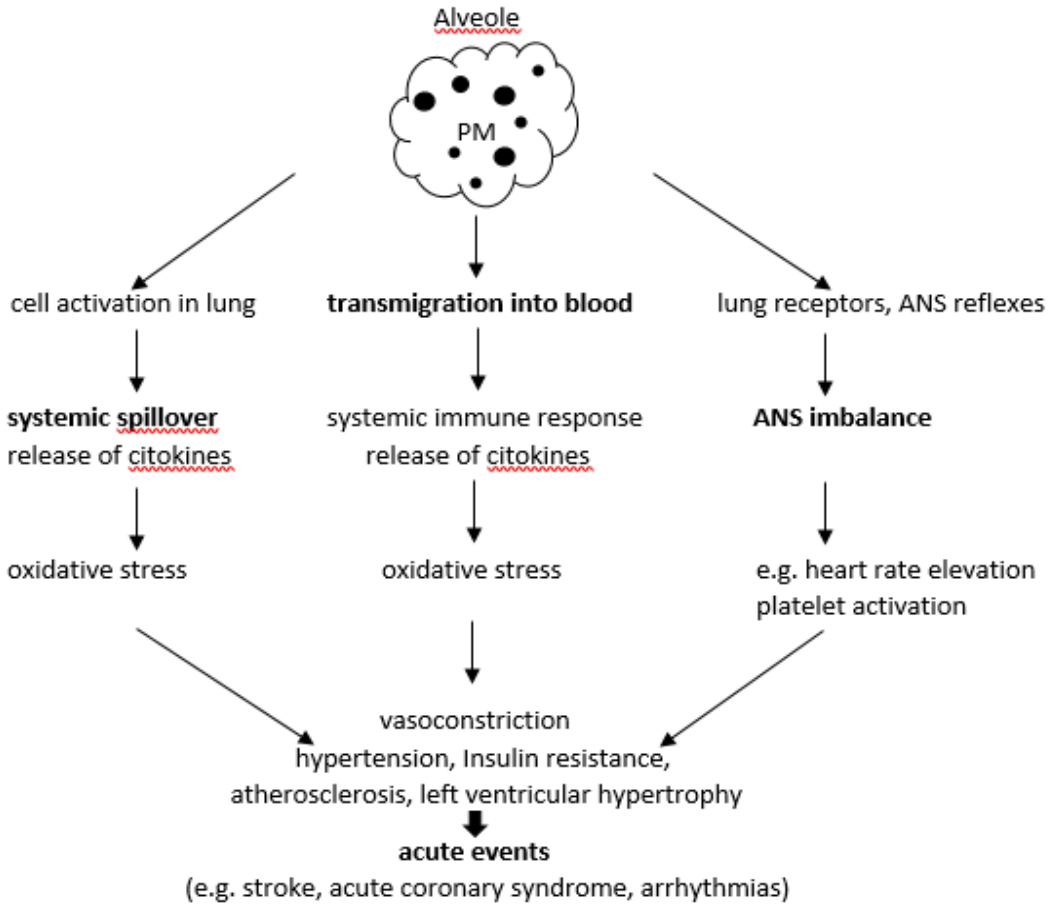

Figure 4*: Three Possible Pathways of health effects after inhalation of PM into alveoles*. *PM: Particulate Matter. ANS: autonomic nervous system. According to (Brook et al., 2010)*

2.3 Linking PM with biomarkers

PM supports the generation of reactive oxygen species (ROS). This process is facilitated through direct entry of PM into cellular tissues, resulting in mitochondrial damage and induction of apoptosis. Furthermore, PM could act as a ROS generator itself, even outside cells, as it contains potential redox-sensitive materials like metals on the surfaces, which propulse a Fenton reaction in various cellular milieus. (Kim et al., 2015)

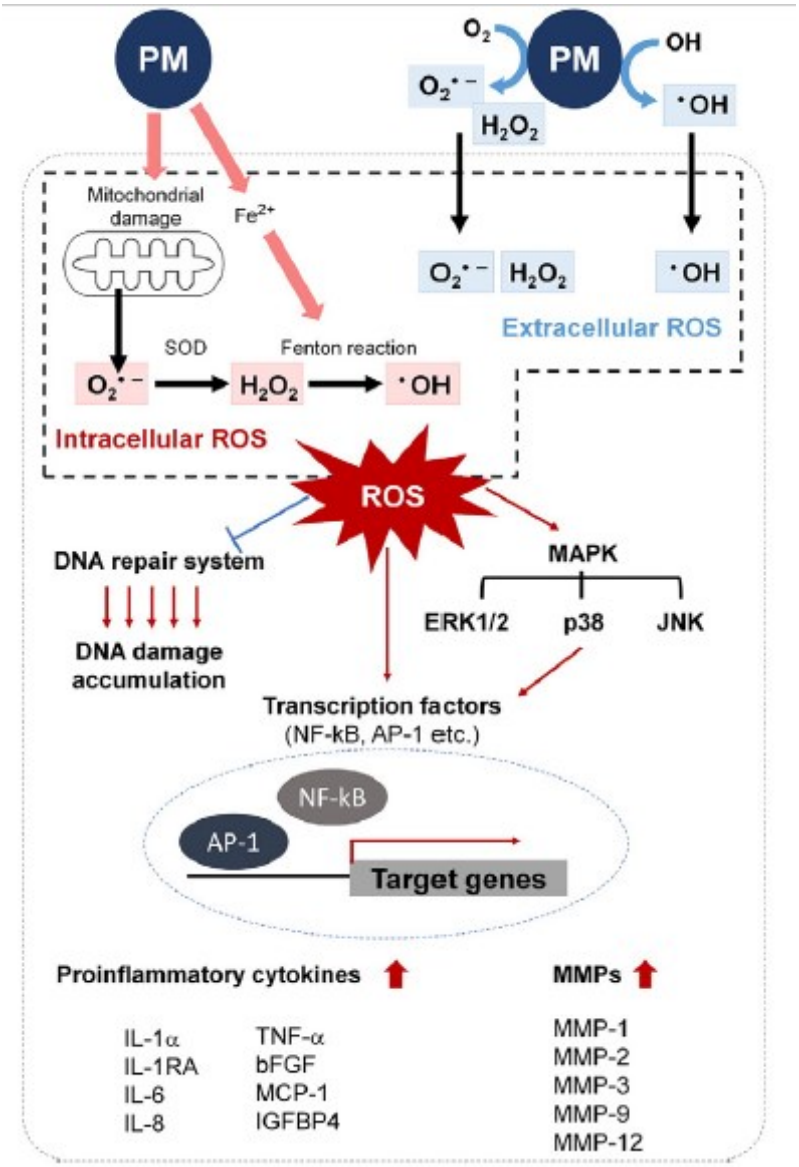

Figure 5: ***Cell damage through PM uptake on a molecular level.*** *The generation of reactive oxygen species (ROS) can be an intra- or extracellular process. Thus, inflammation cascades lead to the upregulation of proinflammatory target genes and provoke a systemic inflammatory reaction via cytokines and proteases.*
PM: Particulate Matter; Fe2+: iron molecule; O_2, H_2O_2,OH: reactive oxygen species; MAPK, ERK1/2, p38, JNK: initiators of inflammatory pathways; NF-kB, AP-1: transcription factors; IL: interleukine; MMP: matrix metallo protease. Reprinted from (Kim et al., 2016), with permission from Elsevier.

ROS, produced extra- or intracellularly, impair the DNA repair system and induce various inflammatory pathways via innate immune responses as Figure 5 shows (Kim et al. 2016). One important mechanism is the *mitogen-activated protein kinase* (MAPK)-pathway. MAPK is a potent activator of transcription factors such as *Nuclear Factor „kappa-light-chain-enhancer" of activated B-cells* (NFkB) and others. These factors regulate innate immunity and inflammation on the genetic level and upregulate target genes coding for proinflammatory

cytokines like *Interleukin-6* (IL-6), IL-8, *tumor necrosis factor alpha* (TNF-α) and many others in various cell types. Also, they induce *matrix metallo proteases* (MMP) that tend to upregulate inflammation via autogenous cell damaging. A variety of proteins involved in innate immune reactions can therefore represent a direct link between PM and adverse clinical outcomes like pulmonary oxidative stress, systemic inflammation, vascular dysfunction or atherosclerosis. (Rückerl et al., 2011)

The following chapters describe biomarkers explored in this work and exemplarily show their physiological reaction after exposure towards fine and ultrafine particles.

2.3.1 PM and CRP in blood

C-reactive protein (CRP) is one of the most common parameters to diagnose, monitor and prognose inflammatory processes and systemic inflammation. It was discovered in the 1930s and thus already looks back on a long research history. As an acute phase protein, CRP is mainly produced in the liver whereas small amounts of CRP mRNA where reported to be found in other tissues. CRP is detectable not only in plasma, but also in mucous membrane secretions of the respiratory tractus and the lungs (Gould and Weiser, 2001) or coronary artery smooth muscle cells. (Calabró et al., 2003)
It is upregulated upon the stimulation of cytokines like TNF-α (Calabró et al., 2003) or IL-6 (Rückerl et al., 2011). It can easily show a 1000-fold increase upon inflammatory stimulation with a fast initial rise after six hours, and a peak around 48 hours after stimulation. Its half-life time is 19 hours, its physiological range in healthy individuals is up to 5 mg/l. (Pepys and Hirschfield, 2003)

CRP is a primarily pentameric molecule with two important binding sites, one for Phosphatidylcholine and similar molecules, which are found for example in degraded cellular material and another binding site for complement factor C1q to activate the complement pathway. It is believed to be important for opsonization and scavenging as an innate host defense mechanism. Furthermore, it upregulates various inflammatory cytokines (Pepys and Hirschfield, 2003; Chandrashekara, 2014).

A soluble pentameric (pCRP) form is turned into a non-soluble monomeric (mCRP) form when binding to non-self or degraded material. The two forms seem to create a self-regulating balance with mCRP being an upregulator of inflammation. Whether (m)CRP is a bystander of critical illness or a causal explanation however remains uncertain. Clinically used highly sensitive CRP

assays like the one used in this work interestingly seem to detect only pCRP and thus not reveal the whole picture of CRP content in plasma (Trial et al., 2016).

Despite the uncertainties about the different functions CRP has in innate immunity, it has proven to have a prognostic value in diseased and apparently healthy individuals. CRP is a risk marker for cardiovascular and metabolic diseases and possibly a mediator of diseases, as it could enhance plaque instability or coronary events (Pepys and Hirschfield, 2003).
CRP is also the most intensively studied inflammatory marker in association with air pollution (Rückerl et al., 2011). Air pollution seems to elevate CRP levels in healthy as well as in diseased individuals (Rückerl et al., 2007). Residential exposure to $PM_{2.5}$ showed to upregulate CRP (Hoffmann et al., 2009). Similar findings could be made in a susceptible population with residential exposure to quasi-ultrafine particles from traffic (Delfino et al., 2008). The reduction of PM through the appliance of air filters in residencies with chronically high exposure towards PM from ambient sources showed a significant reduction of CRP (Allen et al., 2011). We therefore chose it as a valuable marker to detect inflammatory signals after being exposed to indoor particles.

2.3.2 PM and Interleukin-8

Interleukin-8 (IL-8 or CXCL8) is a chemotactic cytokine. It influences immune response and cell migration and was first described as a protein of chemotactic significance in 1987. (Yoshimura et al., 1987)

It is produced by leukocytes such as macrophages and monocytes, neutrophils or T-cells. Furthermore, endothelial and epithelial cells can produce IL-8. Adequate stimuli can be bacterial or viral infection, general cell stress and a resulting increase in chemokines and nuclear factors (Mukaida, 2003). Upon stimulus, IL-8 is upregulated within one hour, and cell production rate returns to baseline levels within a few hours after the end of a stimulus. Similar findings could be made with IL-8 circulating in the blood stream. (Mukaida, 2003; Baggiolini et al., 1989)

IL-8 recruits and activates a broad spectrum of immune cells via interaction with G protein-coupled chemokine receptors and plays a mediator role at sites of inflammation. Its presence alters selectin and integrin expression in the bloodstream and activates various receptors on neutrophils, leading to transmigration from the bloodstream. It initiates degranulation and respiratory burst and at higher concentrations, T cells can be recruited by IL-8 directly or, indirectly, via neutrophil-derived mediators. (Mukaida, 2003; Griffith et al., 2014)

IL-8 is often used as a surrogate parameter to assess inflammation of the airways. Nasal or bronchial epithelium release IL-8 in significant amounts, and chemokine levels antecede clinical symptoms like mucous production after exposure towards irritants. Also, IL-8 levels correlate with symptom severity during acute respiratory diseases. Production levels seem to differ between diseased and healthy individuals and production rate was shown to be higher in atopics or patients with chronic respiratory diseases. (Henriquez et al., 2015; Hackett et al., 2011)

IL-8 plays a role in local and systemic inflammation; thus, it can not only be found on mucous membranes but also in the bloodstream. To assess toxicity of indoor PM sources, IL-8 was repeatedly used in controlled exposure studies. In vitro, lung epithelial cells produce IL-8 following treatment with PM of various sizes (Fujii et al., 2001). In vivo, rises of nearly 100% were reported after exposure to biomass smoke (Banerjee et al., 2012). Also, strong IL-8 responses were found in serum after incubation with fractions of air pollutants (Sigsgaard et al., 2000). We therefore measured IL-8 both in serum and lavage fluid.

The role of IL-8 seems to reach far beyond acute inflammation. It was shown to be present in a wide variety of chronic pathologic conditions. It is of interest in tumor therapy and rheumatology. Also, it is established as a marker for neonatal sepsis. Acknowledging the extensive use in other research fields, this work focusses on the evaluation of acute inflammation in airways and peripheral blood.

2.3.3 PM and ICAM

Intercellular adhesion molecule-1 (ICAM-1or CD54) is a transmembranous glycoprotein that belongs to the immunoglobulin superfamily and is expressed on leukocytes and on various cell types, for example endothelial and epithelial cells, fibroblasts and even in neurons (Witkowska and Borawska, 2004; Ramos et al., 2014). It plays a role in immunologic answers towards inflammatory stimuli by facilitating leukocyte adhesion and trafficking. This is mainly accomplished by binding with *lymphocyte function-associated antigen* (LFA-1), preferentially in a dimerized form of ICAM with higher affinity. Thus, numerous immunologic cascades can be initiated. Expression of the molecule can be upregulated in the presence of cytokines like TNF-α or Interleukins. Therefore, upregulation of ICAM-1 correlates with inflammatory conditions (Ramos et al., 2014). A strong upregulation could be observed within 24 hours and once elevated, the concentration on cell surfaces can remain high for 48 hours and more (Hua, 2013).

ICAM-1 consists of five extracellular domains, a transmembrane domain and an intraplasmatic domain. It was discovered that alternative splicing produces at least 6 isoforms of ICAM. It is believed that the differences in their extracellular domains permit different functions of the isoforms during an inflammatory reaction, but little is known about the true effects of these isoforms. (Ramos et al., 2014)

The soluble form of ICAM-1 (sICAM) is most likely formed by proteolytic cleavage of the membrane bound domain of ICAM-1 by proteases (Sithu et al., 2007). Circulating sICAM forms complexes which can be found in various body fluids of clinical interest like serum, sputum, urine and bronchoalveolar lavage fluid. Soluble ICAM has been associated with a number of diseases, most importantly with cardiovascular diseases like hypertension and acute coronary syndrome. Patients in the top quartile of sICAM values have been shown to be at a higher risk of developing myocardial infarction. The marker is also believed to reflect an ongoing inflammation in various tissues, for example endothelium or plaque structures. Furthermore, sICAM levels seem to rise in malignant diseases and elevated levels have a prognostic factor in gastrointestinal cancers or melanoma. In addition, nutritional aspects could play a role in chronically elevated sICAM levels. (Witkowska and Borawska, 2004)

The marker could be indicative of the populations‘ health state and the absence of chronic diseases and at the same time it has the appropriate dynamics to detect short term inflammatory reactions. In the context of exposure to particulate matter, CAMs and especially sICAM were used multiple times to test for adverse health effects.

2.4 Legislative regulation of Particulate Matter

The body of evidence on health impairment through PM has led to implementation of air quality standards and air quality guidelines in many countries. Air quality standards often set thresholds for larger particle sizes like PM_{10} and $PM_{2.5}$ in both residential and occupational environments. On a global scale, the *World Health Organisation* (WHO) established evidence based air quality guidelines since 1987. They are updated periodically, last in 2021 (see Table 2). They are not legally-binding, but intended to be used as a reference and fundament for local regulatory steps (Chan, 2006).

Yet legislative regulations and thresholds are globally inhomogeneous and do not necessarily reflect WHO guideline values. For example, after the 2021 update, the WHO supports an average outdoor concentration of PM_{10} of 15µg/m³ per year with exceeding 45 µg/m³ on not more than 3 days. The *European Union* (EU) allows twice the WHO benchmark as an annual

mean (40µg/m³) with exceeding 50 µg/m³ on not more than 35 days. (European Environmental Agency, 2016; World Health Organisation, 2015)

The WHO has also set updated guideline values for $PM_{2.5}$, suggesting levels of 5µg/m³ of an annual mean, and 15µg/m³ being exceeded on no more than 3 days in outdoor air. For countries or regions with higher levels and no options for short term changes, higher acceptable interim values were proposed.

Pollutant	Time	Guideline Value 2005	Guideline Value 2021
PM2.5	Average / year	10 µg/m³	5 µg/m³
	Average / day	25 µg/m³	15 µg/m³
PM10	Average / year	20 µg/m³	15 µg/m³
	Average / day	50 µg/m³	45 µg/m³

Table 2: ***WHO air quality guidelines for $PM_{2.5}$ and PM_{10}.*** *"average / day" represents the 99th percentile, i.e. should not be exceeded on 99% of days.*

In many areas of the world, PM concentrations are not monitored or exceed recommendations by far (Chen et al., 2012). Even the EU has not yet accomplished globally recommended target values. From 2012 to 2014 between 16% and 21 % of the urban population were exposed to outdoor PM values exceeding the current annual mean EU limit values for PM_{10} and 90 % of urban EU population lived with $PM_{2.5}$ particle pollution above WHO guideline values of that time (European Environmental Agency, 2016).

WHO guidelines are neither designed for indoor nor for outdoor air, but for ambient air, which comprises households as well as open spaces. Yet the guidelines are usually applied to outdoor air, as most of the measuring takes place in public spaces. Thus, explicit legislative limit values of indoor air pollution are scarce and, if existent, similar to outdoor air recommendations. In many countries, indoor air pollution limit values are only applied to a small number of potentially harmful chemicals, often intended to regulate working conditions in certain occupational settings. (World Health Organisation, 2015)

2.5 Research questions

Now overviewing the topics of research, the following questions could be posed

1. Does short term exposure towards predefined common household particle sources alternate levels of IL-8, CRP and sICAM in blood and nasal lavage?
2. Does the intensity of the particle exposure correlate with the changes in biomarkers levels and is the biological signal homogenous?
3. Is it possible to allocate the effect on innate immune response parameters to a specific particle source or a particle size fraction?

3 Material and Methods

3.1 Study and study design

The *Effects of fine and ultrafine Particles from Indoor Activities–Study* (EPIA-Study) was performed by the *Institute of Energy and Environmental Technology* (IUTA – *Institut für Energie und Umwelttechnik*) in Duisburg in cooperation with the *Leibniz Research Institute for Environmental Medicine* (IUF - *Leibniz-Institut für Umweltmedizinische Forschung*) in Düsseldorf . The study was commissioned and funded by the *German Federal Environmental Agency* (UBA - *Umweltbundesamt*).
The study was intended to
1. investigate indoor particle sources that generate particles mainly in the UFP-range
2. combine characterization and toxicological analyses of particles from these sources
3. investigate biological reactions in humans which reflect short-term mechanisms towards PM exposure.

The study was designed as a sham-controlled cross-over human exposure study. It was approved on 6th July 2012 by the ethics committee of *Heinrich-Heine-Universität Düsseldorf* with reference number 3830. All participants were thoroughly screened for general health conditions, risk factors and in- and exclusion criteria in a pre-study screening process. All study participants gave written and informed consent before participation.

Participants were exposed to various particle sources between October 2012 and June 2013. They were all healthy, non- or ex-smokers, speaking and understanding German. Before, during and after the exposure, participants were examined by specially trained and supervised study personnel and various clinical examinations were conducted in a pre-defined order at pre-defined time points according to pre-defined standard operating procedures. The examinations included measurements of blood pressure, pulse wave analysis, heart rate variability, exhaled nitric oxide, lung function, neurocognition, nasal lavage and venepuncture with storage of specimen for further examination. The measurements were intended to detect local inflammatory changes (through nasal lavage, exhaled nitric oxide), local organ impairments (through testing of lung function), systemic inflammation (through venepuncture and subsequent blood testing) and systemic organ impairment (through cardiovascular function).

3.2 Screening process, in- and exclusion criteria

The recruitment of participants was conducted via advertisements, flyers and public postings in the area of the North Rhine-Westphalian towns of Düsseldorf, Essen, Duisburg and Mülheim. Recruitment was performed two times due to high drop out before the beginning of the field phase, as can be seen in figure 6. A total of 143 individuals responded to the study advertisement. Volunteers were pre-screened for suitability during a telephone interview assessing general health conditions and potential risk factors.

Main inclusion criteria in the pre-screening process were age between 18 and 79 years, non-smoking or ex-smoking for at least 10 years and speaking and understanding German. Exclusion criteria assessed during the telephone interview were smoking or ex-smoking for less than 10 years, regular and severe exposure towards tobacco smoke and occupational or residential exposure towards severely polluted air. Furthermore, preterminal disease, heart attack, embolism and stroke in the past three months were excluded. Uncontrolled hypertension, diabetes mellitus, chronic respiratory disease, chronic infectious disease or neurologic or mental disease, planned pregnancy and planned surgery during the next six months were also excluded. A further exclusion criterion was the anatomical inability to successfully conduct pulse wave analysis.

81 eligible volunteers were invited to a screening examination which was used to confront potential study candidates with typical study situations, especially with examination methods that required knowledge and cooperation. Volunteers were familiarized with lung function measurements, nasal lavage and pulse wave analysis before the collection of personal exposure-related data and material began. As these techniques depend on participants‘ active collaboration, this was believed to reduce invalid measurements in the beginning of the field phase. After the screening examination, 68 individuals were found suitable for inclusion in the study, yet 13 later revoked their participation before the beginning of the field phase.

The 55 volunteers willing to participate in the study gave written and informed consent and anthropometry was performed assessing height and weight to calculate body mass index (BMI). Furthermore, blood pressure and heart rate were measured. Participants were handed a general questionnaire which assessed socioeconomic status, lifestyle, medical history and regular medical treatment. Also, participants received printed documents as a preparation for the exposure days. The documents contained general information about the study and information about the personal behaviour each day before and after a particle exposure to secure interpersonal comparability. Participants were asked to avoid extreme physical exercise and alcohol, beginning 24 hours before an exposure and to abstain caffeine containing drinks 4

hours before an exposure. They were also asked to only have a light breakfast. (Soppa et al., 2017)

3.3 Study population

55 individuals agreed on participation in the study (compare figure 6) and where exposed with particulate matter and examined under controlled conditions at least once.
14 volunteers dropped out during the course of the study, 10 of which due to time constraints. Two were excluded during the field phase. One exclusion was due to an epileptic seizure and one due to uncontrolled arterial hypertension which was not detectable during the screening visit.

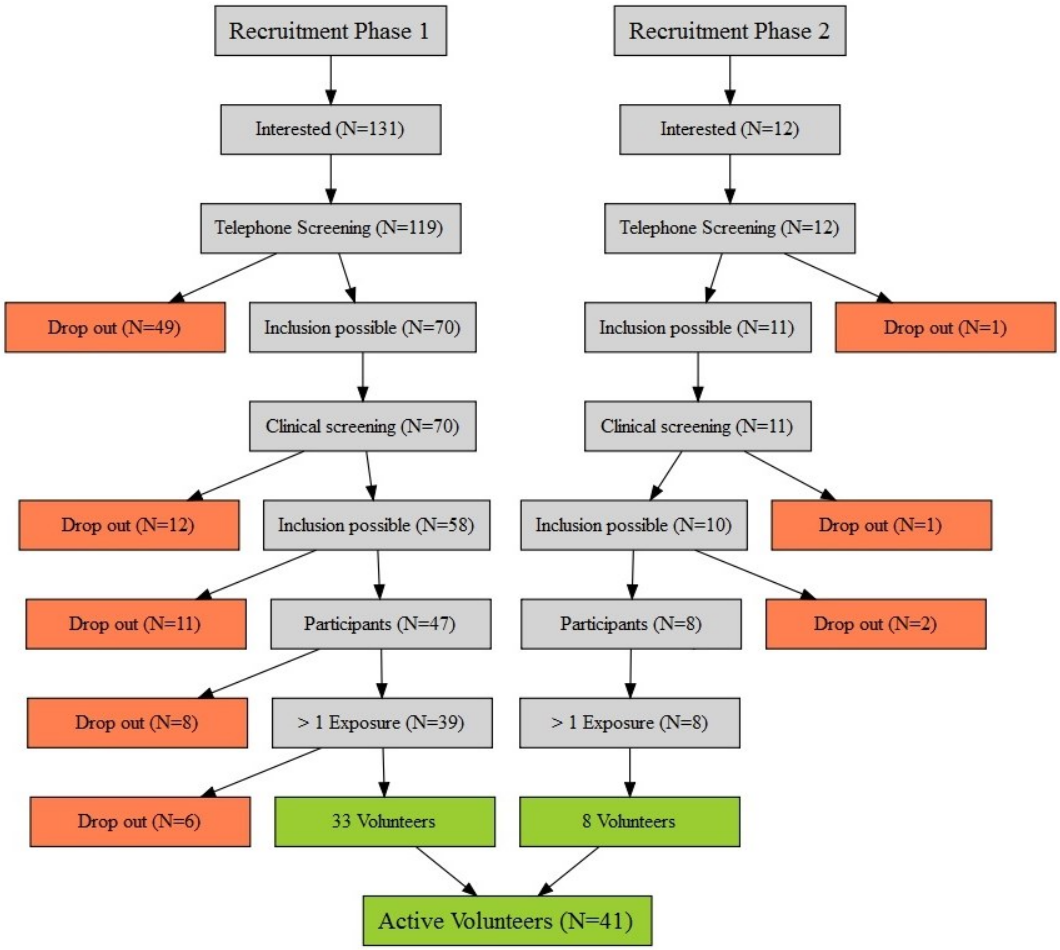

Figure 6: ***Study recruitment and final population with dropouts.*** *The two threads reflect the initial recruitment and the second recruitment phase. N= Number of participants*

3.4 Exposure setting

Identification and characterisation of suitable sources of indoor particulate matter was managed by the IUTA in Duisburg and their *Research Division of Environment and Sustainability*. At their testing site, various typical residential activities were tested regarding their potential to generate fine and ultrafine PM. Simultaneously, the resulting particles were analysed regarding their physicochemical properties.
Among the tested sources were kitchen activities like toasting bread, baking pizza or frying sausages. Vacuum cleaning was tested as a typical household activity. Exposure from resuspended dust by vacuum cleaning was assessed separately from the engine emissions of the vacuum cleaner itself. Furthermore, various indoor combustion sources were assessed, for example candle burning, operating a fireplace and operating butane and spirit burners. Finally, PM emissions were also measured while grinding nanoparticle containing paint and while using a hot air radiator.

The sources considered most reproducible and most relevant where frying sausage, toasting bread and burning candles. These sources showed a stable emittance of particles, a size distribution in the range between PM_{10} and UFP and high particle number concentrations. Other sources were finally discarded because of operational difficulties (for example, a fireplace could not be operated under stable conditions) or because of low relevance in everyday life (for example grinding paint). Furthermore, the discarded sources, when fully operated, caused particle number concentrations in the range of urban outdoor air background concentrations (15.000-100.000 particles/cm³), while burning candles, toasting bread and frying sausages led to number concentrations higher than 1.000.000 particles/cm³.

Participants were exposed to these sources in a specially designed closed chamber at the testing site of IUTA in Duisburg. The chamber measured 16 m² and approximately 48m³ and was built from powder-coated sheet metal with glass windows and a roof covered with an antistatic polyethylene film to limit particle agglomeration on surfaces. The chamber was equipped with the particle sources and an air conditioning system that was operated in a circulating ventilation mode to prevent additional particle entry and to ensure a constant pollutant dispersion. Besides, there was also an active ventilation of filtered outdoor air with a steady air exchange at a flow rate of 90 - 250m³/h. Temperature and humidity in the chamber were controlled and temperature maintained at 24° C.

Exposure towards particles was measured with particle monitors at a temporal resolution of minutes to seconds. A steady state of particle concentrations was reached approximately 30 minutes after the start of a source operation inside the chamber. Participants entered the

chamber only after this steady state was reached. Exposure measurement units outside the chamber then calculated an average two-hour personal exposure for each participant. Sampling ports for air quality measurements were installed in the proximity of the participants‘ seats to precisely reflect personal exposure. Handheld particle monitors (DISCmini, Matter Aerosol, Wohlen, Switzerland) revealed a homogenous distribution of particles in the participants’ surroundings. (Soppa et al., 2014)

3.5 Exposure scenarios

Only toasting bread (TB), candle burning (CB) and frying sausages (FS) showed high particle concentrations, reproducibility and relevance for everyday exposure scenarios at the same time and were thus used for controlled exposure scenarios in the EPIA study. The three different sources were operated on two different levels of intensity, thus creating exposures of intermediate (Level 1) and high particle exposure (Level 2). The higher intensity of exposure was reached by redoubling the amount of exposure sources. An overview of the exposure scenarios can be seen in table 3.

	Source characteristics
RA	Non-operated air ventilator, sham-exposure with room air
CB Level 1	Burning of 20 white candles
CB Level 2	Burning of 40 white candles
TB Level 1	One two-slice toaster, toasting cycles of three minutes
TB Level 2	Two two-slice toasters, toasting cycles of three minutes
FS Level 1	Three sausages in a *Teflon*® pan, fried for 10 minutes without oil, turnover every 150 seconds
FS Level 2	Six sausages in two *Teflon*® pans, fried for 10 minutes without oil, turnover every 150 seconds

Table 3: ***Source abbreviations and characteristics.*** *RA: room air; CB: candle burning; TB: toasting bread, FS: frying sausage*

For CB, 20 commercially available *RAL*-certified white Christmas tree candles were attached to holders on aluminium foil covered plywood on a laboratory desk 1.2 meters above ground. The candles had a distance of approximately 15 cm from one another to avoid melting and air

ventilation was not directly pointed towards the candles to prevent sooting.
Candles were replaced before burning out. For level 2, 40 candles were installed similarly.

For TB on level 1, bread was toasted in a time controlled two-slice toaster (Executive Edition TT 61103, Siemens, Germany). A toasting circle lasted three minutes. To prevent overheating of the toasters and to ensure constant particle emission, three identical toasters were operated alternatingly. The bread (*Buttertoast* from a local discounters) contained wheat flour, water, concentrated butter 3 %, sourdough (wheat flour, water), yeast, salt, grape sugar and sodium diacetate. For level 2, two of the above mentioned toasters were operated simultaneously. Before first use, toasters were heated up outside the chamber for half an hour to remove potential contamination from the production process.

For FS, at level 1 three sausages (*Thüringer Rostbratwürstchen* from a local discounter) were fried without additional fat or oil in a *Teflon*®-coated pan (Tefal-H11506, SEB, France). The sausages contained approximately 90% pork meat, water, sodium chloride, potassium iodide, dextrose, a spice mixture of pepper, onions, nutmeg, ginger, garlic, cardamom and parsnip and the food stabilizer diphosphate. The pan was placed on an electric hotplate (KP 1057, Severin, Germany). The sausages were fried for 10 minutes in a preheated pan with turnovers every 150 seconds. After three frying circles (9 fried sausages), the pan was cleaned from frying residues and frying paused for 10 minutes to cool down the pan. Level 2 followed the same procedure with two pans (6 sausages).

Implementing a control exposure in the experimental setup was difficult to perform, as participants had visual and olfactory contact with the exposures. Therefore, a fourth exposure setting contained a non-operated ventilator in room air (RA), which was presented to the participants as a particle emitting air refresher. This exposure is referred to as sham-exposure in the course of this work.

3.6.1 Measurement of particle metrics and chemical composition

Measurement of particle metrics was conducted continuously to ensure a constant particle pollution of inhaled air. Particles with a size between 5.6 and 560 nm were measured by a *Fast Mobility Particle Sizer Spectrometer* (FMPS, Model 3091,TSI Inc., USA) with a timely resolution of one second. In an FMPS, electrically precharged particles are deflected in an electric field. Depending on their size, they show a unique deflection pattern and hit electrodes on a series of electrometers. The electric charge of the particles is transformed into a current on

the electrode and amplified by the electrometers. An integrated algorithm in the device can calculate back from the charge distribution to particle size distribution.

Size-dependent particle number concentration was calculated with a *Scanning Mobility Particle Sizer* (SMPS, Model 3936, TSI Inc., USA), an established technique used for particle number calculation in the submicron range that follows similar principals as the FMPS at a broader timely resolution. Depending on the unique setup of components (Electrostatic Classifier, Model 3080; Differential Mobility Analyzer, Model 3081 or 3085; Condensation Particle Counter, Model 3776 with Neutralisator Model 3077, all TSI Inc., USA) the SMPS unit was able to detect particle number concentrations in the range of 6.5 to 750 nm with a sampling time of 2 to 4 minutes.

The surface area concentration was measured by a *Nanoparticle Surface Area Monitor* (Model 3550, TSI Inc., USA). This device operates via ion-charging and current release of particles in presence of electrometers and calculates the lung deposited surface area (LDSA) of particles in $\mu m^2/cm^3$ by using calibration factors from known and predescribed particles.

An *Aerodynamic Particle Sizer* (APS, Modell 3321, TSI Inc.,USA) sorted particles between 0.6 to 20 µm according to their aerodynamic diameter. An APS discriminates particles by aerodynamic drag in an air stream. The characteristic flight time of particles is measured by lasers and calculated back to particle size. PM_1, $PM_{2.5}$ and PM_{10} as size-specific mass concentrations were calculated from particle size and number concentrations with the assumption of particles being spherical at a density of 1 g/cm3 (Soppa, Schins et al., 2014).

To constantly monitor the particle pollution outside and inside the exposure chamber, two particle sizers *DiSCMini* (Matter Aerosol, Switzerland) were in use throughout the study. They were randomly given to exposed participants to monitor personal exposure, too. The *DiSCMini* were able to detect particles within a range of 10 to 400 nm of aerodynamic diameter and calculated particle number concentration, mean particle diameter and mean particle surface area.

Chemical composition of particles was assessed by an *Aerosol Mass Spectrometer* (AERODYNE HR-TOF-AMS, Aerodyne Research Inc., USA) which characterized particles within a size range of 60 to 600 nm. Time resolution could be arranged from hours to a few seconds average.

Ultrafine particles were not only measured but also collected with a *Nanometre Aerosol Sampler* (NAS, Model 3089, TSI Inc., USA). Thus, particles could be transferred to additional analysis with *Scanning Electron Microscopy* (SEM) or *Reflection-X-Ray-Fluorescence Spectrometry* (TXRF). Further particle collection for toxicological analysis of redox potential or

radical formation was accomplished with a *Low Volume Sampler* (LVS 3, Derenda, Germany) and a *Particle-into-liquid-sampler* (PILS, Metrohm AG, Switzerland).

Also, an *Organic Carbon-/Elemental-Carbon-Analyzer* (Lab OC-EC Aerosol Analyzer, Sunset Laboratory Inc., USA) and a *Compact-Protontransfer-Reaction-Mass spectrometer* (Compact PTR-MS, Ionicon, Austria) for the analysis of volatile organic compounds (VOC) were operated. Data from these analysers was not used in this work.

3.6.2 Particle chemistry

Chemical analysis of the particle sources was accomplished by members of the IUTA, Duisburg with an *Aerosol Mass Spectrometer* (AMS, AERODYNE HR-TOF-AMS, Aerodyne Research Inc., USA) for particles between 60 and 600 nm of aerodynamic diameter. The AMS unit generally distinguished five different compounds, organic hydrocarbons (OHC), sulphates (SO_4), nitrates (NO_3), ammonium (NH_4) and chlorides (Chl).

Furthermore, liquid suspensions of airborne particles were tested for surface reactivity with elctronspin-resonance spectrometry-based assays at IUTA, Duisburg.

Candle Burning (CB) showed high amounts of NO_3 (50-60 %) and OHC (40-45%) and low amounts of NH_4. The main source of NO_3 were most probably the candle wicks, as they are impregnated with ammonium containing flame-retarding additives. Black or elemental carbon (soot) was only accountable for 3 to 10 % of the hydrocarbons detected during CB. Detectable elements were potassium, calcium, iron, zinc and titan. In toxicological analyses, particles showed no ability to produce radicals, but a surface reactivity could be observed. (Hellack et al., 2014)

Toasting Bread (TB) showed high amounts of OHC (90-95 %) and low amounts of NO_3, NH_4 and SO_4. Carbon detected on filters was almost exclusively OHC, with only 1 % of elemental carbon. Particle mass was to 50 % caused by water adsorbed to the hydrocarbons. The elements detected in the filters were calcium, iron, chloride and zinc, all in the range of a few nanograms. Iron and chloride are believed to arise from roasting processes. Particles from TB showed only a low potential to form radicals. (Hellack et al., 2014)

Frying Sausage (FS) emitted particles of almost exclusively OHC (95-99%). The rest was formed by NO_3 and chloride, probably deriving from salts in the product or from elements embedded in proteins. Elemental carbon was not detectable during the frying process. Other detected elements were iron, calcium and zinc in single-digit nanogram concentration that could

be explicable as background concentration. No potential to form radicals was observed. (Hellack et al., 2014)

3.7 Conduction of Field Work

The cross-over design implied repeated exposures of the same volunteer throughout the course of the study. To avoid carry over effects and to control for biological variability within the course of time, exposures of the same volunteer were carried out with a time lag of two weeks at the same day of the week and the same hour of the day. Each study day, four participants were scheduled to arrive with an interval of 30 minutes to ensure efficient and fluent examination.

The study days began with a physical examination and a health questionnaire which also assessed travel time to the testing site and mode of transportation. Noticed or reported infections before the exposure and the use of anti-inflammatory drugs up to 7 days before the exposure day led to postponement of the exposure.

Each exposure with particles was accompanied by six time points of medical examinations (see Table 4). Shortly before each of these examinations, volunteers filled in a diary, reporting subjective health conditions.

All measurements were conducted once before exposure to generate baseline measurements (t_0). Then participants entered the exposure chamber for two hours, with particle sources already brought to a steady state as mentioned above. After one hour of exposure, blood pressure and pulse rate were measured inside the chamber by a staff member(t_1). After the two-hour exposure, blood pressure and pulse rate were analysed together with pulse wave measurements (t_2). Two hours after exiting the exposure chamber (t_3), the same examination was repeated together with a measurement of exhaled nitric oxide (FeNO), a nasal lavage (NAL) and a venepuncture. Another two hours later (t_4), blood pressure, pulse rate, pulse wave analysis, lung function and neurocognition were evaluated, marking the end of the study day. Participants were instructed to avoid vigorous physical activity and alcohol intake and to return to the study centre 24 hours after the exposure (t_5), when the full range of medical examinations was conducted again.

Degradable specimen like nasal lavage fluids and blood samples were either immediately processed for further analysis according to standard operating procedures or stored in deep freezers and transported to the Institute for Environmental Medicine, Düsseldorf at the end of the week, where long-term storage at -80°C was possible.

	Before Exposure (t_0)	During Exposure (t_1)	Post Exposure (t_2)	2h post Exposure (t_3)	4h post Exposure (t_4)	24h post Exposure (t_5)
Health questionaire	X					
Diary	X	X	X	X	X	X
RR / Pulse	X	X	X	X	X	X
PWA	X		X	X	X	X
PWV / HRV	X		X			X
FeNO-Test	X			X		X
Pulmonary function	X				X	X
Neurocognitive test	X				X	X
Nasal lavage	X			X		X
Blood test	X			X		X

Table 4*: Setup of measurements and chronological order.* *RR: blood pressure; PWA: pulse wave analysis; PWV: pulse wave velocity; HRV: heart rate variability; FeNO: fraction of exhaled nitric oxide.*

3.8 Nasal lavage (NAL)

For this thesis, inflammatory markers in nasal lavage fluid and in serum were analysed. The examination of nasal lavage and its operational technique is therefore described in detail.

NAL is a non-invasive method to obtain an insight into the conditions of the respiratory tract. At rest, the majority of humans are nose breathers, and as such the nasal cavity is the first air space and the first mucosal barrier to come in contact with irritants (Mirowsky und Gordon, 2015). Nasal lavage can be described as an instillation of saline into the nasal cavity and subsequent recovery of the instilled fluid after a predefined dwell time (Scarpa et al., 2014). There is reasonable evidence to consider washing fluid from the nasal cavity as a proxy for airway response and health conditions in the lung (Graham und Koren, 1990). Mediator changes in lavage fluid have been shown to reflect biological effects in the lower airways, for example respiratory worsening in lung function measurements (Scarpa et al., 2014). Thus, investigating mucous membranes with NAL could be seen as a less invasive replacement of methods like bronchial or bronchioalveolar lavage.

An often analysed mediator in NAL fluid is IL-8. Being involved with innate immune responses as described in chapter 2.3.2, IL-8 in NAL was positively associated with air pollution multiple times (Scarpa et al., 2014)

In the EPIA study a standard operating procedure (SOP) was developed for NAL, based on an established technique from respective literature (Graham und Koren, 1990). According to the SOP, volunteers had to sit on a fixed chair, holding a funnel with a collection tube and paper towels to clean their nose afterwards. During the course of the lavage, volunteers were asked to recline their head by 45°, thus exposing the nostrils. They were asked to stop breathing and form a „K"-sound with their tongue and palate to close the nasopharyngeal airspace from the lower pharynx. With a sterile pipette, the examiner speedily applied 5 millilitres of sterile phosphate buffered saline (PBS) pre-warmed to 37°C into each nostril. After 10 seconds, loudly counted by the examiner, the volunteer bent forward and passively drained the PBS into the funnel above the collection tube. In the funnel, the fluid passed a polyamide filter. After fluid collection, the filter was discarded, and the collection tube centrifuged for 5 minutes at 3400 rounds per minute (rpm) at 600*g* and at 4°C.

The collection tube was then taken from the centrifuge, the supernatant decanted into a new 15 millilitre tube and the tube put on ice. The cell pellet on the tube ground was used for separate analyses whereas the supernatant was aliquoted into Micronic® tubes and stored at -20°C until the end of the week. Finally, these samples were transferred in a closed box on ice to be placed in a -80°C deep freezer for long term storage and further analyses of, in this case, IL-8 content.

3.9 Venepuncture

For the analysis of CRP-, IL-8- and sICAM-serum levels, material from venepuncture was used. Each patient was asked for their preferred posture (seated or laid down) during venepuncture and this position registered in a participant's file. Thus, venepuncture was always carried out under the same conditions. A tourniquet was applied for a maximum of one minute before puncture. If no vein was visible, discreet palpitation of the area was done and if no vein was detectable after manipulation, damp heat was applied with a warm and wet towel for a few minutes after loosening the tourniquet. Application of this manipulation technique however had to be registered in the participants' file. A possible area of puncture was cleansed with a pulp swab and covered with disinfectant for 30 seconds. Before or immediately after a successful puncture, the tourniquet was loosened. *Monovettes*® for the analysis of serum and EDTA-diluted blood were filled. After puncture and removal of the needle, the area was bandaged, and the participant asked to apply pressure to prevent hematoma formation.

Monovettes® were slewed five to ten times after venepuncture. Blood intended for direct measurements was sent to a nearby laboratory, blood for further research was immediately centrifuged at 3400 rpm for 10 minutes and 15°C. The supernatant was then aliquoted into Micronic® tubes and deep-frozen at -20°C until the end of the week. Finally, these samples were transferred in a closed box on ice to be placed in a -80°C deep freezer for long term storage and further analyses.

3.10. Laboratory work

3.10.1. Measurement techniques

The analysis of nasal lavage fluids and peripheral blood was carried out at the *Leibniz-Institute for Environmental Medicine* in Düsseldorf, in the research group for particles, inflammation and genome integrity under the lead of Dr. Roel Schins, beginning in February 2014.

Enzyme-linked Immunosorbent Assays (ELISA) were used to detect IL-8 in NAL fluid and blood (IL-8 PeliKine compact™, Sanquin, The Netherlands) and CRP and sICAM in blood samples (Quantikine®ELISA, R&D Systems, Inc., USA). Characteristics of the different assays are found in table 5.
For most of the markers, the samples had to be diluted as the highly sensitive assays would otherwise not be able to detect the correct amount of target biomarker.

The measurement technique of the different ELISAs followed the same mechanistic principles. All assays were so-called *sandwich-ELISAs*. Herein, a 96-well plate is precoated with a capture-antibody that reacts specifically with the target biomarker. Then the plate is filled with samples, each sample duplicated for quality control reasons. At this point, the biomarker of interest already binds to the capture-antibody on the bottom of the well.

After adding the samples, an anti-target antibody is brought into solution that binds to the target biomarker now bound to the capture antibody, thus forming a sandwich of antibodies. Afterwards, an enzyme capable to bind the anti-target antibody is applied. Once bound to the sandwich of antibodies, this enzyme is able to propulse a colour reaction in the solution. The intensity of the colour reaction correlates with the amount of target biomarker initially bound to the coated well. An absorption reader can then calculate from the absorbance of a standard dilution with known amounts of biomarker on the same plate to the amount of biomarker found in a sample of unknown concentration.

Elisa type	Range	Sensitivity	Dilution of original sample
IL-8 in NAL	1 – 240 pg/ml	3 pg/ml	1:10
IL-8 in blood	1 – 240 pg/ml	3 pg/ml	No dilution
CRP in blood	0.8 – 50 ng/ml	0.022 ng/ml	1:100
sICAM in blood	1.6 – 50 ng/ml	0.254 ng/ml	1:20

Table 5: ***Characteristics of the ELISAs used during the laboratory work.*** *Due to the expected range of values, different dilutions were applied to create samples within the range of the assay.*

3.10.2 Calculation of biomarkers

The generation and analysis of biosamples from nasal lavage fluid and venepuncture was reduced to certain time points only. For IL-8 in NAL fluids and blood, samples were taken at timepoints t_0, t_3 and t_5 because a biological reaction on the level of cytokines is expected to appear quickly (see chapter 2.3.2). For CRP and sICAM, only blood samples from timepoints t_0 and t_5 were used, as significant changes in serum levels of these biomarkers have a longer latency (see chapter 2.3.1).

Biosamples had been aliquoted and immediately deep-frozen during the field phase, so the samples were sorted by exposure sources and study dates. In order to measure every exposure of one single volunteer at the same time and on the same plate, these samples had to be resorted and merged first, thus making intraindividual results more comparable. To prevent thawing and freezing of the samples during the sorting process, specimens were placed on dry ice. Afterwards, the merged sets were analysed with ELISA technique or stored in a freezer at circa -80°C until further analysis during the next days.

Before measurement, the sample sets in *Micronic*® tubes (containing aliquots from all available time point and exposure sources of one volunteer) were merged with other sample sets to fully fill in one 96-well plate and thus save laboratory resources. The ELISAs were conducted according to the delivered manual in concordance with procedures established in the working group. The readout was done with a photometric ELISA reader (Multiskan Ascent 96-well Plate reader, Thermo Fisher Scientific, Germany) at 450 nm for IL-8 assays and at 450 and 570 nm for CRP and sICAM assays, respectively (TECAN, Infinite® 200 PRO plate reader, Tecan Group AG, Switzerland) which produced a data set that could be converted into an excel file (Microsoft Excel 97-2003, Microsoft Corporation, USA).

The calculation of the measured absorbtions was also carried out with Microsoft Excel (Microsoft Excel 97-2003, Microsoft Corporation, USA). To explain the final calculation of amounts of biomarkers, an exemplary excel sheet is displayed in figure 7. First, the light absorption of a standard dilution with known amounts of biomarker („conc“ in Figure 7) is measured in duplicate at a light wavelength of 450 nm and 570 nm („abs450(1)“ and „(2)“ and „abs570(1)“ and „(2)“).

Then the differences of these absorptions are calculated. („abs450-abs570(1)“ and „(2)“ in Figure 7), and for a better precision of the two absorptions, the average is calculated („av of abs diff“). Then the absorption of a blank (or empty) well is subtracted to correct for the absorption of the transparent plastic plate that contains the samples („average abs-blanco“ in Figure 7).

Concentration and absorption values are transformed logarithmically („log conc“ and „log gem abs“) to calculate a graph with a line of best fit as shown in figure 7. As the line of best fit is calculated from a known degree of absorption and a known amount of sample, unknown amounts of sample can now be determined by light absorption values only. This estimation technique is very accurate, as the coefficient of determination shows („R^2=0,9953“ in Figure 7).

conc	abs450(1)	abs450(2)	abs570(1)	abs570(2)	abs450-abs570(1)	abs450-abs570(2)	av of abs diff	average abs-blanco	log conc	log gem abs
50,00	2,467	2,292	0,047	0,044	2,420	2,249	2,334	2,327	1,69897	0,3668617
25,00	1,478	1,490	0,039	0,032	1,439	1,458	1,449	1,441	1,39794	0,158799582
12,50	0,922	0,898	0,038	0,034	0,884	0,864	0,874	0,867	1,09691	-0,0619809
6,25	0,572	0,526	0,033	0,030	0,539	0,496	0,517	0,510	0,79588	-0,29230211
3,12	0,319	0,312	0,033	0,033	0,286	0,279	0,283	0,276	0,494155	-0,55956323
1,56	0,180	0,178	0,029	0,029	0,151	0,148	0,150	0,143	0,193125	-0,84588047
0,78	0,115	0,113	0,033	0,036	0,082	0,077	0,079	0,072	-0,107905	-1,14056146
0,00	0,046	0,044	0,039	0,037	0,007	0,007	0,007	0,000		#ZAHL!

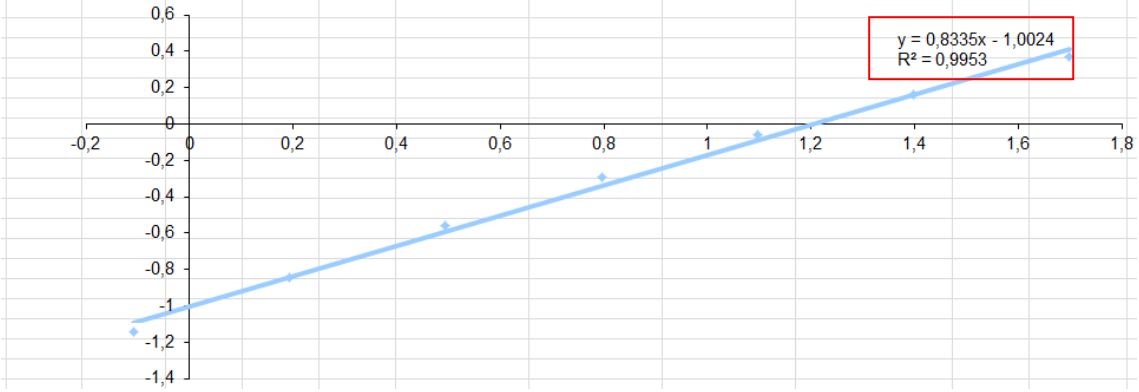

Figure 7*: Standard curve for the detection of CRP values in an ELISA measurement. Conc: standard dilution; abs1+2: absorptions at 450 nm and 570 nm wavelength. Av of abs diff: average of absorption differences; log conc: logarithm of concentration in standard dilutions; log gem abs: logarithm of absorptions differences. X-axis: logarithmic concentration of standard dilution, Y-axis: logarithmic mean absorption of standard dilution, R^2: coefficient of determination*

The term of the standard curve (framed red in figure 7) is then used to calculate from the absorption of the remaining samples to an unknown amount of biomarkers. This is achieved by log-transformation of absorption values as shown above. The absorption values are then placed

in the formula of the standard curve (framed in red) as y-value. The result of this term is the logarithmic amount of biomarker. Thus, it is retransformed into natural numbers. The last step is an adjustment for the dilution factor if a biosample was diluted in the first place.

3.10.3 Quality control and inclusion criteria for biosamples

The laboratory analyses were only carried out if a volunteers' sample set contained samples from a full sham exposure including t_0, t_3 and t_5 and at least one completed true exposure scenario with each of these time points.

As laboratory analyses required demanding manual work prone to human errors, measurement imprecisions or a lack of sample quality, the results of the ELISA measurements were controlled for internal concordance. This was performed using a variation coefficient as a quality criterion for precision of the duplicate absorbances of one sample, according to a working group procedure (Variation Coefficient = Standard deviation/ mean of duplicates * 100). All measurements with a coefficient >15 for CRP, sICAM and IL-8 in NAL, and >20 for IL-8 in blood were excluded. The reason for a higher imprecision tolerance with IL-8 in blood was that the variation coefficient reacts stronger for small absorbance values. IL-8 contents in blood of healthy volunteers were on the lower limit of the assay's detection range.

If the exclusion criteria were met in one of the analysed time points, all time points of the respective exposure where excluded. If a sham exposure was affected by these quality criteria limits and no material for a second measurement was available, the sham exposure was considered as non-existent and all observations of one volunteer were excluded (this was the case only once). The number of measurements in nasal lavage fluid and blood therefore differ from the number of samples originally taken from the study population in the field phase.

3.11 Statistical analysis

3.11.1 Inclusion criteria for statistical analysis

A completed sham exposure was considered as an obligatory precondition to enter the data set, thus 12 of the initial 55 study participants had to be excluded due to incomplete sham exposure. Two participants were excluded retrospectively as they had unnoticedly met exclusion criteria during the course of the study. Single individual exposures had to be excluded as scorching of a toast resulted in an unintentionally high exposure to coarse PM and another pair of observations

had to be excluded because a participant showed up for material collection 48 hours instead of 24 hours after the exposure.

Finally, a total of 41 volunteers entered the analysis. Due to technical difficulties during the field phase and due to volunteer compliance during the study, not all volunteers conducted every planned measurement. Especially venepuncture was sometimes unsuccessful or refused by volunteers. In some cases, the total amount of blood samples was insufficient to carry out further tests in the laboratory. Taken these reasons together, the final amount of measured observations in this study can be found in Table 7.

	Excluded observations due to laboratory constraints, %	**Excluded observations due to study constraints, %**	**Included observations, %**	**Volunteers, N**
IL-8 in NAL	18 of 693 = 2.5 %	24 of 693 = 3.5 %	651 of 693 = 94.0 %	41
IL-8 in blood	47 of 557 = 8.4 %	39 of 557 = 7.0%	471 of 557 = 84.6 %	34
CRP in blood	28 of 414 = 6.7 %	28 of 414 = 6.8 %	358 of 414 = 86.5 %	33
sICAM in blood	6 of 414 = 1.4 %	30 of 414 = 7.3 %	378 of 414 = 91.3 %	34

Table 6*: Final exclusions and inclusions of observations.*

3.11.2 Variables

Statistical analysis was performed at the *Institute of Occupational, Social and Environmental Medicine* of the *Heinrich-Heine University Düsseldorf* under the supervision of Prof. Dr. Barbara Hoffmann.

The independent variables of the following analysis reflect exposure-related data. The following continuous and categorial variables are of interest.

Continuous variables:

- Particle mass [PM_{10}, $PM_{2.5}$, PM_1] in [µg/m³] with an assumed density of 1 g/cm³
- particle surface area concentration [PSC] in [µm²/cm³]
- particle number concentration [PNC] for particles from 10 nm to 500 nm in [number/cm³]

Categorial variables:

- Frying sausage (FS)

- Toasting Bread (TB)
- Burning Candles (CB)
- Room Air (RA)

The dependent variables reflect the outcome-related data. The following continuous variables are used as markers of outcome:

- IL-8 in nasal lavage fluid in [pg/ml]
- IL-8 in blood samples in [pg/ml]
- CRP in blood samples in [ng/ml]
- sICAM in blood samples in [ng/ml]

The following covariates are used in different adjustment sets:

- Gender [male/female] (categorial), assessed by self-report in general questionnaire
- Age in [years] (continuous), assessed as difference between study date and reported day of birth
- Height in [cm] (continuous), assessed with an ultrasonic measurement unit (MZ10020, ADE GmbH&Co, Germany)
- Weight in [kg] (continuous), assessed with a standard weight scale (Soehnle, LEIFHEIT AG, Germany)
- Body Mass Index (BMI) in [kg/m^2] from weight and height
- Temperature in [°C] and humidity in [%](continuous), assessed as 2-hours average in the exposure chamber with a moisture and temperature measuring device (Hygro-Sens, Germany)
- Travel time to the study centre in [minutes] (continuous), assessed by self-report
- Means of transportation [car, train and bus, on foot] (categorial), assessed by self-report
- Ambient $PM_{2.5}$ concentrations at residence address during the last five days before study participation in [$\mu g/m^3$] (continuous), recorded by the *State Agency for Nature, Environment and Consumer Protection of North Rhine-Westphalia* (LANUV) at the monitoring station closest to the volunteer's residence address
- Temperature in [°C] (continuous) during sample drawing

Smoking status, medical and educational background were also assessed via self-report in the general questionnaire. These variables were not considered as covariates because they showed a

very homogenous distribution. All participants were never or long-time ex-smokers and the population mainly consisted of healthy young adults, many of them recruited at universities.

3.11.3 Analysis approaches

We calculated descriptive statistics for each dependent and independent variable. Continuous variables are generally reported with mean, standard deviation, median, first and third quartile and range. Categorial variables are reported with number and percentage. Additionally, dependent variables of biomarkers were split up by source of exposure, level of exposure and time of exposure and descriptive statistics for each of these observations was calculated.

In a first step, a pre-analysis was conducted. To quantify the exposure source-related changes of biomarker levels, we developed a linear mixed regression model with random participant intercept and an indicator variable for each source of exposure. The dependent variable in this analysis is the intraindividual difference of a biomarker level between any timepoint (t_n) and the baseline measurement (t_o). A separate analysis for each difference of time points was conducted, thus performing two separate regression analyses for IL-8 (t_3-t_0 and t_5-t_0) in serum and NAL and one analysis for CRP and sICAM (t_5-t_0).

$$Y_i = \beta_0 + u_i + \beta_{CB} I_{CB_i} + \beta_{FS} I_{FS_i} + \beta_{TB} I_{TB_i} + \sum_{i=1}^{k} \beta_i X_{ki}$$

Y_i : ΔIL-8, ΔCRP, ΔsICAM: change in biomarkers as difference t3-t0 and t5-t0

β_0 : intercept

u_i : random intercept for participant i

$\beta_{CB\ TB\ FS}$: Coefficients: absolute change in a biomarker level between baseline (t0) and post-exposure time t_x due to a specific source

$I_{CB\ TB\ FS}$: Indicator variables for exposure source (CB=Candle Burning, TB=Toasting Bread, FS=Frying Sausages, reference: room air) in person i

$\sum_{i=1}^{k} \beta_i X_{ki}$: Vector of coefficient for independent variables of adjustment set in person i

As covariates, age, BMI, sex, temperature and humidity in the exposure chamber, travel time to the study centre, means of transportation, background $PM_{2.5}$ concentration at the residence

address averaged over the last 5 days before a study day and temperature during sample collection, were considered.

Models were built up by first adding personal data to the crude model (Model 1). It was then tried to add the main implications of the study surrounding by appending temperature and humidity to the personal data (Model 2). The next set of covariates tried to add the implication of commuting to and from the study centre (Model 3). Next, the background concentration of PM at the volunteer's home address was added to the set of covariates, captured by a 5 days average of $PM_{2.5}$ at a public measurement site in the proximity of a volunteer's home address (Model 4). As a last extension, conditions during the withdrawal of bio-samples were integrated by adding the temperature during sample collection (Model 5).

Adjustment sets thus formed the following models:

- Model 0: crude model
- Model 1: + age, BMI, sex
- Model 2: Model 1+ temperature and humidity in the exposure chamber
- Model 3: Model 2+ travel time to the study centre, means of transportation
- Model 4: Model 3+ background $PM_{2.5}$ concentration at the residence address averaged over the last 5 days before a study day
- Model 5: Model 4+ temperature during sample collection

In a second step of the statistical analysis, it was tried to quantify continuous changes of biomarkers, using various metrics of particle exposure in a linear mixed regression model with a random participant intercept. The dependent variable in this analysis was the difference in outcome between timepoints after and before a controlled exposure towards a certain particle metric, without differentiating between different sources of exposure. The independent variable was a two-hours personal particle exposure. Again, a separate analysis for each difference of time point and for different particle size fractions was conducted. The covariates and adjustment sets correspond to the pre analysis.

This approach however did not take different particle sources with specific particle emission patterns into account and was therefore discarded in further analyses.

Instead, in a third step, a new model was developed as a main model. It was supposed to examine the time-dependent influence of personal average exposure to a certain source and its particulate matter of a certain metric. This was accomplished by implementing interaction terms for source of exposure and metrics of exposure. Again, the outcome is a change in biomarker levels, with separate regression analyses for time points t_3-t_0 and t_5-t_0 for IL-8 and t_5-t_0 for CRP

and sICAM. Thus, single pollutant metrics can be assigned to a certain exposure source and their influence on changes of outcome parameters can be quantified. Potential effects are hence directly assigned to chemical and physical compositions of a particle source, transferring the first two steps of analysis into a single third analysis.

The covariates and adjustment sets correspond to the pre analysis.

$$Y_i = \beta_0 + u_i + \beta_E E_i + \beta_S S_i + \beta_{IA} E_i S_i + \sum_{i=1}^{k} \beta_i X_{ki}$$

Y_i = ΔIL-8, ΔCRP, ΔsICAM: change in biomarkers as difference of t3-t0 and / or t5-t0

β_0 : intercept

u_i : random intercept for participant i

β_E : Coefficient of exposure related effect

E_i : Exposure of participant i towards a certain metric of PM [UFP >= 100 nm; < 100 nm; < 50 nm; 30-50 nm; 10-30 nm; < 10 nm; Particle Surface Area; PM_{10}; $PM_{2.5}$; PM_1]

β_S : Coefficient of source related effect

$S_i = \begin{cases} \text{FS} \\ \text{CB} \\ \text{T} \\ \text{RA} \end{cases}$: with sources of person i as factors

β_{IA} : Coefficient of interaction term

$\sum_{i=1}^{k} \beta_i X_{ki}$: Vector of coefficient for independent variables of the adjustment set in person i

Biomarker changes were calculated per fixed increment of a particle metric to be able to compare between sources and source specific effects. For PM_{10}, $PM_{2.5}$, PM_1 an increment of 10 µg/m3, for PNC 10.000 particles/cm³, for PSC 1000 µm²/cm³ was chosen. Changes in biomarkers were also calculated per interquartile range (IQR) to compare the effects of different particle metrics within one source of exposure.
Statistical analyses were performed with *SAS* (SAS/STAT version 9.2, SAS Institute Inc., USA) and *RStudio* (R version 3.4.3, Development Core Team, Austria).

3.11.4 Sensitivity analysis

To test robustness of the data set, the same analyses mentioned above were carried out after adjustment to additional aspects and covariates not considered in the main analysis. Exemplarily, two variables were chosen and the analysis was then rerun and compared to prior findings.

The added covariates for the sensitivity analysis were reported symptoms of a cold in the past few weeks and the amount of $P.M_{2.5}$ at the participants' home address.

In the sensitivity analysis of reported cold, all observations with a close timely relation to a reported cold were excluded. This analysis should test if individual health aspects and subclinical but prolonged signs of infection might play an important role in the amount of measured biomarkers.

The above mentioned adjustment set of Model 4 was later used as the second sensitivity analysis, after it was decided to limit the amount of covariates and use the covariates of Model 2 as main model.

Model 4 took the volunteers $PM_{2.5}$ exposure at the volunteers' home address into account. This was achieved by calculating the 5-days-average of $PM_{2.5}$ levels at a PM measurement site close to the volunteers' residency. Presuming that, including night hours, participants spent at least half of their time at home, this analysis should help to show individual effects of background particle exposure.

4 Results

4.1 Description of the study population

Personal characteristics	**value**
Age [years], mean (SD)	33.0 (17.3)
Male; female, N (%)	20; 21 (49; 51)
Weight [kg], mean (SD)	71.7 (13.3)
Height [cm], mean (SD)	173.4 (9.3)
BMI[kg/m²], mean (SD)	23.7 (3.2)
Underweight (< 18.5 kg/m²), N (%)	1 (2.4)
Normal weight (>18.5, < 25 kg/m²), N (%)	25 (61.0)
Overweight (> 25 kg/m²), N(%)	15 (36.6)
Level of school education, N (%)	
Low	2 (4.9)
Medium	3 (7.3)
High	32 (78)
Missing	4 (9.8)
Born in Germany, N (%)	25 (62.5)
Employed, N (%)	15 (38.5)
Never-Smoker, N (%)	38 (92.7)
Frequency of sporting activity, N (%)	
No sport	13 (31.7)
1x per week	8 (19)
2-3x per week	18 (43.9)
More than 3x per week	1 (2.45)
Missing	1 (2.45)
Allergy diagnosed in the past, N (%)	14 (34.1)
Mold or mold stain present at residence, N (%)	4 (9.8)
Residence with major road within a range of 100 meters, N (%)	18 (43.9)
Traffic in proximity of residence	
Resident traffic, N (%)	26 (63.4)
Commuter traffic, N (%)	3 (7.3)
Transit traffic, N(%)	11 (26.8)
Missing, N (%)	1 (2.4)
Frequent traffic jam in proximity of residence, N (%)	2 (4.9)
Linear distance from residence to testing site [km], mean (SD)	20.9 (11.6)
Driven distance to testing site [km], mean (SD)	28.6 (13.3)
Time of travel to testing site [hours], mean (SD)	1.1 (0.6)
Means of transportation before testing, N (%)	
Car	245 (37.8)
Public transport	356 (54.9)
Missing	50 (7.3)
Mean temperature in exposure chamber [°C], mean (SD)	23.8 (1.1)
Mean humidity in exposure chamber [%], mean (SD)	34.9 (7.8)
$PM_{2.5}$ concentration at residence during last 5 days before exposure at testing site, data from closest monitoring station to residence [µg/m³], mean [SD]	19.0 (9.4)

Table 7: ***Description of study population and exposure-related personal data.*** *SD: Standard deviation, N: Number of participants. Total participants: 41.*

The population of the statistical analysis comprised 41 healthy volunteers, 20 males and 21 females with an average age of 33 years and an average body-mass-index of 23.7. Only two of them were ex-smokers for at least ten years, the rest never-smokers. 32 volunteers reported a general qualification for university entrance as educational level, whereas only 15 reported to be employed, a finding that was due to the many students and some pensioners comprised in the study population. Two thirds of the volunteers reported to do sports at least once a week. The volunteers‘ self-reported living conditions reflected a predominantly urban microenvironment. While 18 out of 41 reported proximity of less than 100 meters to a major road, the majority reported only residential traffic in front of their home address. Four people reported mold or mold stain to be present at their residence. On average, the volunteers had to travel 66 minutes for a mean of 30 kilometres to arrive at the study centre, a distance for which the majority used public transports.

During the exposure, temperature and humidity were controlled within a comfortable range of around 24°C and a relative humidity of 35 % in order to prevent an additional stress response due to meteorological preconditions. Further descriptional figures of anthropometry and population characteristics can be found in table 7.

4.2 Description of exposure

Figures 8 and 9 are supposed to give an overview on the personal exposure during a volunteers' stay in the exposure chamber. All figures therefore represent the mean and standard deviation of the average 2-hour personal particle exposures which volunteers were exposed to during the study. The results are separated by sources of exposure and particle metrics and rounded for better legibility.

All operated particle sources led to a high particle concentration inside the chamber, with values considerably above WHO guideline values for PM_{10} and $PM_{2.5}$. Also, the amount of UFP produced in the exposure chamber exceeded the amount of UFPs in an urban background concentration by far. The range of particle size and mass distribution differed strongly between the particle sources.

Frying sausages (FS) resulted in a high concentration of PM_{10} (224 ± 145 [µg/m³]) and $PM_{2.5}$ (178 ± 108 [µg/m³]) and in a high amount UFP (467 000 ± 169 000 [particles/cm³]). The amount of UFP in contrast to the other sources of exposure however was lowest during FS.

Candle burning (CB) instead led to a comparatively low amount and mass of larger particles like $PM_{2.5}$ (70 ± 20 [µg/m³]) but resulted in an extensive production of UFPs smaller 100 nm (2 330 000 ± 421 000 [particles/cm³]).

Toasting bread (TB) resulted in a distribution of larger particles similar to CB, and also showed high amounts of emitted UFP (1 280 000 ± 348 000 [particles/cm³]).

Within the fraction of UFPs, the exposure sources showed unique patterns of particle distribution. UFP from FS consisted of a large fraction of particles in the range of 50 nm to 30 nm and a very small number of total particles in fractions smaller than 30 nm. TB and CB instead showed a first peak of particle numbers in the range of 100 nm to 50 nm and a second peak in the range of 30 nm to 10 nm size. This effect was clearer for CB than for TB. CB also emitted a notable fraction of particles smaller than 10 nm (361 000 ± 93 000 [particles/cm³]).

Particle surface area was comparable between all sources and ranged from 3070 ± 917 [µm²/cm³] for CB to 2453 ± 1426 [µm²/cm³] for FS.

The sham exposure showed a low concentration of particle pollution with $PM_{2.5}$ values of 4.9± 5.5 [µg/m³] and UFPs smaller 100 nm of 3408 ± 1931 [particles/cm³]. These values represent an exposure well below the range of urban background concentration at the volunteer's residence. A residual particle entry was due to ventilation of filtered outdoor air to ensure oxygen supply inside the chamber and possibly also due to particles transported into the chamber on the volunteer's surfaces.

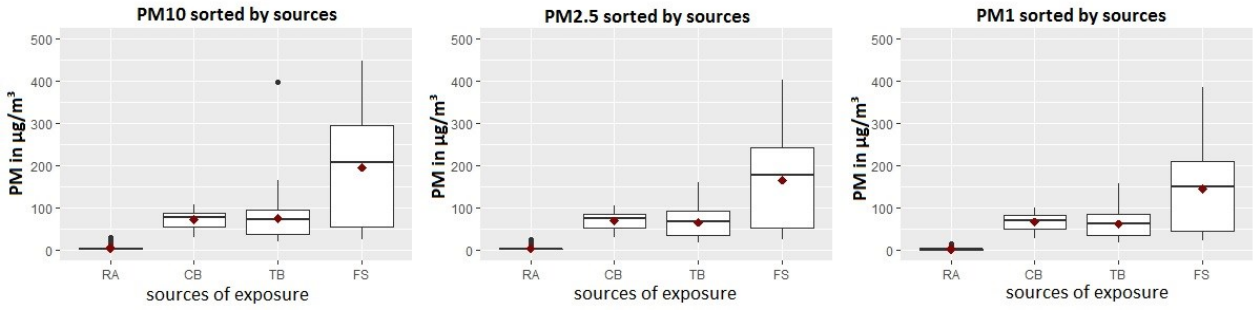

Figure 8 ***Particle Mass (PM) sorted by size of particles and sources of exposure.*** *X-Axis: Source of exposure; RA: Room Air, CB: Candle Burning, TB: Toasting Bread, FS: Frying Sausage. Y-Axis: Particle Mass in µg/m³. Box: upper and lower quartile; Line: Median; Whiskers: lowest and highest value; Red dot: Mean.*

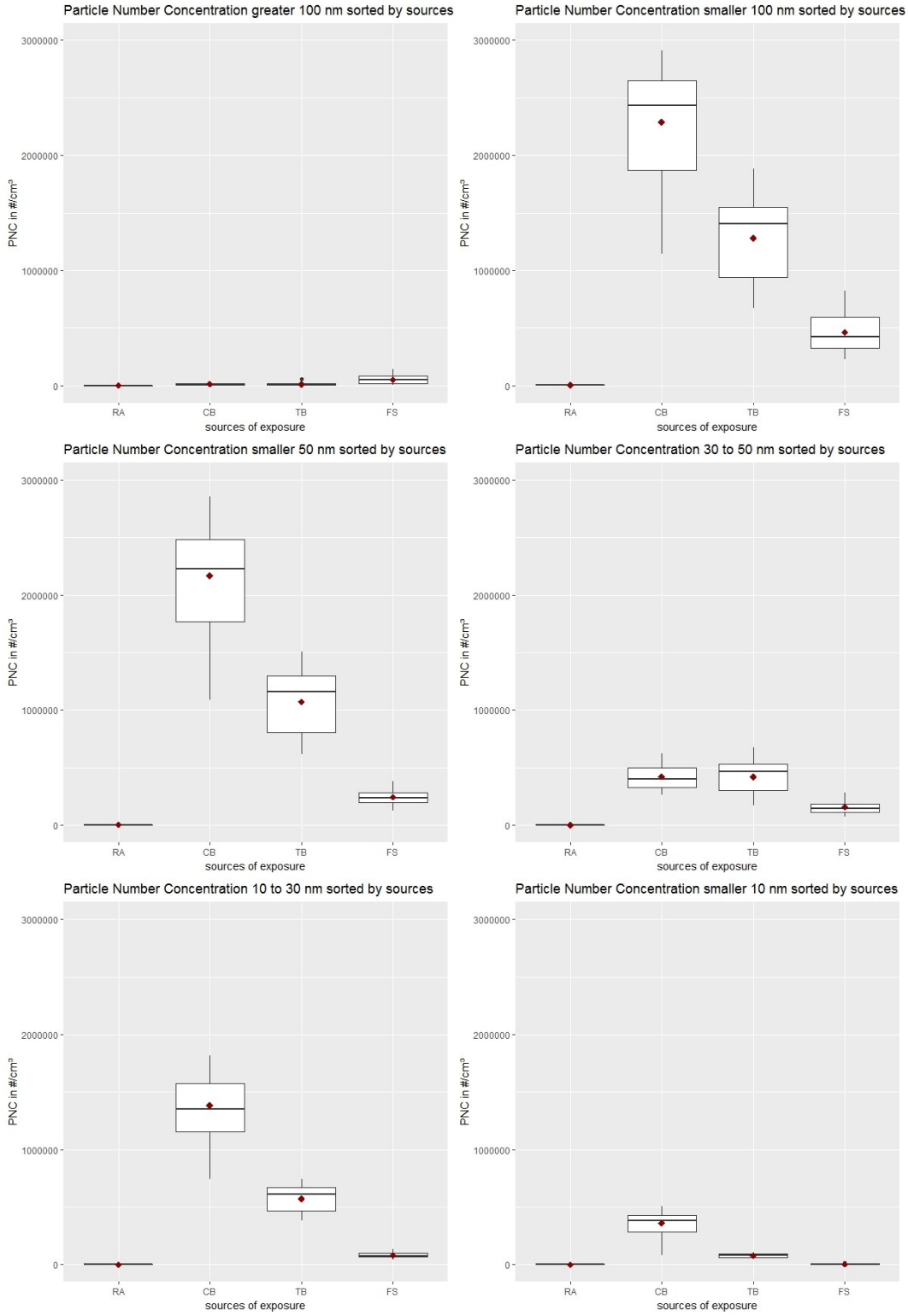

Figure 9: ***Particle number concentration (PNC) sorted by size of particles and sources of exposure.*** *X-Axis: Source of exposure; RA: Room Air, CB: Candle Burning, TB: Toasting Bread, FS: Frying Sausage. Y-Axis: Particle Number Concentration in number/cm³. Box: upper and lower quartile; Line: Median; Whiskers: lowest and highest value; Red dot: Mean.*

Doubling the intensity of true exposure sources as described in chapter 3.5, led to a strong augmentation of particle emission. Generally, it can be said that an intensified exposure towards the particle sources was reflected by all particle metrics. It was most visible within the metrics Particle Surface Area Concentration and Particle Number Concentration, metrics which are predominantly influenced by UFPs, as can be seen in figure 10.

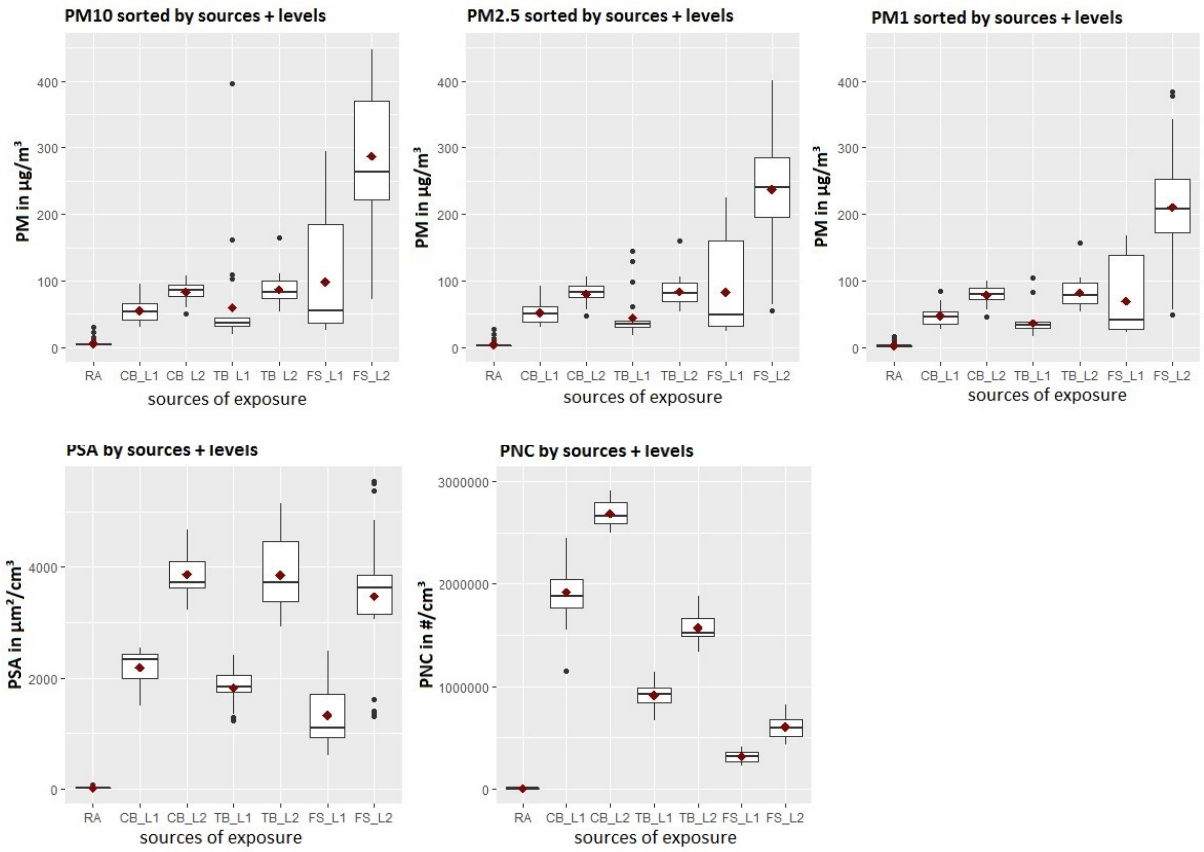

Figure 10: ***Particle metrics sorted by source of exposure and level of intensity.*** *X-Axis: Source of exposure; RA: Room Air, CB: Candle Burning, TB: Toasting Bread, FS: Frying Sausage. L1: Level 1, L2: Level 2.*
Y-Axis: PM: Particle Mass in µg/m³. PSA: Particle Surface Area in µm²/cm³, PNC: Particle Number Concentration in number/cm³, Box: upper and lower quartile; Line: Median; Whiskers: Range between 2,5%- and 97,5%-Quantile; Black dots: Outliers; Red dot: Mean.

4.3 Description of outcomes

According to chapter 3.11.1, biosamples were only chosen for the analysis if certain quality criteria were reached. Furthermore, single observations or entire volunteers were excluded when exclusion criteria were reached. This resulted in varying numbers of observations between outcome variables and time points. Table 8 shows final numbers of observations per source, time point and outcome variable. A total of 1858 observations were included with a focus on IL-

8, contributing 1122 observations to the outcome, 651 from IL-8 in NAL and 471 from IL-8 in blood.

532 observations were made during candle burning on the two levels of intensity (CB L1 and L2), 485 in the during toasting bread (TB L1 and L2), 494 during frying sausage (FS L1 and L2) and 347 during exposure to room air with only one level of intensity (RA).

	Before exposure (t0)				**Post 2 hours (t3)**		**Post 24 hours (t5)**			
Outcome	**IL-8 in NAL**	**IL-8 in**	**CRP**	**sICAM**	**IL-8 in NAL**	**IL-8 in blood**	**IL-8 in NAL**	**IL-8 in blood**	**CRP**	**sICAM**
Room Air	41	30	33	34	41	30	41	30	33	34
Candle Burning Level 1 (CB L1)	29	20	26	26	29	20	29	20	26	26
Candle Burning Level 2 (CB L2)	32	23	29	29	32	23	32	23	29	29
Toasting Bread Level 1 (TB L1)	26	19	19	21	26	19	26	19	19	21
Toasting Bread Level 2 (TB L2)	30	24	26	28	30	24	30	24	26	28
Frying Sausage Level 1 (FS L1)	28	20	22	23	28	20	28	20	22	23
Frying Sausage Level 2 (FS L2)	31	21	24	28	31	21	31	21	24	28
Total observations	217	157	179	189	217	157	217	157	179	189

Table 8: ***Total number of observations.*** *Table sorted per exposure source (RA, CB, TB, FS), level of intensity (L1, L2), time point (t0, t3, t5) and outcome variable (IL-8 in NAL and blood, CRP, sICAM).*

The majority of biological markers were skew-distributed. IL-8 and CRP showed a clear skewness to the right, whereas sICAM was almost normally distributed (see figure 11 and corresponding table 9). IL-8 in nasal lavage and blood samples showed a multimodal distribution because single volunteers showed a continuously high profile of IL-8 in biosamples throughout the whole course of the study or during certain phases of the study. This phenomenon could not generally be traced back to a reported disease, personal characteristics, a history of medical treatment or single events of illness during the study time. The markers are therefore considered as chronically or temporarily elevated for unknown reason in single individuals.

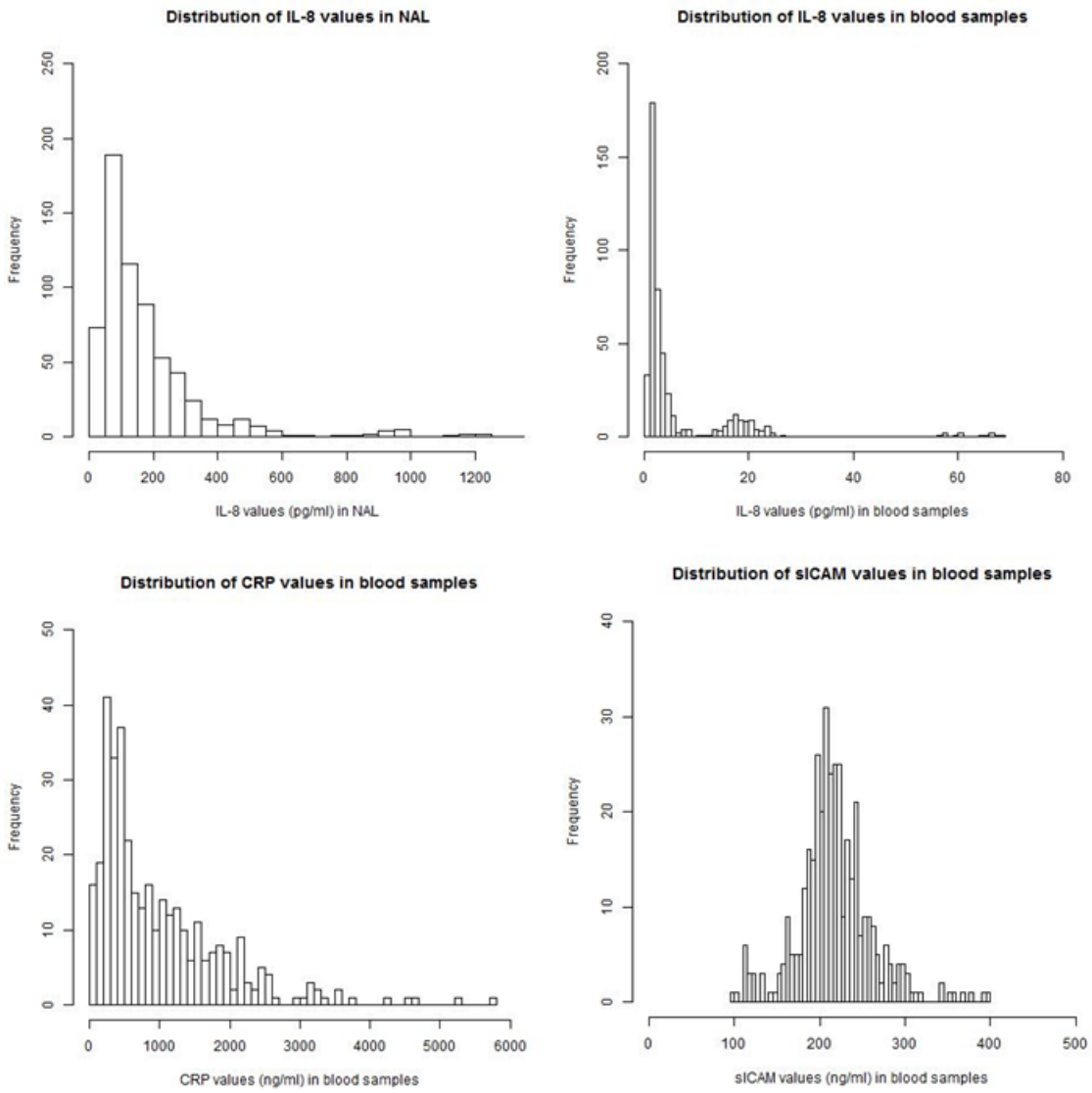

Figure 11: ***Distribution of outcome variables (CRP, sICAM, IL-8 in blood and nasal lavage fluid).*** *Frequency of observations (y-axis) is sorted per total amount of biomarkers (x-axis) in pg/ml for IL-8 and ng/ml for CRP and sICAM .*

	Median	Mean	Standard deviation	Number of observations
IL-8 in NAL (pg/ml)	126.25	181.58	193.34	651
IL-8 in blood (pg/ml)	2.22	6.51	11.03	471
CRP (ng/ml)	659.72	970.75	901.28	471
sICAM (ng/ml)	213.63	216.65	44.78	358

Table 9: ***Distribution and number of outcome variables.*** *Figures are rounded for better legibility.*

A transformation into logarithmus naturalis (ln) led to an approximatively normal distribution. It was however not performed before regression analysis because the outcome variables are calculated from differences of the biological markers. Calculating logarithmic differences would have led to hardly interpretable results if transformed before difference calculation or it would have caused a significant number of dropouts if logarithms would have been calculated from negative differences.

As written in chapter 3.11.3, outcome variables are differences of biological markers between time points. Calculating these differences showed an approximately normal distribution, so the differences entered the regression without further transformation (exemplarily see figure 12).

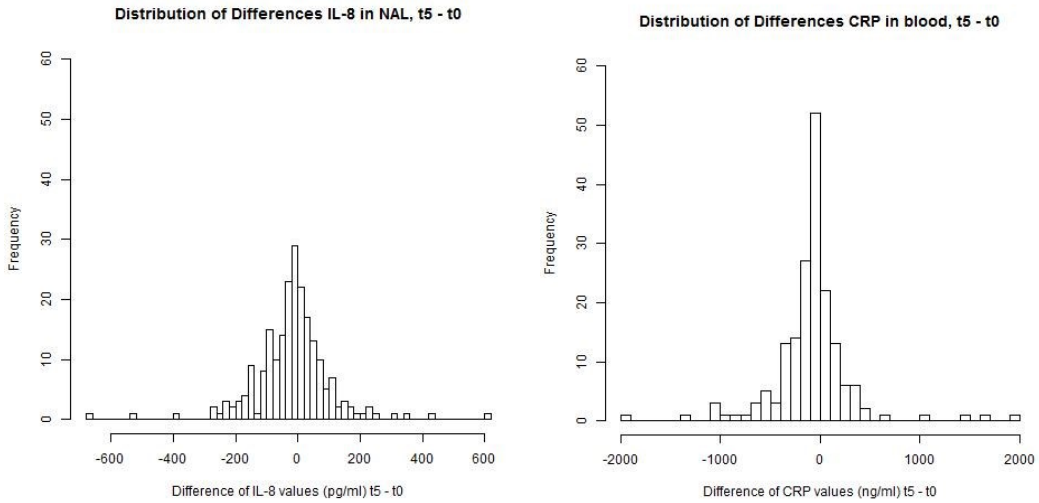

Figure 12: ***Distribution of differences between timepoints t5 (24 hours after exposure) and t0 (before exposure) in IL-8 and CRP content.*** *Frequency of observations (y-axis), difference of post- and preexposure values (x-axis) in pg/ml. The calculated differences are the dependent variables in the regression. They show a normal distribution.*

4.4 Coherence analysis

Splitting the outcome variables by source of exposure and time points of measurement, confirmed a skew distribution for all exposure scenarios with the largest amount of outliers among the IL-8 measurements in blood and nasal lavage. The total amount of biomarker showed only slight signals of change following an exposure and in entirety moved only within very narrow confines. The clearest pattern could be observed with IL-8 in nasal lavage, where the coherence analysis showed a decline comparing the crude biomarker medians at two hours after exposure with the pre exposure values. Interestingly, the sham exposure room air showed the same pattern of decline at two hours after exposure.

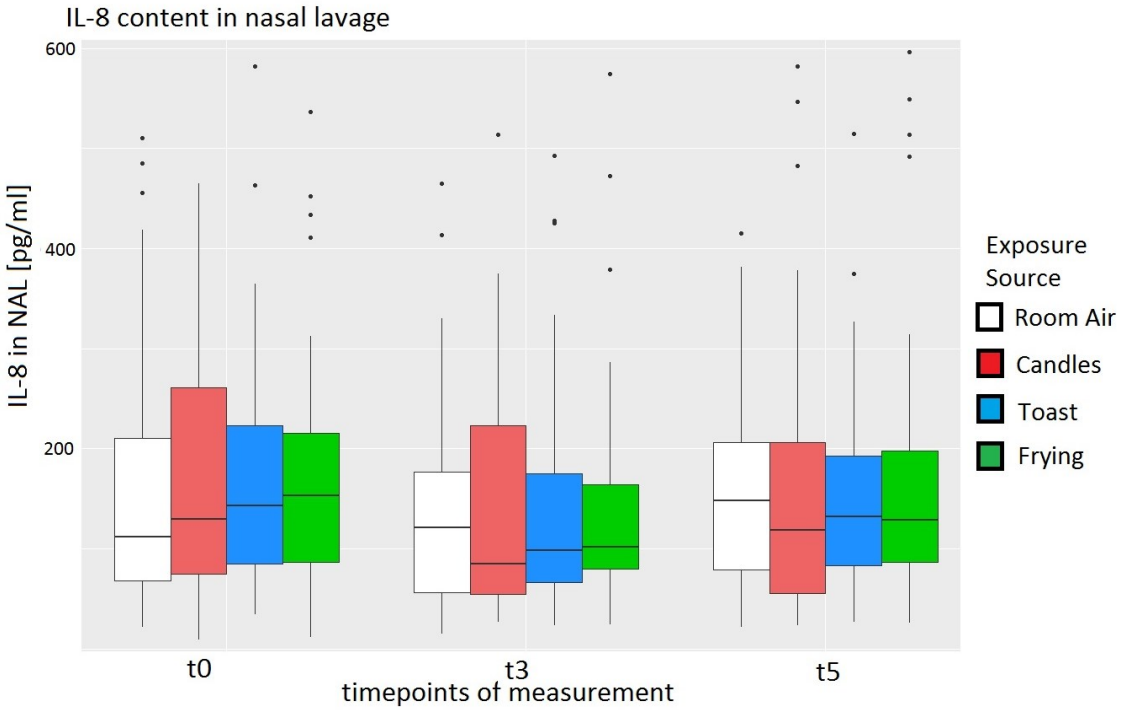

Figure 13*: Crude distribution of IL-8 in NAL.* *Boxplots sorted by time course and by source of exposure. Y-axis: Il-8 content in NAL in pg/ml. Lines in boxplot represent medians. t0: pre exposure, t3: 2 hours post exposure, t5=24 hours post exposure.*

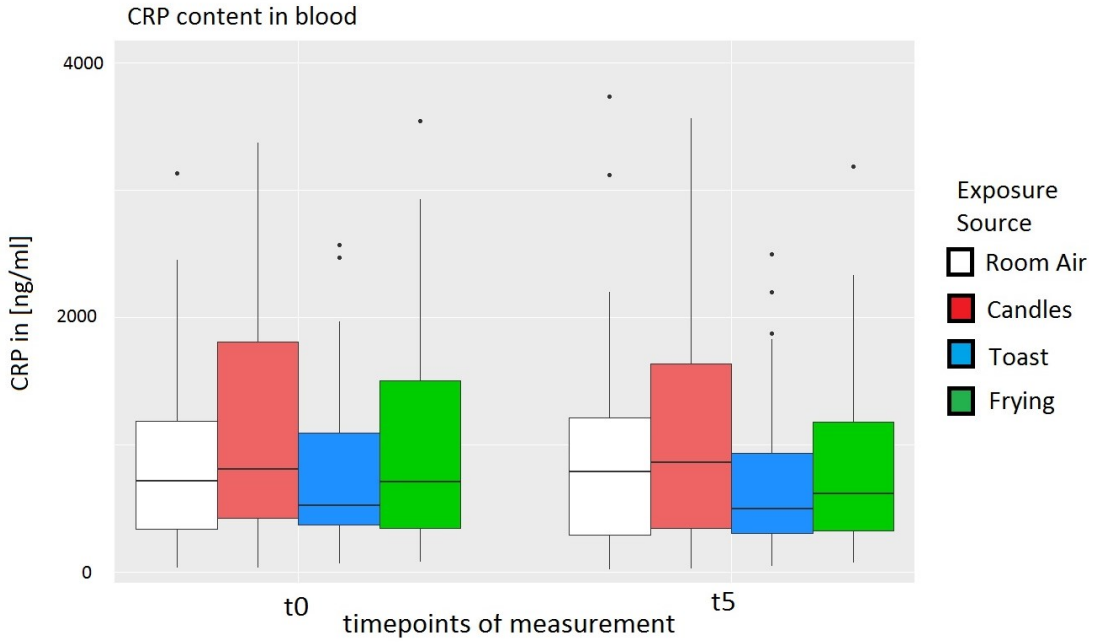

Figure 14: *Crude distribution of CRP.* *Boxplots sorted by time course and by source of exposure. CRP content in blood. Y-axis: CRP content in ng/ml. Lines in boxplot represent medians. t0: pre exposure, t5=24 hours post exposure.*

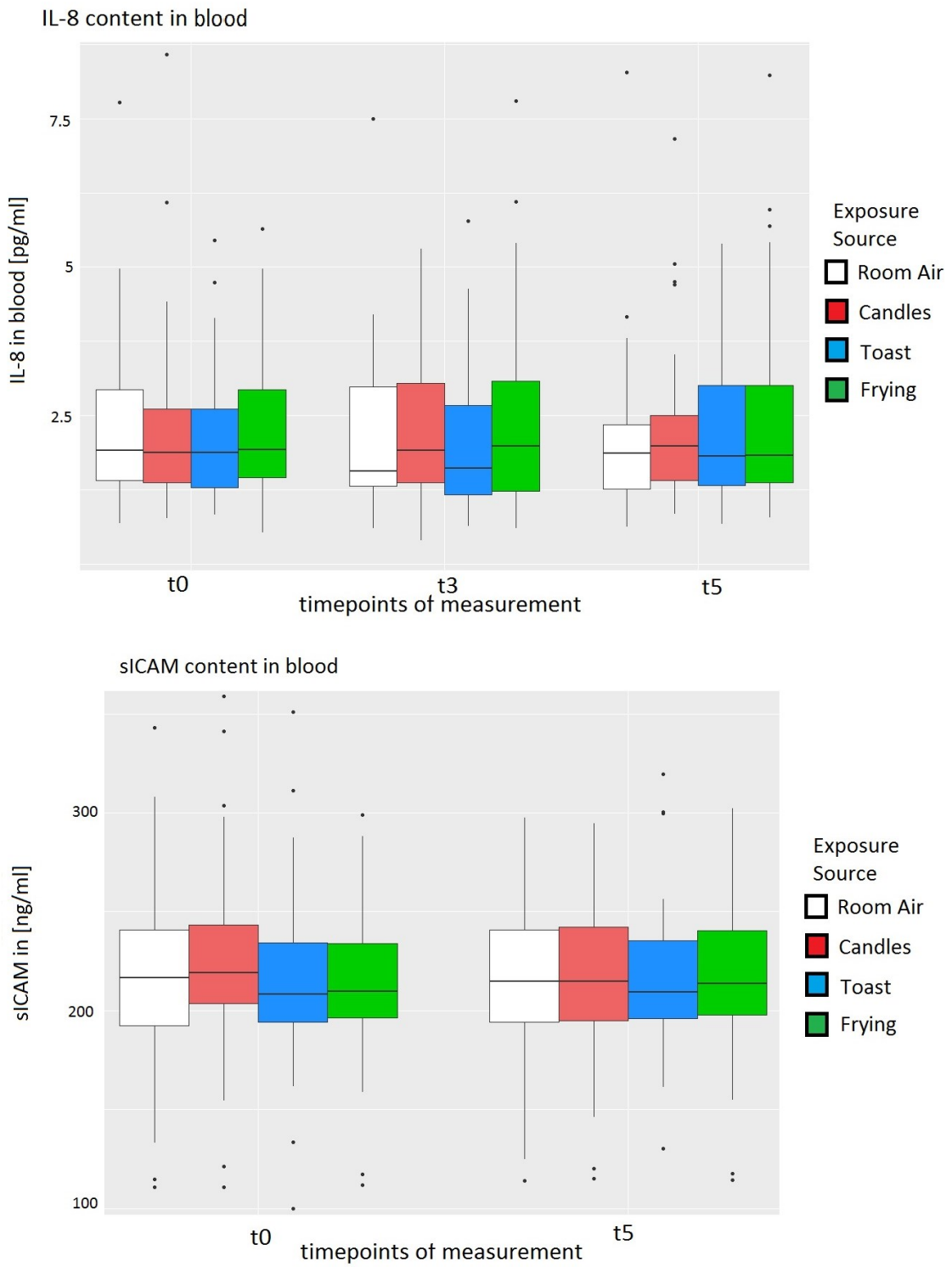

Figure 15 ***Crude distribution of NAL and sICAM in blood.*** *Boxplots sorted by time course and by source of exposure. From top to bottom:IL-8 in blood, sICAM in blood. Y-axis: IL-8 content in pg/ml, sICAM content in ng/ml. Lines in boxplot represent medians. t0: pre exposure, t3: 2 hours post exposure, t5=24 hours post exposure.*

IL-8 in blood, CRP and sICAM changed within a very small range, showing close relation amongst time series measurements. Figure 13-15 show the crude outcome values for each timepoint and exposure source in boxplots, whereas table 10 presents the corresponding means and medians in a tabular overview.

	Before exposure (t0)		**2 hours post exposure (t3)**		**24 hours post exposure (t5)**	
	Mean	**Median**	**Mean**	**Median**	**Mean**	**Median**
IL-8 in NAL (pg/ml)						
Room Air	159.12	111.98	140.50	121.19	159.44	147.87
Candles	229.8	168.78	195.34	93.40	186.66	122.51
Toasting	201.22	147.57	154.31	98.56	200.06	136.32
Frying	191.66	153.48	161.90	106.18	175.81	131.04
IL-8 in blood (pg/ml)						
Room Air	6.41	2.4	6.89	2.15	7.17	2.17
Candles	6.22	2.22	6.16	2.4	6.6	2.16
Toasting	6.62	2.26	6.38	2.11	6.65	2.19
Frying	6.58	2.55	6.64	2.39	6.44	2.14
CRP (ng/ml)						
Room Air	898.41	711.62	Not determined	Not determined	916.23	788.20
Candles	1226.80	806.06			1066.47	858.99
Toasting	910.39	538.61			806.24	498.39
Frying	982.22	705.61			928.15	615.26
sICAM (ng/ml)						
Room Air	218.42	216.72	Not determined	Not determined	219.13	214.64
Candles	225.17	219.16			219.10	214.83
Toasting	214.82	208.35			212.31	208.33
Frying	212.71	209.59			217.68	213.63

Table 10: ***Means and Medians of tested biomarkers, ordered by timepoint of measurement and by source of exposure.***

4.5 Differences between time points of exposure

Before regression analysis, the differences between timepoints t_3 and t_0, and t_5 and t_0 respectively, were calculated for each outcome variable. This calculation should show the crude effect of exposure to particles from the tested indoor sources by subtracting the pre-exposure value from the post-exposure value. Histograms were plotted and statistical descriptions of differences was calculated.

The differences of time point showed a normal distribution, which made them suitable to enter the regression analysis without further transformation. All crude intrapersonal differences (t3-t0 and t5-t0) show negative means and medians, indicating that biosamples from latter timepoints mostly contain a smaller amount of biomarkers than the biosamples taken before the beginning of the exposure. Nevertheless, a large standard deviation indicates a broad spread of results.

Subsetting the crude intrapersonal differences of outcomes by exposure sources (RA, CB, TB, FS) did not alter this pattern, as the majority of differences remained negative. Interestingly, the sham exposure led to positive means of differences for CRP, sICAM and IL-8 in NAL at 24 hours after exposure, as can be seen in table 11.

	Room Air	**Candle Burning**	**Toasting Bread**	**Frying Sausage**
IL-8 in NAL, t3-t0 in [pg/ml]	-18.62 (75)	-34.46 (174)	-46.90 (111.5)	-29.75 (101.7)
IL-8 in NAL, t5-t0 in [pg/ml]	0.32 (110)	-43.14 (156)	-1.16 (121.6)	-15.85 (99.72)
IL-8 in blood, t3-t0 in [pg/ml]	-0.52 (1.72)	-0.06 (1.27)	-0.23 (0.73)	0.07 (0.89)
IL-8 in blood, t5-t0 in [pg/ml]	-0.24 (1.74)	-0.15 (1.49)	-0.04 (1.93)	-0.14 (0.87)
CRP, t5-t0 in [ng/ml]	17.82 (395)	-160.33 (474)	-104.15 (284.2)	-54.08 (384.6)
sICAM, t5-t0 in [ng/ml]	0.72 (15)	-6.07 (25.5)	-2.51 (15.8)	4.97 (24.74)

Table 11*: Mean (standard deviation) of differences between the post-exposure and pre-exposure values of all outcome variables, sorted by source of exposure.*

4.6 Correlations

The exposure variables generally show a strong correlation among the fraction of larger PM metrics and among the fraction of UFP. Correlations between large particles and UFPs smaller than 100nm are weak, as can be seen in table 12.

	PM10	PM2.5	PSA	>100 nm	<100 nm	<50 nm	30-50 nm	10-30 nm	< 10 nm
PM10	1	0.97	0.54	0.94	-0.07	-0.17	0.02	-0.21	-0.20
PM2.5		1	0.63	0.97	-0.01	-0.11	0.10	-0.16	-0.16
PSA			1	0.56	0.70	0.60	0.83	0.53	0.44
>100 nm				1	-0.05	-0.15	0.03	-0.20	-0.18
<100 nm					1	0.99	0.89	0.98	0.92
<50 nm						1	0.84	0.99	0.95
30-50 nm							1	0.78	0.64
10-30 nm								1	0.97
<10 nm									1

Table 12*: Pearson correlation coefficient of independent variables used in further statistical analysis.*

The outcome variables generally show no or weak correlations between each other, tested for spearman correlation coefficient and also tested for Pearson correlation coefficient after logarithmic transformation of the outcome variables. Also, after splitting them up by timepoints t_0, t_3 and t_5 there is no or weak correlation.

Correlation of the covariates used for the following regression analysis was also calculated to prevent problems of collinearity, as can be seen in table 13. Generally, correlations were weak. Also, no correlation was seen between the covariates and the two most important groups of particles, $PM_{2.5}$ and UFP.

	$PM_{2.5}$	UFP	Age	BMI	Temp.	Humidity	Time in Travel	$PM_{2.5}$ at residence	°C at sample collect.
$PM_{2.5}$	1	-0.01	0.01	-0.02	-0.34	0.08	-0.01	0.10	-0.14
UFP		1	0.01	0.01	0.30	0.08	-0.04	0.18	-0.07
Age			1	0.24	0.04	0.05	-0.25	-0.06	0.08
BMI				1	-0.07	0.19	-0.10	-0.12	-0.03
Temp.					1	-0.27	-0.06	-0.02	0.08
Humidity						1	-0.04	-0.49	-0.12
Time in Travel							1	0.19	0.07
$PM_{2.5}$ at residence								1	0.07
°C at sample collect.									1

Table 13*: Pearson correlation coefficient of numeric covariates used in further statistical analysis.*

4.7 Pre analysis - Regression analysis by source of exposure

For the regression analysis with indicator variables for each exposure source, various models with the above mentioned covariates were developed. Adding new covariates and building up models as described in chapter 3.11.3, resulted in a very limited shift of confidence intervals, as can exemplarily be observed for CRP during toasting bread in figure 14. Adding age, BMI and the sex category to the models did not alter results substantially, as can be seen in Model 1. Also, adjusting for temperature and humidity in the exposure chamber did not alter the data set much (Model 2). Adding more covariates did not change estimates and confidence intervals into a significant direction. The data displayed in this paragraph will therefore be limited to the crude model containing only indicator variables for exposure sources and a full model containing age, height, sex, temperature and humidity in the exposure chamber, referred to as Model 2 (compare figure 16). This model was chosen because it contains all important and potentially distorting factors by using a limited and comprehensible amount of covariates.

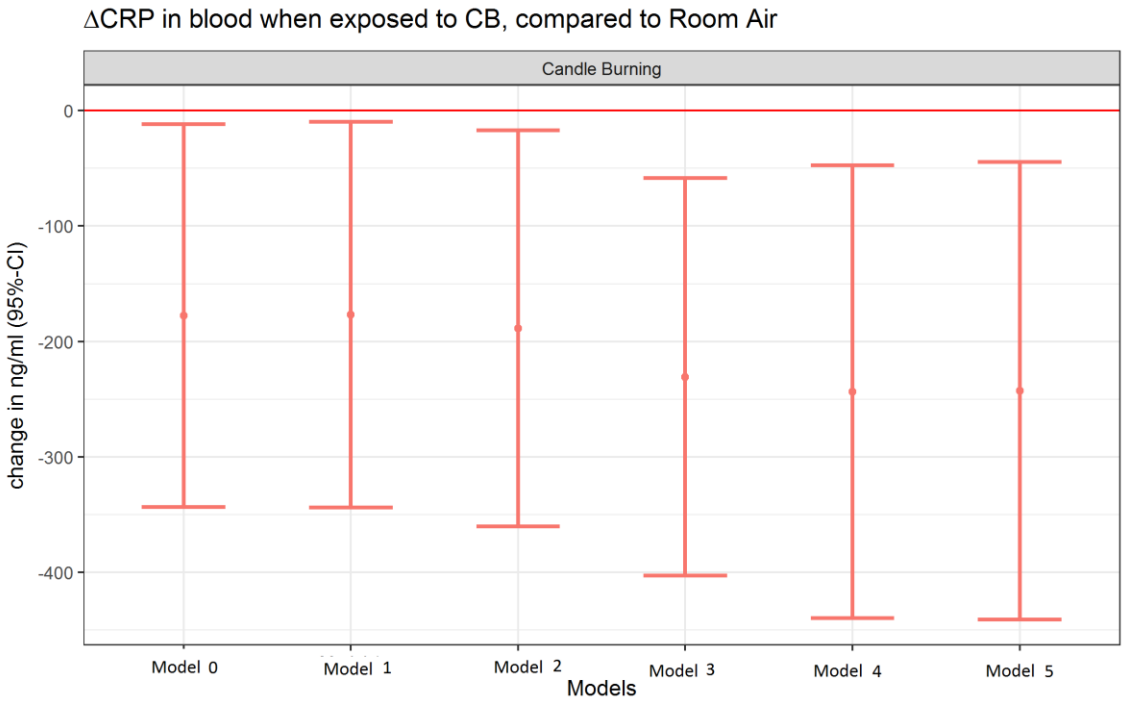

Figure 16*: Estimates of different regression models for CRP level changes in [ng/ml] after exposure to Candle Burning.* *The models correspond to a setup of covariates according to chapter 3.11.3. Y-axis: Difference of post- vs pre-exposure CRP content in ng/ml. Red dot: Estimate; Whiskers: 95%-Confidence Interval. (n=45)*

Compared with room air, a significant decline of CRP after exposure towards CB could be observed at 24 hours after exposure. The effect was calculated as -177.6 ng/ml (95%-CI : -11.6; -343.6) in the crude model (Model 0 in figure 16, n=45) and -181.5 ng/ml (95%-CI: -17.1; -360.1) in the full model (Model 2 in figure 15, n=45). TB led to a decrease in CRP of 183,9

ng/ml (95%-CI: 11.3; -378.9, n=45) in the full model. A similar trend could be seen for frying sausages as a particle source (see figure 17).

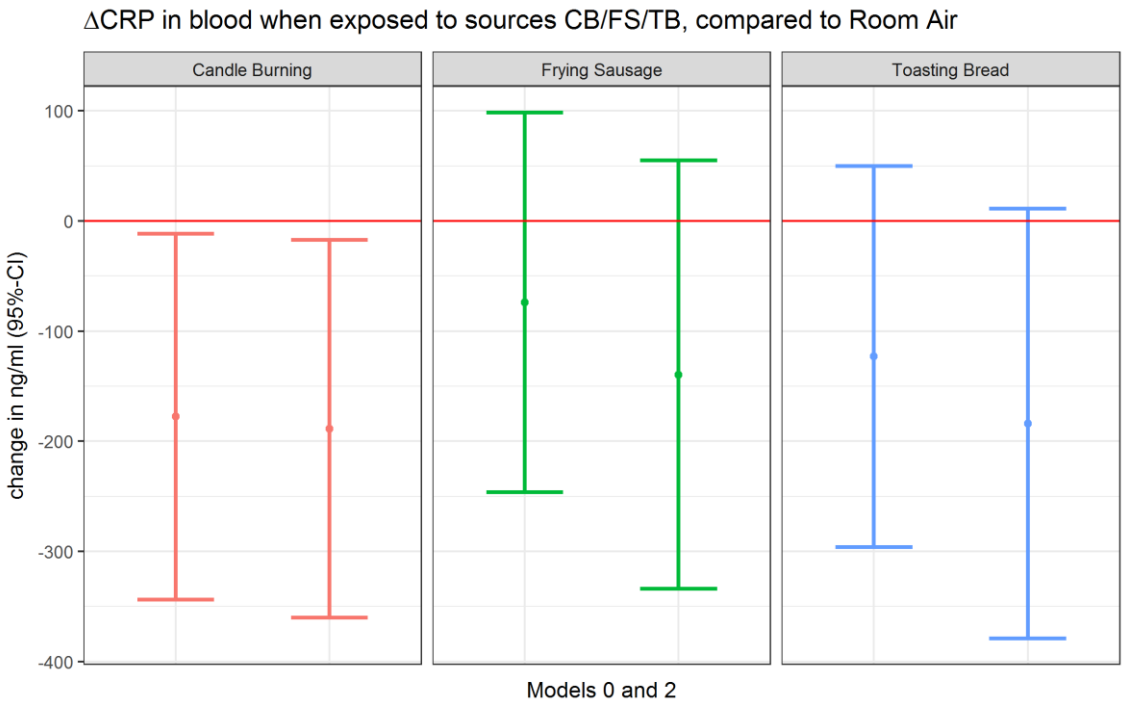

Figure 17*: Change in CRP content in [ng/ml] at 24 hours after exposure.* *A decline is seen for Candle Burning (CB) and Toasting Bread (TB) after adjustment, similar signs are observed for Frying Sausage (FS). Dots: Estimates; Whiskers: 95%-Confidence Interval. (Model 0: n=45, Model 2: n=45)*

IL-8 in blood instead showed an increase in the crude model (Model 0 in figure 18) of 0,59 pg/ml ([95%-CI: 0,08; 1,08]; n=43) and 0.68 pg/ml ([95%-CI: 0,07; 1,29]; n=42) in the full model at 2 hours after exposure to FS, compared with room air. This signal could not be observed a day later, indicating a transient reaction. IL-8 levels showed no difference to the reference exposure room air when measured 24 hours after exposure. The signals for a short-term increase could be observed after exposure to CB and TB, too, whereas confidence intervals were broader, comprising 0. These signals decreased in the time course, too, showing a similar reaction as after exposure towards FS.

IL-8 in nasal lavage and sICAM in blood showed no changes in the crude and in the full model. They were largely uninfluenced by adjustment to different sets of covariates.

The full data set of the pre analysis, comprising estimates and confidence intervals, is displayed in table 14.

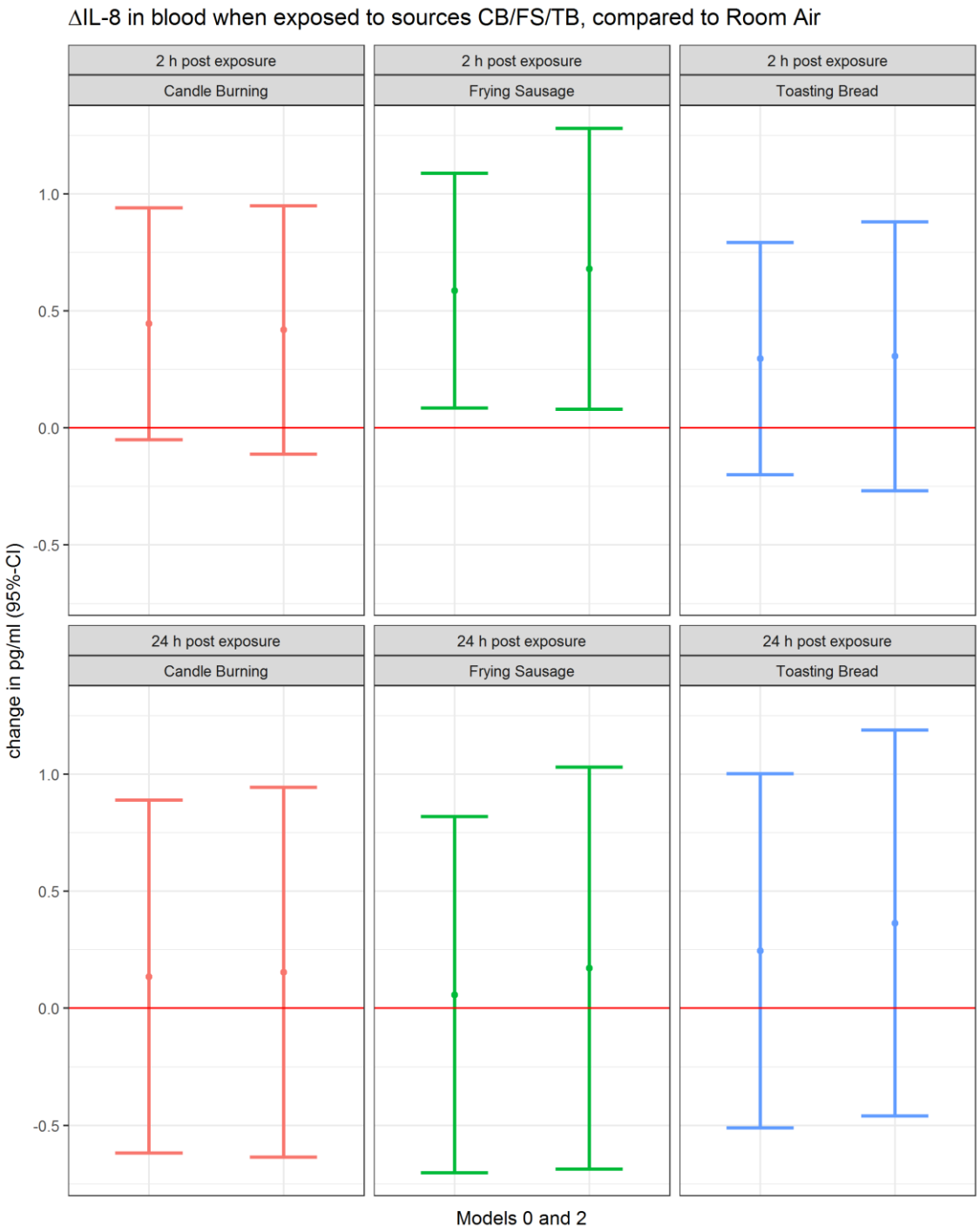

Figure 18*: IL-8 content change in blood in [pg/ml] at 2 and 24 hours post exposure, compared to room air.* *An increase at 2 hours after Frying Sausages (upper row) returns to baseline values at 24 hours after exposure (bottom row). Dots: Estimates; Whiskers: 95%-Confidence Interval.(CB Model 0: n=43, TB Model 0: n=43, FS Model 0: N=41; CB Model 2: n=42, TB Model 2: n=42, FS Model 2: n=41)*

	IL-8 in NAL 2 hours	IL-8 in NAL 24 hours	Il-8 in blood 2 hours	IL-8 in blood 24 hours	CRP 24 hours	sICAM 24 hours
Candle burning	-16.68 (-66.7; 33.4)	-26.5 (-77.8; 24.8)	0.42 (-0.11; 0.95)	0.15 (-0.64; 0.94)	-188.6 (-360; -17.1)	-7.9 (-17.6; 1.76)
Toasting bread	-36.73 (-90.9; 17.42)	10.3 (-44.6; 65.3)	0.31 (-0.27; 0.88)	0.36 (-0.46; 1.19)	-193.9 (-379; 11.3)	-5.69 (-16.3; 4.93)
Frying Sausage	-24.3 (-78; 29.5)	-29.7 (-84.4; 25.1)	0.68 (0.08; 1.28)	0.17 (-0.69; 1.03)	-139.5 (-334; 55)	5.85 (-4.8; 16.5)

Table 14: ***Summary of effect estimates (and 95% confidence intervals) of the analysis by source, compared to sham exposure room air in the full model (model 2).*** *IL-8 in NAL and blood in [pg/ml], CRP and sICAM in [ng/ml]. Figures are rounded.*

4.8 Main analysis – comparison of association of particle fractions between sources of exposure

The analysis in this approach tries to investigate the impact of particle metrics and particle sources on the outcome variables in one step. This way, we could compare between the different particle sources and calculate the effects of a known amount of particles of a certain size. The multiplicity of particle metrics measured in the field phase, leads to 10 possible subclass analyses for each exposure source (PM_{10}, $PM_{2.5}$, PM_1, PSA, PNC >100 nm, <100 nm, <50 nm, 30 – 50 nm, 10 – 30 nm, <10 nm). We could thus calculate increasing levels of biomarkers in concordance to increasing levels of air pollutants. We could better understand the most relevant source of pollutants among the tested sources.

4.8.1 Main analysis – CRP per fix increment of particles

An increment of 10.000 particles/cm³ smaller 100 nm from FS was associated with a CRP increase of 6,95 ng/ml ([95%-CI: 0.46; 13,43]; n=46) in the crude model (Model 0). The effect remained stable after adjusting for personal characteristics (Model 2) which is visualised in figure 19. A similar trend was observed for fix increments in PNC 30 – 50 nm (19,27ng/ml; [95%-CI: 0,04; 38,51]; n=46) in both models and for fix increments of PNC < 50 nm in the adjusted model (16.2 ng/ml; [95%-CI: -0.85; 33,25]; n=46), indicating that the strongest association of augmented CRP levels is seen with UFP from Frying Sausages.

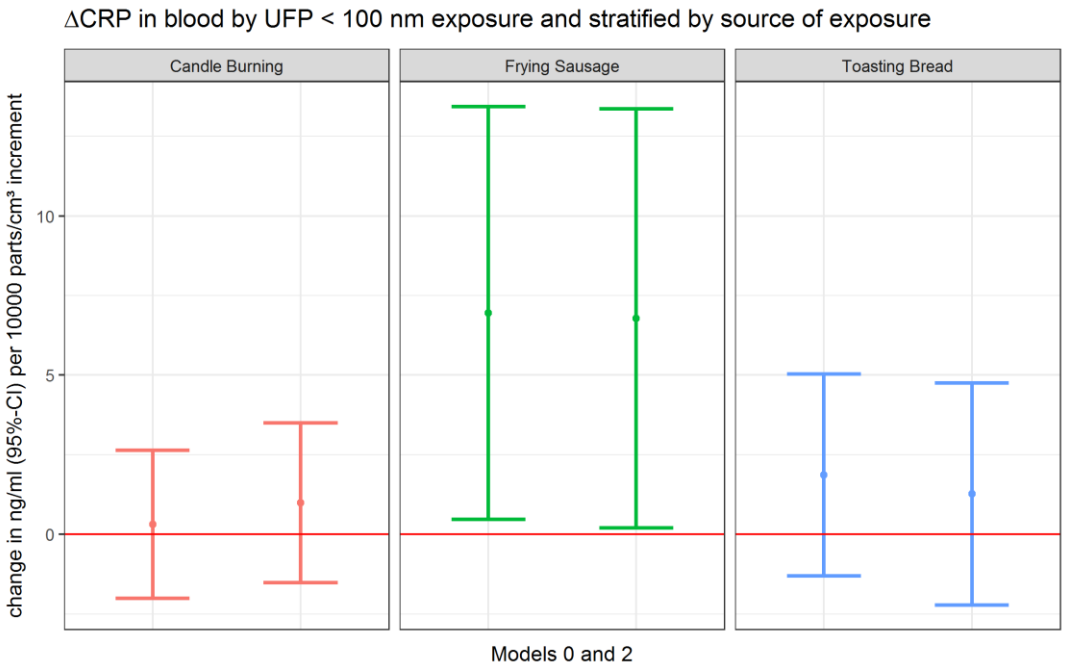

Figure 19: ***Incremental effects of UFP < 100 nm from Candle Burning, Frying Sausage and Toasting Bread (CB, FS, TB) on CRP level in blood.*** *A source dependent effect can be observed. Dots: Estimates; Whiskers: 95%-Confidence Interval. (CB: n=55, FS: n=46, TB: n=45)*

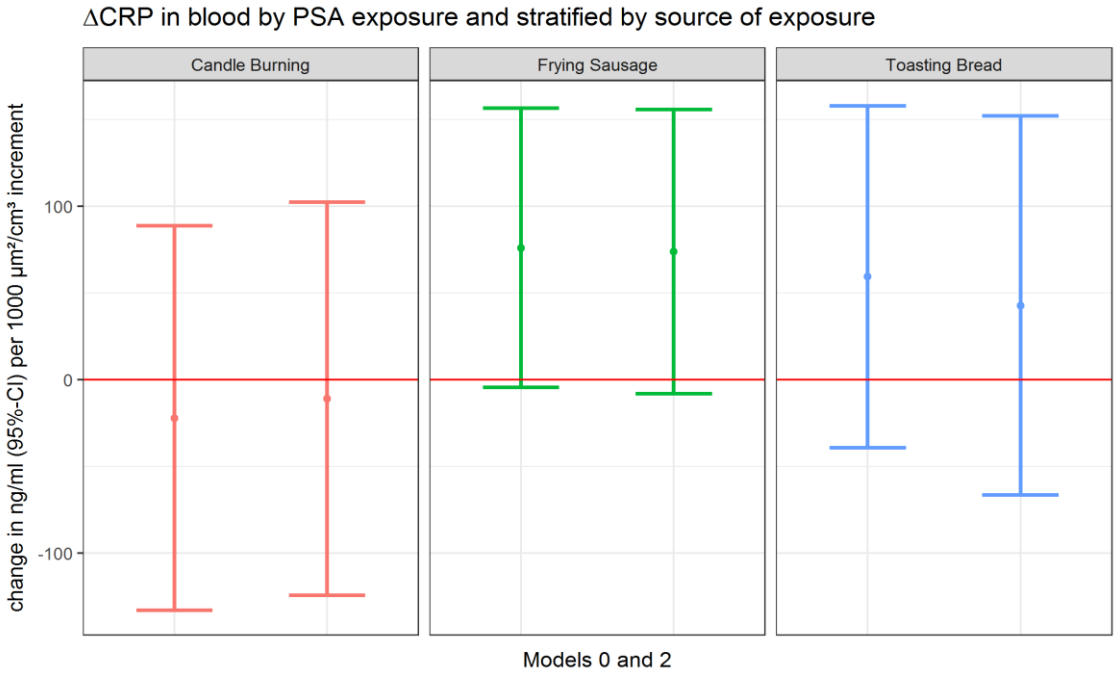

Figure 20: ***Incremental effects of particle surface area (PSA) from Candle Burning, Frying Sausage and Toasting Bread (CB, FS, TB) on CRP level in blood.*** *A source dependent effect can be observed. Dots: Estimates; Whiskers: 95%-Confidence Interval. (CB: n=55, FS: n=46, TB: n=45)*

CRP increments were also associated with the metric of Particle Surface Area (PSA). During FS, PSA increments of 1000 µm²/cm³ were associated with an increase in CRP of 76,07 ng/ml ([95%-CI: -4,45; 156,59]; n=45), as can be seen in figure 20.

Fix increments in PM_{10}, $PM_{2.5}$ and PM_1 from FS showed similar signs of association with CRP content in blood, but with smaller estimates and broader confidence intervals (CRP increase per 10µg/m³ increment of PM2.5 from FS: 8.90 ng/ml [95%-CI: -2.91; 20.71]; Model 0: n=46, Model2: n=44). Fix increments of particle fractions from all other sources showed weak association with CRP levels. Despite a generally positive association, confidence intervals were broad and no clear signal could be observed. We could thus observe that among the tested sources, increasing levels of fine and ultrafine particles from Frying Sausages were associated with a CRP increase at 24 hours after exposure. The full data set of CRP content change per fix increments of particles is shown in table 15.

CRP (per fix increment of particles)	**Candle Burning**	**Frying Sausage**	**Toasting Bread**
PM_{10}	19.69 (-39.59; 78.96)	5.24 (-3.44; 13.92)	6.6 (-15.61; 28.81)
$PM_{2.5}$	20.06 (-40.66; 80.78)	8.05 (-4.01; 20.11)	22.71 (-21.69; 67.11)
PM_1	15.77 (-44.3; 75.9)	9.56 (-3.8; 22.9)	26.4 (-22.67; 75.46)
PSA	-11.0 (-124.5; 102.5)	73.19 (8.0; 155.8)	42.8 (-66.4; 152.1)
UFP >100 nm	42.5 (-105.3; 190.2)	21.9 (-9.1; 53.0)	58.1 (-117.6; 233.7)
UFP <100 nm	0.99 (-1.52; 3.5)	6.78 (0.2; 13.4)	1.27 (-2.22; 4.8)
UFP <50 nm	1.39 (-1.4; 4.22)	16.2 (-0.9; 33.3)	1.65 (-3.2; 6.47)
UFP 30-50 nm	-1.32 (-11.5; 8.84)	19.28 (0.05; 38.5)	3.67 (-5.38; 12.7)
UFP 10-30 nm	3.09 (-1.69; 7.87)	8.51 (-37.96; 54.98)	3.4 (-7.9; 14.72)
UFP <10 nm	8.39 (-3.93; 20.72)	-55.11 (-451.3; 341.1)	24.55 (-54.44; 103.6)

Table 15: Mean effect estimates *(and 95% confidence interval) of CRP in [ng/ml] per fix increment of particles.* *Results at 24 hours after exposure towards three particle sources (Candle Burning, Frying Sausages, Toasting Bread) in the full model. Increment in PM_1, $PM_{2.5}$ and PM_{10} per 10µg/m³; increment in UFP fractions per 10.000 parts/cm³; increment in PSA per 1000µm²/cm³.*

4.8.2 Main analysis - IL-8 in NAL per fix increment of particles

An increment of UFP from CB was associated with incrementing IL-8 levels in NAL, but only two hours after exposure, indicating a transient reaction after UFP exposure. The increase of IL-8 in NAL was visible for CB UFPs > 100 nm in both models (model 0: 46.87 pg/ml; [95%-CI: 3.39; 90.35]; n=61) and for particles < 100 nm in the full model (0.82 pg/ml; [95%-CI: 0.04;

1.52]; n=61). Again, particle surface area showed a strong association with IL-8 content in NAL in both models after exposure towards CB, showing an increase of 48.15 pg/ml ([95%-CI: 14.85; 81.45]; n=61) per 1000 µm²/cm³ in the full model. At 24 hours after exposure, all mentioned effects of CB particle exposure turned non-significant again and showed no difference in effects when compared to the other particle sources, as shown in figure 21.

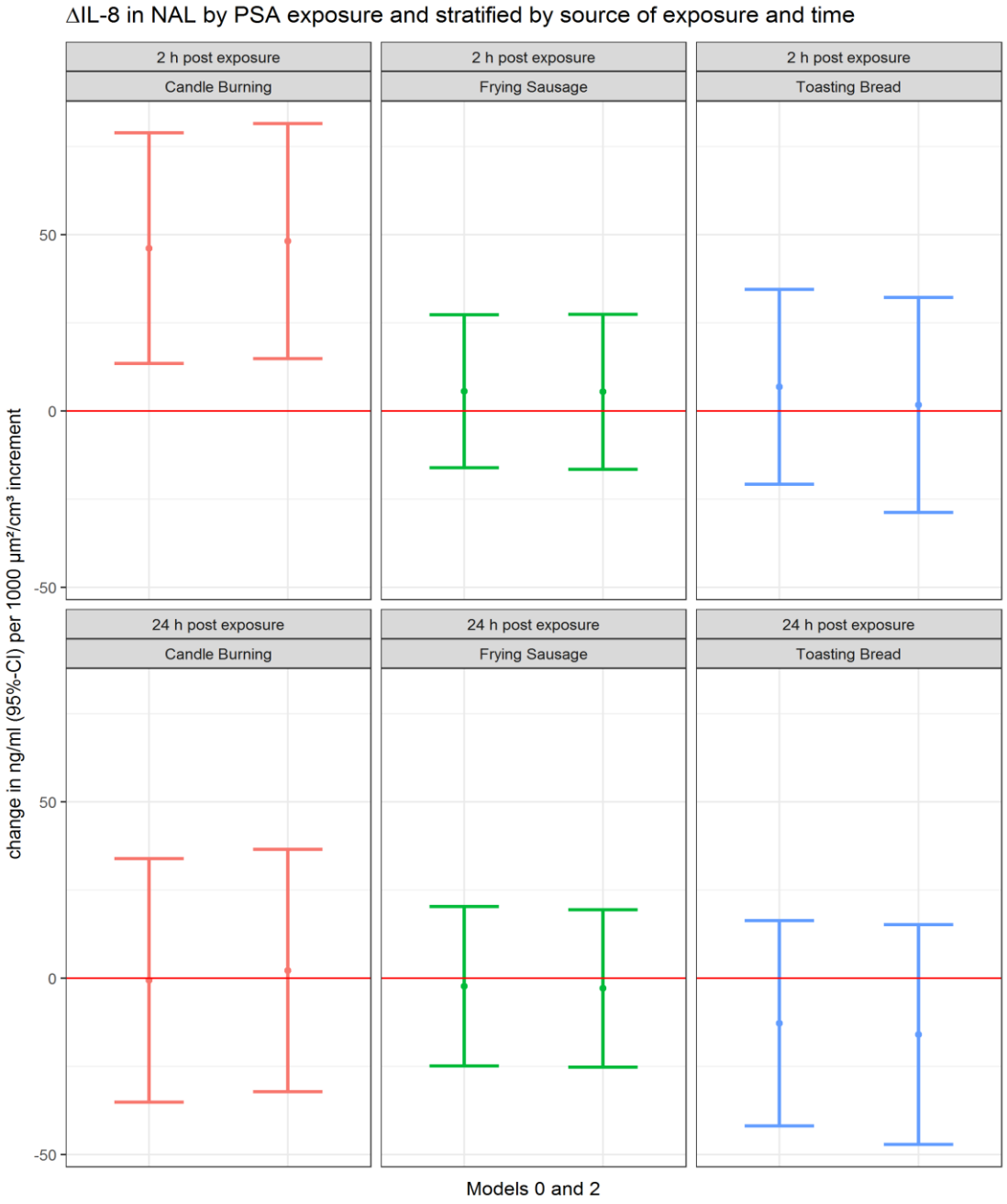

Figure 21: ***Incremental effects of particle surface area (PSA) from Candle Burning, Frying Sausage and Toasting Bread (CB, FS, TB) on IL-8 level in NAL.*** *An increment of 1000 µm²/cm³ (PSA) of particles from Candle Burning (CB) was associated with an IL-8 increase of 48,15 pg/ml (95%-CI: 14,85; 81,45) in NAL. The short-term increase returned to baseline after 24 hours. All other sources show no effects on IL-8 in NAL. Dots: Estimates; Whiskers: 95%-Confidence Interval. (CB Models: n=61, FS Models: n=59, TB Models: n=56)*

For particle fractions from TB, an inverse effect could be observed after increments of the large PM fractions at 24 hours after exposure in the crude (-6.39 pg/ml; [95%-CI: -12.57; -0.21]; n = 56) and the full model (-7.95 pg/ml; [95%-CI: -14.16; -1.74]; n=56). Increments of TB particles in the UFP size range where not associated with IL-8 changes in nasal lavage.

Exposure towards other sources and particle fractions showed no or little association with changes of IL-8 content in NAL. The full data set of IL-8 content change in NAL per fix increments of particles is shown in table 16.

IL-8 in NAL (per fix increment of particles)	**Candle Burning 2 hours**	**Candle Burning 24 hours**	**Frying Sausage 2 hours**	**Frying Sausage 24 hours**	**Toasting Bread 2 hours**	**Toasting Bread 24 hours**
PM_{10}	10.21 (-7.99; 28.41)	-4.29 (-21.73; 13.14)	-0.44 (-2.85; 1.95)	-0.76 (-3.05; 1.54)	-1.17 (-7.77; 5.42)	-7.96 (-14.2; -1.74)
$PM_{2.5}$	10.1 (-8.45; 28.65)	-4.05 (-21.96; 13.85)	-0.41 (-3.65; 2.82)	-0.44 (-3.56; 2.67)	-1.15 (-13.04; 10.73)	-11.5 (-22.81; -0.2)
PM_1	11.22 (-6.87; 29.3)	-1.3 (-19.1; 16.46)	-0.2 (-3.81; 3.41)	0.11 (-3.4; 3.63)	-0.08 (-13.11; 12.95)	-6.75 (-19.4; 5.91)
PSA	48.15 (14.86; 81.45)	2.16 (-32.2; 36.52)	5.44 (-16.55; 27.4)	-2.92 (-25.2; 19.36)	1.71 (-28.77; 32.2)	-16.0 (-47.17; 15.2)
UFP >100 nm	49.95 (5.54; 94.36)	-9.39 (-54.5; 35.73)	0.68 (-7.6; 8.97)	-1.95 (-10.25; 6.35)	6.75 (-29.99; 43.49)	-11.12 (-48.2; 26.0)
UFP <100 nm	0.82 (0.05; 1.6)	0.45 (-0.32; 1.21)	0.73 (-1.14; 2.61)	0.34 (-1.53; 2.21)	-0.1 (-1.13; 0.92)	-0.72 (-1.74; 0.3)
UFP <50 nm	0.82 (-0.05; 1.69)	0.53 (-0.34; 1.39)	1.21 (-3.86; 6.11)	2.85 (-1.97; 7.67)	-0.17 (-1.56; 1.22)	-0.95 (-2.31; 0.42)
UFP 30-50 nm	3.67 (0.67; 6.67)	1.22 (-1.82; 4.27)	2.53 (-2.94; 8.0)	1.65 (-3.86; 7.16)	-0.26 (-2.87; 2.35)	-1.82 (-4.44; 0.8)
UFP 10-30 nm	1.1 (-0.34; 2.55)	0.96 (-0.46; 2.37)	-4.52 (-16.8; 7.8)	8.57 (-3.35; 20.49)	-0.27 (-3.42; 2.89)	-1.77 (-4.86; 1.33)
UFP <10 nm	2.41 (-1.49; 6.31)	0.75 (-3.07; 4.58)	-67.14 (-166.2; 31.8)	48.89 (-47.1; 144.8)	-1.03 (23.46; 21.41)	-14.42 (-36.57; 7.73)

Table 16: ***Mean effect estimates (and 95% confidence interval) of IL-8 in NAL in [pg/ml] per fix increment of particles****. Results from 2 and 24 hours after exposure towards three particle sources (Candle Burning, Frying Sausages, Toasting Bread) in the full model. Increment in PM_1, $PM_{2.5}$ and PM_{10} per 10µg/m³; increment in UFP fractions per 10.000 parts/cm³; increment in PSA per 1000µm²/cm³.*

4.8.3 Main analysis - IL-8 in blood per fix increment of particles

As serum levels of IL-8 turned out to be very low compared to the ELISAs‘ lower detection limit, serum level changes shifted only within very narrow confines when comparing single particle fractions in the regression. With few exceptions there was no clear pattern for an association between IL-8 serum levels and particles of a certain source per size fraction. Only at 24 hours after exposure towards TB particles, an increment in the coarse fraction (PM_{10}) showed a decrease in IL-8 blood levels in both models (model 0: -0.08 pg/ml; [95%-CI: -0.15; -0.01]; n=43). Although a specific and single finding, this is still in concordance with the above mentioned inverse effect after 24 hours, which was observed for IL-8 in NAL after PM_{10}–exposure from TB. Thus, both IL-8 in serum and nasal lavage were lowered in association with a fix increment of PM_{10} from TB. The full data set is shown in table 17.

IL-8 in blood (per fix increment of particles)	Candle Burning 2 hours	Candle Burning 24 hours	Frying Sausage 2 hours	Frying Sausage 24 hours	Toasting Bread 2 hours	Toasting Bread 24 hours
PM_{10}	0.101 (-0.085; 0.287)	-0.006 (-0.259; 0.246)	0.013 (-0.014; 0.04)	-0.008 (-0.042; 0.027)	-0.052 (-0.116; 0.012)	-0.084 (-0.158; -0.009)
$PM_{2.5}$	0.099 (-0.094; 0.293)	-0.005 (-0.27; 0.26)	0.023 (-0.016; 0.063)	-0.026 (-0.077; 0.026)	-0.033 (-0.167; 0.101)	-0.019 (-0.192; 0.154)
PM_1	0.084 (-0.107; 0.276)	-0.025 (-0.286; 0.236)	0.028 (-0.017; 0.073)	-0.032 (-0.091; 0.026)	0.05 (-0.097; 0.198)	0.169 (-0.034; 0.373)
PSA	-0.058 (-0.401; 0.285)	-0.236 (-0.729; 0.257)	0.194 (-0.077; 0.466)	-0.183 (-0.526; 0.159)	0.109 (-0.216; 0.436)	0.371 (-0.077; 0.819)
UFP >100 nm	0.049 (-0.423; 0.522)	-0.125 (-0.794; 0.544)	0.063 (-0.039; 0.165)	-0.057 (-0.187; 0.074)	0.242 (-0.275; 0.759)	0.586 (-0.122; 1.294)
UFP <100 nm	-0.007 (-0.015; 0.001)	-0.006 (-0.019; 0.003)	0.018 (-0.003; 0.04)	-0.012 (-0.042; 0.019)	0.003 (-0.006; 0.013)	0.011 (-0.003; 0.026)
UFP <50 nm	-0.009 (-0.018; 0.001)	-0.009 (-0.02; 0.004)	0.045 (-0.009; 0.099)	-0.013 (-0.089; 0.062)	0.004 (-0.01; 0.018)	0.014 (-0.006; 0.034)
UFP 30-50 nm	-0.006 (-0.036; 0.023)	-0.026 (-0.07; 0.018)	0.055 (-0.008; 0.117)	-0.025 (-0.117; 0.066)	0.003 (-0.023; 0.029)	-0.026 (-0.011; 0.064)
UFP 10-30 nm	-0.018 (-0.03; -0.003)	-0.014 (-0.035; 0.007)	0.034 (-0.109; 0.178)	0.024 (-0.155; 0.203)	0.007 (-0.027; 0.041)	0.025 (-0.022; 0.072)
UFP <10 nm	-0.044 (-0.083; -0.005)	-0.01 (-0.068; 0.037)	0.004 (-1.299; 1.307	0.092 (-1.51; 1.696)	0.033 (-0.197; 0.264)	0.156 (-0.17; 0.483)

Table 17: ***Mean effect estimates (and 95% confidence interval) of IL-8 in blood in [pg/ml] per fix increment of particles.*** *Results at 2 and 24 hours after exposure towards three particle sources (Candle Burning, Frying Sausages, Toasting Bread) in the full model. Increment in PM_1, $PM_{2.5}$ and PM_{10} per 10µg/m³; increment in UFP fractions per 10.000 parts/cm³; increment in PSA per 1000µm²/cm³.*

4.8.4 Main analysis – sICAM per fix increment of particles

Regression analysis did not show an effect of increments in specific particle fractions and particle sources on serum sICAM levels. In general, fix increments resulted in small changes of a few nanograms.

The full data set of sICAM content change in blood per fix increments of particles is shown in table 18.

sICAM (per fix increment of particles)	Candle Burning	Frying Sausage	Toasting Bread
PM_{10}	0.45 (-2.65; 3.55)	0.23 (-0.21; 0.67)	0.44 (-0.71; 1.6)
$PM_{2.5}$	0.31 (-2.88; 3.51)	0.28 (-0.32; 0.89)	0.58 (-1.72; 2.88)
PM_{1}	-0.14 (-3.3; 3.03)	0.36 (-0.31; 1.02)	0.12 (-2.43; 2.68)
PSA	-1.95 (-8.35; 4.45)	1.43 (-2.8; 5.66)	1.06 (-4.87; 6.99)
UFP >100 nm	-2.26 (-10.53; 6.02)	0.82 (-0.77; 2.42)	1.32 (-8.21; 10.87)
UFP <100 nm	-0.07 (-0.21; 0.08)	0.1 (-0.26; 0.46)	0.03 (-0.16; 0.22)
UFP <50 nm	-0.08 (-0.24; 0.08)	0.04 (-0.89; 0.97)	0.05 (-0.21; 0.31)
UFP 30-50 nm	-0.16 (-0.73; 0.4)	0.07 (-0.99; 1.13)	0.06 (-0.43; 0.55)
UFP 10-30 nm	-0.12 (-0.39; 0.14)	-0.2 (-2.6; 2.19)	0.13 (-0.49; 0.74)
UFP <10 nm	-0.39 (-1.07; 0.29)	1.74 (-18.87; 22.35)	1.12 (-3.19; 5.42)

Table 18: ***Mean effect estimates (and 95% confidence interval) of sICAM in [ng/ml] per fix increment of particles.*** *Results at 24 hours after exposure towards three particle sources (Candle Burning, Frying Sausages, Toasting Bread) in the main model. Increment in PM_1, $PM_{2.5}$ and PM_{10} per 10µg/m³; increment in UFP fractions per 10.000 parts/cm³; increment in PSA per 1000µm²/cm³.*

4.9 Main analysis – comparison of association of particle fractions with outcomes within one source of exposure

To directly compare the impact of different particle size fractions on outcome variables within one source of exposure, a change of biomarker per interquartile range (IQR) was calculated. The underlying idea is to detect the particle size amongst the range of particles within one source of exposure, which shows the clearest attributable effects on biomarker changes.

4.9.1 Main analysis – CRP per interquartile range

Associations could be observed during FS, in concordance with the analysis by fix increments. In the full model, the interquartile approach associated particles smaller 100 nm with a CRP increase of 176.5 ng/ml (95%-CI: 1.51; 351.59) per IQR of 285516 particles/cm³ at 24 hours after the exposure to Frying Sausage. Figure 22 shows that particles in the range of 100 to 30 nm and PSA were more strongly associated with a CRP increase than coarse particles or particles < 30 nm**.** The effect for particles larger than 100 nm was by trend less strong and diminished after adjustment to the full model. For CRP and exposure towards CB, TB and RA, the interquartile approach did not reveal effects after adjusting to the full model.

The full data set of CRP content change in blood per IQR of particles is shown in table 19.

Figure 22: ***Mean effect estimates and 95% confidence interval of CRP change at 24 hours after the exposure to Frying Sausage per IQR.*** *Interquartile Ranges: PM_{10}: 248.4 µg/m³; $PM_{2.5}$: 188.7 µg/m³; PM_1: 162.9 µg/m³; PSA: 2575.2 µm²/cm³; UFP > 100 nm: 69486 #/cm³; UFP < 100 nm: 285516 #/cm³; UFP < 50 nm: 86803 #/cm³; UFP 30 - 50 nm: 72840 #/cm³; UFP 10 - 30 nm: 41723 #/cm³; UFP < 10 nm: 3936#/cm³. Dots: Estimates; Whiskers: 95%-Confidence Interval.*

CRP (per IQR)	Candle Burning	Frying Sausage	Toasting Bread
PM_{10}	101.65 (-112.9; 316.2)	111.49 (-97.12; 320.1)	47.3 (-32.8; 127.4)
$PM_{2.5}$	104.82 (-128.3; 337.9)	120.78 (-101.6; 343.2)	76.19 (-86.7; 239.1)
PM_{1}	93.36 (-143; 329.8)	127.7 (-81.74; 337.1)	47 (-125.2; 219.2)
PSA	-5.89 (-176.7; 164.9)	175.4 (-24.02; 374.9)	47.03 (-123.2; 217.2)
UFP >100 nm	33.47 (-162.8; 229.8)	141.19 (-61.76; 344.1)	13.13 (-158.6; 184.2)
UFP <100 nm	-14.9 (-247.1; 217.3)	176.55 (1.51; 351.6)	56.63 (-110.9; 224.2)
UFP <50 nm	-16.58 (-260.5; 227.3)	128.56 (-12.29; 269.4)	63.29 (-114.2; 240.8)
UFP 30-50 nm	-5.29 (-190.4; 179.8)	131.05 (0.15; 261.96)	51.1 (-103.2; 205.4)
UFP 10-30 nm	-12.49 (-249.1; 224.1)	25.89 (-168.3; 220.1)	59.29 (-110.9; 229.5)
UFP <10 nm	-38.57 (-293.4; 216.1)	-1.73 (-158.8; 155.3)	84.36 (-90; 258.7)

Table 19: ***Mean effect estimates (and 95% confidence interval) of CRP change in [ng/ml] per IQR.*** *Change at 24 hours after the exposure to Candle Burning, Frying Sausage and Toasting Bread per IQR of particle fraction. The data displayed corresponds to the full model (model 2).*

4.9.2 Main analysis – IL-8 in NAL per interquartile range

The same dependency of the effect on source and metrics could be observed for IL-8 in NAL. During CB, a short- and long-term association could be discovered for metrics reflecting particles of the UFP spectrum. An IQR of 1387.8 $\mu m^2/cm^3$ in PSA was associated with an IL-8 increase of 51.64 pg/ml (95%-CI: -1.73; 105.01) in the full model at 2 hours after exposure. At 24 hours after the exposure to CB, there was an association with particles smaller than 100 nm, most visible in the fraction of particles from 10 to 30 nm. Herein, an IQR of 400571 particles/cm^3 was associated with an increase of 71.21 pg/ml (95%-CI: 1.48; 140.94) of IL-8 in NAL fluid (see figure 23). Coarse particles instead could not reveal similar associations with IL-8 content in NAL fluid.

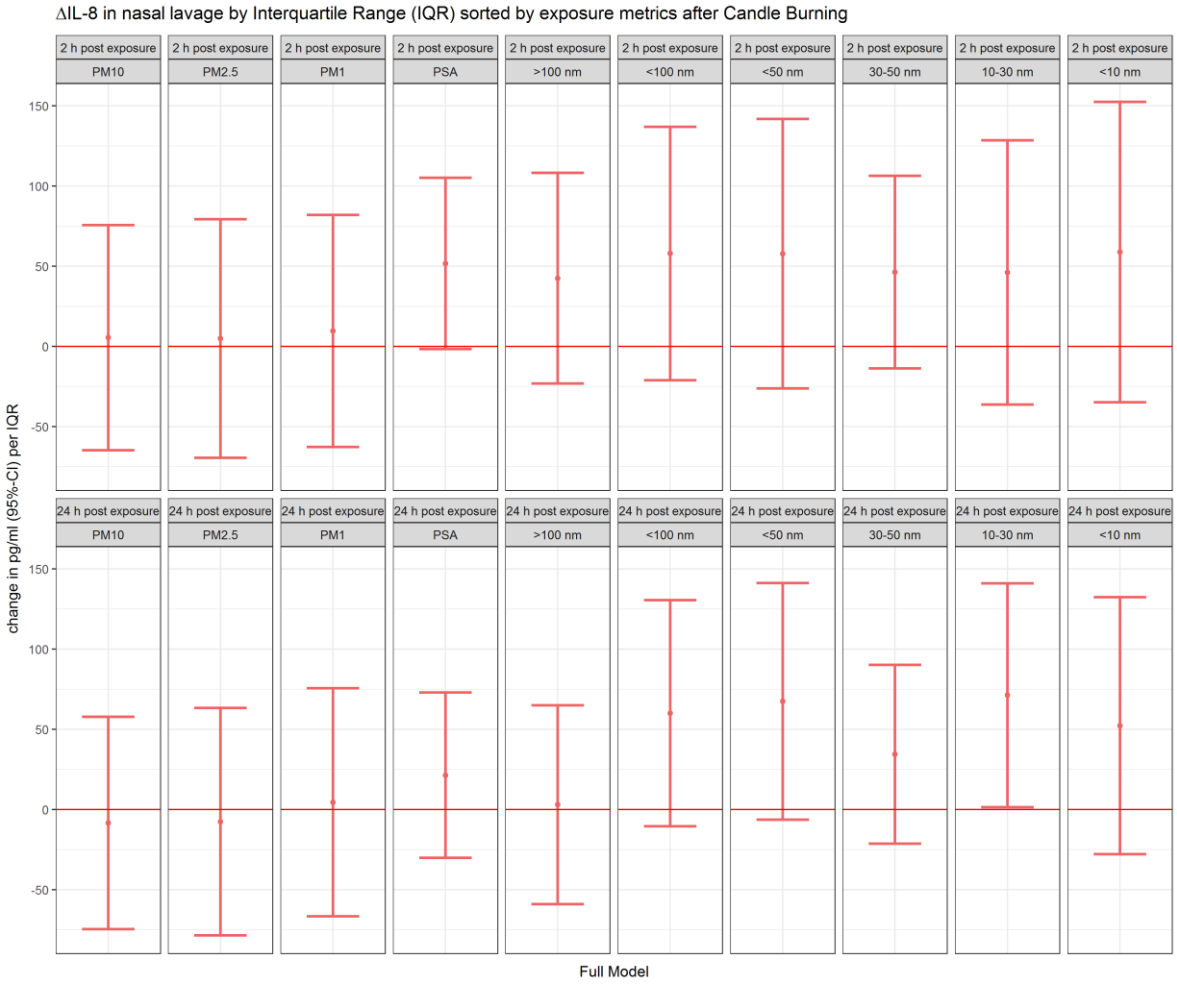

Figure 23: ***Mean effect estimates and 95% confidence interval of IL-8 change in nasal lavage fluid at 2 hours and at 24 hours after exposure to Candle Burning per IQR.*** *Interquartile Ranges: PM10: 31.1 µg/m³; PM2.5: 32.8 µg/m³; PM1: 33.8 µg/m³; PSA: 1387.8 µm²/cm³; UFP > 100 nm: 12199 #/cm³; UFP < 100 nm: 793090 #/cm³; UFP < 50 nm: 716597 #/cm³; UFP 30 - 50 nm: 169006 #/cm³; UFP 10 - 30 nm: 400572 #/cm³; UFP < 10 nm: 145582 #/cm³. Dots: Estimates; Whiskers: 95%-Confidence Interval.*

Similar associations could be discovered for exposure towards FS, as particles smaller than 50 nm were associated with an increased IL-8 in NAL by 33.08 pg/ml (95%-CI: -0.69; 66.86) at 24 hours after exposure (per IQR of 86803 particles/cm³). Larger particles in contrast were not associated with IL-8 changes, suggesting that the strongest association with biomarker changes is seen with particles of the ultrafine size range. This pattern is reflected in figure 24.

The full data set of IL-8 content change in NAL per IQR of particles is shown in table 20.

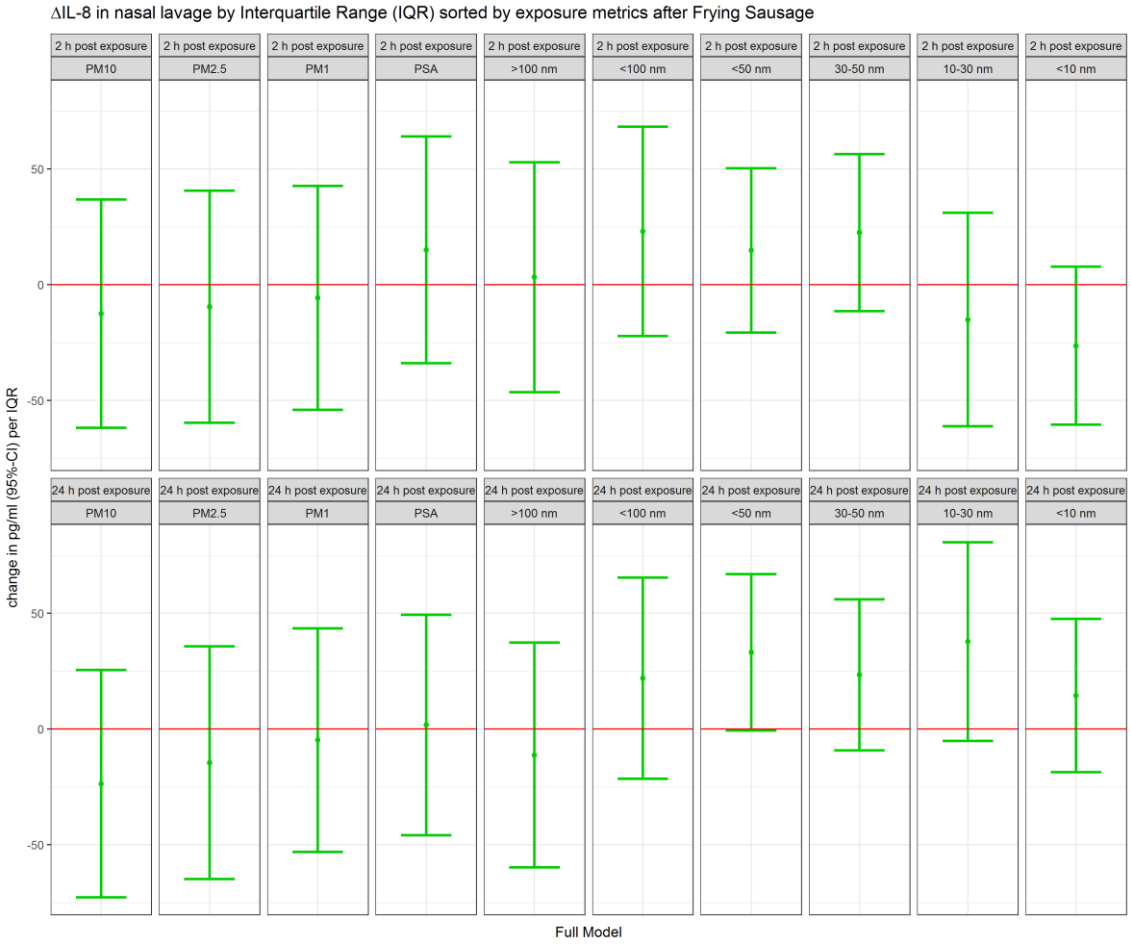

Figure 24: ***Mean effect estimates and 95% confidence interval of IL-8 change in nasal lavage fluid at 2 hours and at 24 hours after exposure to Frying Sausage per IQR.*** *Interquartile Ranges: PM_{10}: 248.6 µg/m³; $PM_{2.5}$: 188.7 µg/m³; PM_1: 162.7 µg/m³; PSA: 2575.2 µm²/cm³; UFP > 100 nm: 69485.9 #/cm³; UFP < 100 nm: 285515.5 #/cm³; UFP < 50 nm: 86803.2 #/cm³; UFP 30-50 nm: 72840.5 #/cm³; UFP 10-30 nm: 41722.9 #/cm³; UFP < 10 nm: 3935.6 #/cm³. Dots: Estimates; Whiskers: 95%-Confidence Interval.*

IL-8 in NAL (per IQR)	Candle Burning 2 hours	Candle Burning 24 hours	Frying Sausage 2 hours	Frying Sausage 24 hours	Toasting Bread 2 hours	Toasting Bread 24 hours
PM 10	5.42 (-64.75; 75.6)	-8.26 (-74.6; 57.8)	-12.55 (-61.83; 36.73)	-23.6 (-72.7; 25.5)	-5.86 (-35.3; 23.6)	-33.68 (-68.8; 1.4)
PM2.5	4.85 (-69.46; 79.15)	-7.58 (-78.5; 63.35)	-9.52 (-59.67; 40.6)	-14.55 (-64.8; 35.6)	-4.2 (-60.6; 52.2)	-36.15 (-100.4; 28.1)
PM1	9.56 (-62.7; 81.8)	4.49 (-66.7; 75.64)	-5.69 (-54.02; 42.6)	-4.74 (-53.02; 43.5)	2.43 (-59.0; 63.9)	-7.9 (-76.5; 60.7)
PSA	51.64 (-1.73; 105.01)	21.35 (-30.2; 72.9)	14.99 (-33.97; 63.96)	1.77 (-45.8; 49.34)	-8.75 (-73.9; 56.4)	-5.84 (-78.5; 66.9)
UFP >100 nm	42.4 (-23.26; 108.1)	3.02 (-58.97; 65.0)	3.26 (-46.4; 52.9)	-11.19 (-59.7; 37.3)	6.99 (-38.03; 52.0)	-4.27 (-55.5; 46.96)
UFP <100 nm	57.87 (-21.1; 136.82)	60.02 (-10.5; 130.5)	23.06 (-22.16; 68.3)	21.94 (-21.5; 65.4)	-10.46 (-78.5; 57.6)	-6.98 (-82.27; 68.3)
UFP <50 nm	57.75 (-26.3; 141.8)	67.4 (-6.27; 141.1)	14.79 (-20.66; 50.25)	33.08 (-0.7; 66.9)	-12.29 (-82.06; 57.5)	-6.77 (-84.5; 70.9)
UFP 30-50 nm	46.26 (-13.8; 106.35)	34.34 (-21.4; 90.04)	22.53 (-11.4; 56.5)	23.41 (-9.2; 55.99)	-16.23 (-77.6; 45.2)	-7.08 (-75.3; 61.2)
UFP 10-30 nm	45.95 (-36.42; 128.3)	71.21 (1.48; 140.9)	-15.08 (-61.2; 31.04)	37.79 (-5.16; 80.73)	-6.58 (-71.2; 58.1)	-4.55 (-77.1; 68.0)
UFP <10 nm	47.73 (-34.8; 152.3)	52.24 (-27.9; 132.4)	-26.37 (-60.4; 7.7)	14.44 (-18.7; 47.5)	3.28 (-63.8; 70.4)	-7.07 (-82.1; 67.95)

Table 20: ***Mean effect estimates (and 95% confidence interval) of IL-8 in NAL in [pg/ml] per IQR.*** *Change at 2 and at 24 hours after the exposure to Candle Burning, Frying Sausage and Toasting Bread per IQR of particle fraction. The data displayed corresponds to the full model (model 2).*

4.9.3 Main analysis – IL-8 in blood per interquartile range

A transient effect at 2 hours after exposure towards UFP FS particles was seen in the interquartile range approach. Estimates showed an increase of IL-8 in serum (0.36 pg/ml; [95%-CI: 0.02; 0.69]; n=41) per increase of 86803 particles/cm³ smaller than 50 nm.

After exposure towards CB particles, a consistent sign of decrease of IL-8 in blood could be observed in the IQR approach. Again, the effect seemed to be primarily driven by UFP in the range of 100 – 10 nm. And although marginal by total amount of biomarker change, the effect remained stable after 24 hours for this particle fraction (see figure 25).

The full data set of IL-8 content change in blood per IQR of particles is shown in table 21.

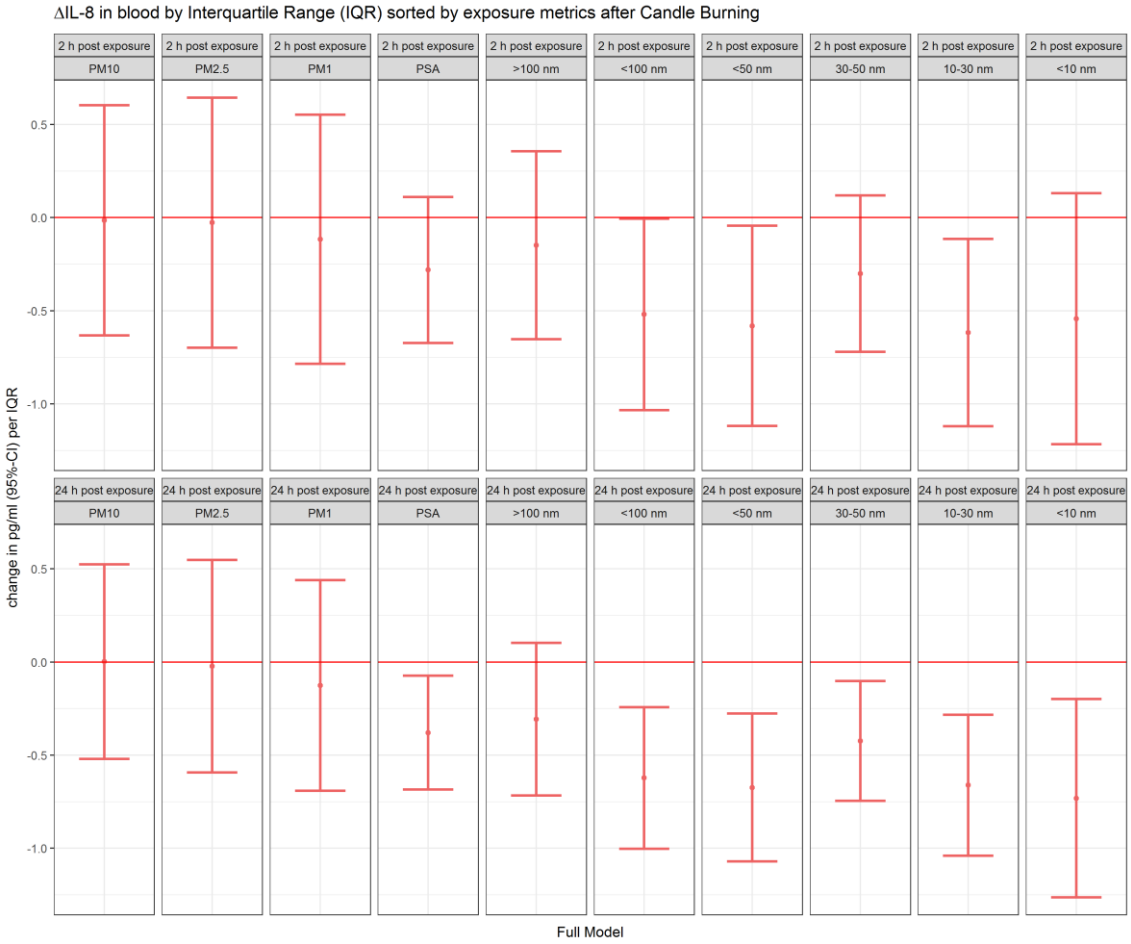

Figure 25: ***Mean effect estimates and 95% confidence interval of IL-8 change in blood at 2 hours and at 24 hours after exposure to Candle Burning per IQR.*** *Interquartile Ranges: PM_{10}: 31.1 µg/m³; $PM_{2.5}$: 32.8 µg/m³; PM_1: 33.8 µg/m³; PSA: 1387.8 µm²/cm³; UFP > 100 nm: 12199 #/cm³; UFP < 100 nm: 793090 #/cm³; UFP < 50 nm: 716597 #/cm³; UFP 30 - 50 nm: 169006 #/cm³; UFP 10 - 30 nm: 400572 #/cm³; UFP < 10 nm: 145582 #/cm³. Red dots: Estimates; Whiskers: 95%-Confidence Interval.*

IL-8 in blood (per IQR)	Candle Burning 2 hours	Candle Burning 24 hours	Frying Sausage 2 hours	Frying Sausage 24 hours	Toasting Bread 2 hours	Toasting Bread 24 hours
PM_{10}	-0.02 (-0.63; 0.6)	0.002 (-0.52; 0.52)	0.258 (-0.25; 0.77)	-0.008 (-0.49; 0.47)	-0.107 (-0.23; 0.02)	-0.261 (-0.87; 0.35)
$PM_{2.5}$	-0.03 (-0.69; 0.64)	-0.022 (-0.59; 0.55)	0.343 (-0.22; 0.91)	0.028 (-0.51; 0.56)	-0.127 (-0.42; 0.16)	-0.107 (-1.41; 1.19)
PM_{1}	-0.116 (-0.78; 0.55)	-0.126 (-0.69; 0.44)	0.338 (-0.21; 0.89)	0.044 (-0.47; 0.56)	0.108 (-0.28; 0.49)	0.399 (-0.90; 1.7)
PSA	-0.281 (-0.67; 0.11)	-0.379 (-0.68; -0.07)	0.364 (-0.17; 0.9)	-0.083 (-0.59; 0.43)	0.092 (-0.32; 0.51)	0.275 (-0.87; 1.42)
UFP >100 nm	-0.148 (-0.65; 0.356)	-0.307 (-0.72; 0.103)	0.289 (-0.26; 0.84)	-0.017 (-0.53; 0.49)	0.064 (-0.33; 0.46)	0.456 (-0.83; 1.74)
UFP <100 nm	-0.519 (-1.03; -0.005)	-0.62 (-1.002; -0.24)	0.403 (-0.06; 0.86)	-0.028 (-0.46; 0.41)	0.043 (-0.39; 0.48)	0.209 (-0.9; 1.32)
UFP <50 nm	-0.581 (-1.12; -0.04)	-0.67 (-1.07; -0.28)	0.363 (0.03; 0.7)	0.058 (-0.27; 0.38)	0.033 (-0.44; 0.5)	0.167 (-1.0; 1.34)
UFP 30-50 nm	-0.3 (-0.72; 0.12)	-0.42 (-0.75; -0.1)	0.32 (-0.02; 0.66)	-0.006 (-0.33; 0.32)	0.039 (-0.36; 0.43)	0.223 (-0.81; 1.26)
UFP 10-30 nm	-0.617 (-1.12; -0.11)	-0.66 (-1.04; -0.28)	0.382 (-0.11; 0.87)	0.271 (-0.19; 0.73)	0.011 (-0.45; 0.47)	0.075 (-1.04; 1.19)
UFP <10 nm	-0.542 (-1.22; 0.13)	-0.731 (-1.26; -0.2)	0.069 (-0.35; 0.49)	0.119 (-0.28; 0.52)	0.062 (-0.41; 0.53)	0.097 (-1.02; 1.21)

Table 21: ***Mean effect estimates and 95% confidence interval of IL-8 in blood in [pg/ml] per IQR.*** ***C****hange at 2 and at 24 hours after the exposure to Candle Burning, Frying Sausage and Toasting Bread per IQR of particle fraction. The data displayed corresponds to the full model (model 2).*

4.9.4 Main analysis – sICAM per interquartile range

As according to the previous findings during sICAM analysis, the IQR approach did not reveal patterns attributable to a certain particle metric (see corresponding table 22).

sICAM (per IQR)	Candle Burning	Frying Sausage	Toasting Bread
PM_{10}	0.38 (-11.39; 12.14)	7.99 (-3.29; 19.27)	1.23 (-3.07; 5.52)
$PM_{2.5}$	0.87 (-13.08; 14.83)	7.02 (-4.56; 18.59)	1.47 (-7.44; 10.37)
PM_{1}	-0.68 (-14.97; 13.61)	7.47 (-3.13; 18.07)	-0.34 (-10.16; 9.47)
PSA	-1.88 (-12.77; 9.02)	6.01 (-5.17; 17.18)	2.76 (-7.24; 12.77)
UFP >100 nm	-2.98 (-15.43; 9.47)	6.85 (-4.35; 18.05)	3.58 (-6.61; 13.76)
UFP <100 nm	-6.61 (-21.13; 7.91)	6.06 (-3.93; 16.05)	1.69 (-8.28; 11.67)
UFP <50 nm	-7.87 (-23.02; 7.29)	3.14 (-5.27; 11.55)	1.68 (-8.93; 12.28)
UFP 30-50 nm	-2.11 (-13.7; 9.48)	3.69 (-3.94; 11.34)	1.13 (-8.0; 10.26)
UFP 10-30 nm	-7.92 (-22.56; 6.73)	-0.68 (-12.33; 10.97)	1.91 (-8.34; 12.16)
UFP <10 nm	-11.16 (-26.17; 3.85)	0.66 (-8.94; 10.27)	1.88 (-8.58; 12.33)

Table 22: ***Mean effect estimates and 95% confidence interval of sICAM in [ng/ml] per IQR.*** *Change at 2 and at 24 hours after the exposure to Candle Burning, Frying Sausage and Toasting Bread per IQR of particle fraction. The data displayed corresponds to the full model (model 2).*

4.10 Sensitivity Analysis

The sensitivity analysis led to minor changes of confidence intervals, as can exemplarily be seen in figure 26. The main findings were not influenced by the sensitivity testings and there was no detectable effect pattern.

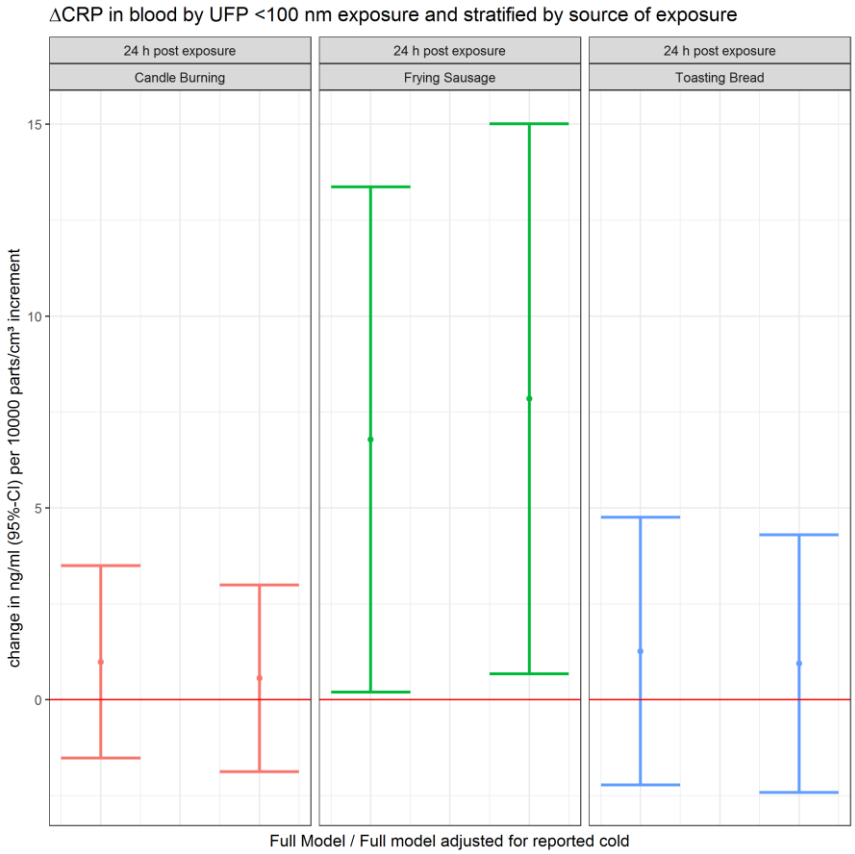

Figure 26: ***Sensitivity analysis, change of CRP levels in blood per increment of 10.000 particles <100 nm.*** *Full Model and model adjusted for reported cold in the weeks before the examination. Estimates were not changed substantially. Dots: Estimates; Whiskers: 95%-Confidence Interval.*

A similar finding could be made after including the 5-days-average of the $PM_{2.5}$ value at the volunteer's home address into the regression. The integration of home address PM exposure did not significantly alter the pre-existing estimates to a degree that could be interpreted as a response pattern.

5 Discussion

5.1 Main results

The study results show that common household particle sources can lead to a substantial particle exposure in closed rooms. We could show that total particle number and particle mass concentration in closed rooms can exceed particle concentration in outdoor air by far. We hereby confirm findings from other authors who designed similar exposure scenarios (Afshari et al., 2005).

In the main analysis, biomarker changes per fix increment of pollutants were calculated. It could be shown that the intensity of particle exposure was associated with the level of some circulating biomarkers. Although total measured amounts of biomarkers in the EPIA study vary only within narrow confines and sometimes even show an overall decrease in the course of time, the study reveals associations between intensity of exposure and biomarker levels. This could be shown for CRP levels and also IL-8 levels in nasal lavage and blood.

The biological reactions we observed can be associated with certain particle sources. Results indicate that not all tested sources have the same potential to alter biomarkers. Comparing between the sources, FS and CB were repeatedly associated with biomarker changes, whereas after TB we only rarely observed changes. One could therefore speculate that some household particle sources, especially FS and CB, might be a stimulus to inflammation just like particles from occupational or ambient air pollution.

CB and FS differ significantly regarding their particle composition, with CB emitting a comparatively high amount of UFP, and FS emitting a comparatively high amount of PM_{10}. Calculating an interquartile range increase, it could be shown that a biomarker alteration is mainly associated with particles of the UFP range. This is true for FS and for CB. After regression analysis, the main effects are observed in the quasi-UFP-reflecting metric of PSA and in particle fractions with a diameter less than 100 nm. In some cases, the most relevant biomarker changes seemed to be driven by particles with a diameter of 50 nm and less. Therefore, it can be speculated that especially small UFP fractions from certain common household sources can lead to biomarker alterations.

As a consequence, it should be highlighted that UFP and numeric particle measurements might more adequately reflect associations between particle exposure and biomarker changes. The main effects were continuously driven by UFP and particle sizes that primarily reflect UFP and quasi-UFP metrics, such as particle surface area. When trying to understand health outcomes, it might be worth to assess individual exposure to UFP in the future.

5.2 Interpreting the pre-analysis with indicator variables

In the pre analysis with indicator variables, we found changes in biomarker levels of innate immunity after exposure towards particulate matter from indoor sources. We discovered a tendency of intraindividual decline in total biomarker levels after exposure to all indoor PM sources when compared with room air. This was surprising, as the adverse health effects of outdoor particles through increasing inflammatory markers are well established (Rückerl et al., 2011; Brook et al., 2010; Hajat et al., 2015).

Despite the repeated measurements and a comparatively long exposure time inside the exposure chamber, volunteers were always exposed to significant amounts of outdoor particles before and after particle exposure at the study centre. Comparing outdoor and indoor particle exposure, other authors stated that outdoor particles show stronger signals of adverse health effects (Delfino et al., 2008). Olsen et al found that outdoor particle sources might be related to inflammation indicated by leukocyte counts, whereas sources from inside the home could have less effect, especially on healthy volunteers (Olsen et al., 2014). Thus, results could contribute to the finding, that indoor-generated PM and UFP might be less harmful than outdoor generated PM when directly compared with one another.

It has been speculated that this could be traced back to the different chemical compositions and physical properties of particles. Metal contaminants are often missing in indoor-generated particles, which makes particles less redox-reactive. For example, Di et al. reported lower mortality hazard ratios in a large US-cohort after exposure to organic carbon, nitrates and sulphates, but higher hazard ratios for all-cause mortality after exposure to particles containing significant amounts of metals (Di et al., 2017). Similar conclusions could for example be drawn by authors, who showed transition metals to be associated with inflammation, but not organic compounds (Sørensen et al., 2005).

In the EPIA-study, particles were dominated by organic carbon and nitrates, whereas metals were almost negligible in proportion. The observed tendency of declining inflammatory marker levels after indoor PM exposure could therefore be interpreted as a less redox reactive environment through presence of comparatively less toxic particles inside the study chamber.

Furthermore, there is a direct physiological link between the perception of stress and the activity of the hypothalamic–pituitary–adrenal axis and the sympathetic nervous system, resulting in mediation of cortisol levels and eventually interleukins and acute phase proteins (Chrousos, 2009). In a review of 30 studies, authors could show a significant effect of psychological stress

on CRP levels (Steptoe et al., 2007). The experimental setting of the exposure scenarios in the EPIA study resulted in an environment that was designed to reduce sources of physical or psychological stress to a minimum. Volunteers could follow a seated activity of their choice and hence influence their subjective stress level. Thus, their stay in the exposure chamber and the procedure of repeated measurements could have led to a downregulation of stress-related hormone axes. The reduction of CRP serum levels, especially after the burning of candles, when compared with room air, could thus be explained by a psychological effect during rest and relief.

It should also be considered that the olfactory system can play a role in the central nervous stress response, as it triggers endocrinological axes. Odours and subjective unpleasantness were shown to induce a significant stress response under experimental conditions (Hirasawa et al., 2019), whereas aromata such as aetheric oils were shown to reduce stress responses in healthy individuals (Jung et al., 2013).

Aromata were omnipresent in our study design because volunteers and particle sources were merged in a narrow chamber, and aromata were clearly noticeable during the whole exposure. Although no information was collected on the volunteers‘ perception of the aromata in the exposure scenarios, we could speculate that the olfactory contact with candle burning or food preparation, could down-regulate the sympathetic nervous system and consecutively the hypothalamic-pituitary-adrenal axis.

Another important factor for counterintuitive biomarker reactions after exposure to high quantities of indoor PM might be the general fitness of the study cohort. Subclinical and null findings were multiple times reported for healthy study cohorts. A large US cohort found a stronger increase of biomarker levels after exposure towards PM 2.5 among people with metabolic syndrome, comparing people with no cardiovascular risk factors (Dabass et al., 2018). For healthy volunteers instead, Dabass found that CRP levels after PM exposure sunk significantly. A study within a group of Chinese college students found only weak associations between total PM levels and CRP-content in blood among healthy individuals (Wu et al., 2012). Similar downregulations or null findings in healthy populations could be observed for sICAM levels after exposure towards PM (Calderón-Garcidueñas et al., 2008; Fang et al. 2010). The EPIA cohort was healthy and cardiovascular risk factors led to exclusion. This could explain the marginal total changes in biomarker levels.

Other authors have observed the tendency of nano-sized particles to suppress direct innate immune reactions which would eventually lead to stronger infections (Nemmar et al., 2013). As all particle sources emitted high amounts of UFP, this would provide another possible explanation for a decrease in biomarkers at 24 hours after exposure.

5.3 Interpreting the main analysis

Although total serum levels showed a decline when compared with room air, biomarker changes for a fix increment of particle exposures could be calculated. This finding is in line with current literature, as the association between intensive PM exposure and altered biomarkers has been proved multiple times (European Environmental Agency, 2016). Recent literature suggests that rising PM exposure has a strong influence on CRP levels. There is reviewed evidence of short term CRP elevations after exposure to PM workplace concentrations similar to those in the EPIA study (Li et al., 2012). Results of this work show a change in CRP and IL-8 levels when increasing the exposure to CB and FS particles of the UFP size range.

A relevant short-term increase in NAL IL-8 was calculated after a strong increase in the fraction of UFP-sized CB particles, whereas augmentation of other sources with a smaller fraction of UFPs was not associated with IL-8 changes in NAL. Among the tested sources, CB with the highest particle number concentration is associated with the clearest short term reaction in the airways. This is in line with other authors, for example (Sigsgaard et al., 2000), who reported that excessive nasopharyngeal particulate stimuli upregulated IL-8 expression in serum and NAL.

The interquartile range approach could show that changes in innate immunity markers are mainly associated with particles of the ultrafine size range, whereas larger particles were weakly associated with biomarker changes. One could therefore speculate that the fraction of UFP and the particle number concentration might be more relevant for specific health signals than the fraction of PM_{10} and mass surrogates in general. In concordance with these findings, other authors could show that associations are clearer when calculating the amount of inhaled pollutants by number per cm^3 rather than by mass only (Lanzinger et al., 2016).

However, the mere existence of elevated UFP fractions cannot fully explain biomarker augmentation, as UFP from TB did not show the same signals. Given that all particle sources emitted an extensive amount of particles with a comparable chemical composition, the heterogeneous results of the statistical analysis cannot fully answer the question, which property makes a particle especially reactive.

It should be noticed that by direct comparison of the sources, the most reactive ones (CB and FS) are combustion sources. Burning scented candles might be similar to a fossil fuelled combustion source. Through extremely hot surfaces and incomplete combustion of organic material during the frying process, FS might also be interpreted as a combustion of organic

matter, whereas TB is less of a combustion. Indoor use of fossil fuels and cooking on indoor fire places was multiple times associated with adverse health outcomes and subclinical biomarker changes (Dutta et al., 2012; World Health Organisation, 2015).

5.4 Clinical relevance / Practical implications

Results show that a relevant particle pollution in indoor air is reached through use of regular consumer goods. Choosing usual household activities as exposure sources, this study puts a focus on an often overseen exposure field. The strong particle exposure in our experimental setup might provide a useful database to model air quality in closed rooms. It also highlights, that a correct individual quantification of particle exposures is only possible if indoor particle exposure is included in measurements.

Furthermore, it could be shown that household particle sources lead to biomarker alteration in a healthy population. As a consequence, this study is relevant for individuals in the proximity of such sources. The experimental setup resembles occupational settings. It is probable, that in the food industry, in gastronomy and in various jobs of the service sector, working conditions can lead to exposures as high as in our study. The results provide good reasons for assessment of workplace air pollution and to evaluate the need for additional regulation.

Study results are also relevant for individuals who frequently operate potential household particle sources. The results could lead to more awareness and a conscious use of potential particle sources in households and closed environments, acknowledging that air quality is a good that can be managed on the very individual level. Individuals should be encouraged through these findings to actively manage room climate, for example through filter technologies or ventilation habits.

Results should be of special interest for individuals at risk for adverse cardiovascular or cardiopulmonary health outcomes. We could show that indoor air pollution can affect the same markers and pathways that are associated with adverse health effects in the (pre-)diseased. Lowering the individual indoor pollution exposure is therefore likely to be beneficial for diseased subgroups. Results could lead to a more conscious design of living habits, for example in healthcare facilities, where people at risk for adverse health effects are gathered in small volumes of indoor air.

5.5 Strengths and limitations

A strength of the EPIA study was the efficient and continuous exposure of volunteers to high amounts of indoor particles, when comparing the exposure to real world data (Morawska et al., 2017; He et al., 2007). We could show that in mass units and particle number, indoor particle sources can easily compete with outdoor exposures in street canyons or roadsides. Furthermore, the microenvironment we created in the EPIA study is comparable with many modern room climates. The comparatively low air exchange rate inside the exposure chamber might effectively mimic modern low energy constructions, where ventilation is reduced to save energy costs.

Another strength of this work is that results were calculated from 4 particle sources on 2 levels of intensity, 10 PM size categories and 4 outcome parameters at 3 time points measured, which leads to a great amount of temporarily consistent data. Also, the controlled exposure scenarios were operated under atmospherically stable conditions. This created a stable and interindividually comparable microenvironment, thus reducing confounding factors.

Chemical and physical properties of PM were screened precisely. One of the most remarkable aspects of particle measurement in the EPIA study is the quantification of size categories in the ultrafine range. To our knowledge, this is one of very few controlled human exposure studies that quantified particles from daily household activities in a range down to 10 nm. The vast majority of research on PM and health effects is found with PM_{10} or $PM_{2.5}$ or addresses UFP as a summarized size category, ignoring that it can be subdivided into further size categories. The study and this work try to elucidate effects of single particle metrics in the UFP range, thus trying to gain information on the most relevant particle fractions among the heterogenous group of UFP.

Another strength of this work is that it examines not one but various parameters of the innate immune response. Although an almost uncountable number of biological parameters can give information about the innate immune status of an individual after an environmental stimulus, we think to provide a set of biomarkers that could be seen as a sequence in the pathway of inflammation. By using highly-sensitive ELISA tests, subclinical findings in a healthy population could be detected. This helps to better understand the possible health impacts in a diseased individual without exposing it to the danger of potential adverse health effect.

Last but not least, our study cohort was screened very thoroughly, thus reducing possible confounders to a minimum. By observing a physically healthy cohort without medical preconditions or medication intake, we increase the probability that measured biomarkers have a causal relation with the experimental setup.

In contrast, some limitations of the study have to be discussed. One limitation is the comparatively low number of volunteers. To some degree, this was compensated by repeated measurements and an experimental setup where a single volunteer was repeatedly exposed and acted as their own control exposure. Yet measured effects can still be the cause of chance due to low numbers of volunteers.

Another limitation to the results is the limited time of post-exposure surveillance, which was reduced to 24 hours. It might be possible, that physiological changes have a longer latency, thus not being recognized by the time points of post-exposure measurements.

Another limitation is given by the short stay of the volunteers inside the exposure chamber and the consecutive period of the day which was not monitored under experimental conditions. The exposure of particles in the chamber was high and probably contributed the majority of total number of particles uptaken by a volunteer during the study day. Yet we cannot tell for certain which other exposures were also relevant for volunteers after exiting the study facility. Repeated measurements and the source-dependent alterations of biomarker levels increase the probability that the experimental exposure was responsible for biomarker changes. Yet it is still possible that a confounder, located outside the study centre, is responsible for changes of biomarkers 24 hours after exposure. For example, commuting to the study centre could have been an artificial and singular event that exposed volunteers to more or less particles in comparison to normal workdays. Also, volunteers were only asked to restrain vigorous physical activity but were not asked to explicitly protocol their activities afterwards. It is possible that for example the extra monetary income of a study day and the free time after the end of a study day might have changed the course of a normal volunteers' workday to a degree that influences biomarkers in subclinical ranges.

Another limitation of the study is the selection of volunteers. By focussing on healthy individuals, we cannot foresee the clinical implication of a particle exposure in the diseased. It is moreover possible that by focussing on a healthy population, we completely excluded individuals at risk for adverse effects through particle exposure and that particles in this subgroup would be associated with different kinetics in biomarkers.

Study results must be handled with care because particle generation took place under comparatively stable conditions. Particle sources were operated without scorching, sooting or overheating the products. It is hard to tell, if the same degree of exposure is reached in a real-life exposure scenario. On the one hand, particle forming events could be more drastic (e.g. burning of food remains, using overheated oils, burning wax additives), on the other hand they could be less intensive through correct use of exhaust hoods, room air filters or constant ventilation. A generalizable conclusion can therefore not be drawn from the study results.

6 Conclusion

6.1 Summary of results, gain of knowledge

A qualitative and quantitative analysis of indoor air pollution sources was performed. It could be shown that indoor sources create a relevant particle exposure in terms of particle number and particle mass concentration.

The tested sources showed varying associations with biomarkers, indicating that different particle sources have individual implications on human health. The most relevant sources in this study were Frying Sausages and Candle Burning.

It could be shown that an increase of certain indoor pollutants is associated with biomarker changes in healthy individuals. When calculating fixed increments of pollutants, short-term increases for CRP and IL-8 in NAL were discovered.

Amongst the whole range of particle size fractions, an interquartile range increase of particle fractions revealed that particles smaller than 100 nm in diameter were consistently associated with biomarker changes. In comparison to larger particles, they were identified to be the most relevant particle group in the association with biomarker changes.

6.2 Research outlook

Further research is needed in the field of indoor particle exposure. It is very challenging to gather information on long term health effects of indoor particle exposure. A next step could therefore be to extend the post-exposure follow-up, for example to days or weeks. Another approach could be to extend the stay in the exposure scenario to eliminate potential confounding through commuting and other unintended individual exposures.

Another important aspect should be to create similar exposure studies with chronically diseased individuals and find out more about their innate immune answer to indoor PM. It might be an effective prevention strategy to identify groups at risk and actively manage their microenvironments in terms of air pollution.

Also, it could be of special interest to isolate fractions of particulate matter of the ultrafine particle spectrum and perform separate controlled exposure studies. This would create a more differentiated picture of possible health effects. More research is needed to understand which fraction of particles has to be primarily eliminated from the spectrum of pollutants and how we could manage an effective pollutant control in households.

Bibliography

Afshari, A.; Matson, U.; Ekberg, L. E. (2005): Characterization of indoor sources of fine and ultrafine particles. A study conducted in a full-scale chamber. In: *Indoor air* 15 (2), S. 141–150. DOI: 10.1111/j.1600-0668.2005.00332.x.

Allen, Ryan W.; Carlsten, Chris; Karlen, Barbara; Leckie, Sara; van Eeden, Stephan; Vedal, Sverre et al. (2011): An air filter intervention study of endothelial function among healthy adults in a woodsmoke-impacted community. In: *American journal of respiratory and critical care medicine* 183 (9), S. 1222–1230. DOI: 10.1164/rccm.201010-1572OC.

Baggiolini, M.; Walz, A.; Kunkel, S. L. (1989): Neutrophil-activating peptide-1/interleukin 8, a novel cytokine that activates neutrophils. In: *The Journal of clinical investigation* 84 (4), S. 1045–1049. DOI: 10.1172/JCI114265.

Balti, Eric V.; Echouffo-Tcheugui, Justin B.; Yako, Yandiswa Y.; Kengne, Andre P. (2014): Air pollution and risk of type 2 diabetes mellitus. A systematic review and meta-analysis. In: *Diabetes research and clinical practice* 106 (2), S. 161–172. DOI: 10.1016/j.diabres.2014.08.010.

Banerjee, Anirban; Mondal, Nandan Kumar; Das, Debangshu; Ray, Manas Ranjan (2012): Neutrophilic inflammatory response and oxidative stress in premenopausal women chronically exposed to indoor air pollution from biomass burning. In: *Inflammation* 35 (2), S. 671–683. DOI: 10.1007/s10753-011-9360-2.

Bekö, Gabriel; Weschler, Charles J.; Wierzbicka, Aneta; Karottki, Dorina Gabriela; Toftum, Jørn; Loft, Steffen; Clausen, Geo (2013): Ultrafine particles. Exposure and source apportionment in 56 Danish homes. In: *Environmental science & technology* 47 (18), S. 10240–10248. DOI: 10.1021/es402429h.

Brook, Robert D.; Rajagopalan, Sanjay; Pope, C. Arden; Brook, Jeffrey R.; Bhatnagar, Aruni; Diez-Roux, Ana V. et al. (2010): Particulate Matter Air Pollution and Cardiovascular Disease. In: *Circulation* 121 (21), S. 2331–2378. DOI: 10.1161/CIR.0b013e3181dbece1.

Calabró, Paolo; Willerson, James T.; Yeh, Edward T. H. (2003): Inflammatory cytokines stimulated C-reactive protein production by human coronary artery smooth muscle cells. In: *Circulation* 108 (16), S. 1930–1932. DOI: 10.1161/01.CIR.0000096055.62724.C5.

Calderón-Garcidueñas, L.; Villarreal-Calderon, R.; Valencia-Salazar, G.; Henríquez-Roldán, C.; Gutiérrez-Castrellón, P.; Torres-Jardón, R. et al. (2008): Systemic inflammation, endothelial dysfunction, and activation in clinically healthy children exposed to air pollutants. In: *Inhalation toxicology* 20 (5), S. 499–506. DOI: 10.1080/08958370701864797.

Chan, Margaret (2006): Air quality guidelines. Global update 2005 ; particulate matter, ozone, nitrogen dioxide and sulfur dioxide. Copenhagen: WHO Regional Office for Europe. Online verfügbar unter http://www.euro.who.int/__data/assets/pdf_file/0005/78638/E90038.pdf?ua=1.

Chandrashekara, S. (2014): C - reactive protein. An inflammatory marker with specific role in physiology, pathology, and diagnosis. In: *IJRCI* 2 (S1). DOI: 10.15305/ijrci/v2iS1/117.

Chen, Jie; Hoek, Gerard (2020): Long-term exposure to PM and all-cause and cause-specific mortality. A systematic review and meta-analysis. In: *Environment international* 143, S. 105974. DOI: 10.1016/j.envint.2020.105974.

Chen, Renjie; Kan, Haidong; Chen, Bingheng; Huang, Wei; Bai, Zhipeng; Song, Guixiang; Pan, Guowei (2012): Association of particulate air pollution with daily mortality. The China Air Pollution and Health Effects Study. In: *American journal of epidemiology* 175 (11), S. 1173–1181. DOI: 10.1093/aje/kwr425.

Chrousos, George P. (2009): Stress and disorders of the stress system. In: *Nature reviews. Endocrinology* 5 (7), S. 374–381. DOI: 10.1038/nrendo.2009.106.

Cohen, Aaron J.; Brauer, Michael; Burnett, Richard; Anderson, H. Ross; Frostad, Joseph; Estep, Kara et al. (2017): Estimates and 25-year trends of the global burden of disease attributable to ambient air pollution. An analysis of data from the Global Burden of Diseases Study 2015. In: *The Lancet* 389 (10082), S. 1907–1918. DOI: 10.1016/S0140-6736(17)30505-6.

Dabass, Arvind; Talbott, Evelyn O.; Rager, Judith R.; Marsh, Gary M.; Venkat, Arvind; Holguin, Fernando; Sharma, Ravi K. (2018): Systemic inflammatory markers associated with cardiovascular disease and acute and chronic exposure to fine particulate matter air pollution (PM2.5) among US NHANES adults with metabolic syndrome. In: *Environmental research* 161, S. 485–491. DOI: 10.1016/j.envres.2017.11.042.

Delfino, Ralph J.; Sioutas, Constantinos; Malik, Shaista (2005): Potential role of ultrafine particles in associations between airborne particle mass and cardiovascular health. In: *Environmental health perspectives* 113 (8), S. 934–946. DOI: 10.1289/ehp.7938.

Delfino, Ralph J.; Staimer, Norbert; Tjoa, Thomas; Gillen, Dan; Kleinman, Michael T.; Sioutas, Constantinos; Cooper, Dan (2008): Personal and ambient air pollution exposures and lung function decrements in children with asthma. In: *Environmental health perspectives* 116 (4), S. 550–558. DOI: 10.1289/ehp.10911.

Di, Qian; Wang, Yan; Zanobetti, Antonella; Wang, Yun; Koutrakis, Petros; Choirat, Christine et al. (2017): Air Pollution and Mortality in the Medicare Population. In: *The New England journal of medicine* 376 (26), S. 2513–2522. DOI: 10.1056/NEJMoa1702747.

Díaz-Robles, Luis A.; Fu, Joshua S.; Vergara-Fernández, Alberto; Etcharren, Pablo; Schiappacasse, Luis N.; Reed, Gregory D.; Silva, María P. (2014): Health risks caused by short term exposure to ultrafine particles generated by residential wood combustion. A case study of Temuco, Chile. In: *Environment international* 66, S. 174–181. DOI: 10.1016/j.envint.2014.01.017.

Dutta, Anindita; Ray, Manas Ranjan; Banerjee, Anirban (2012): Systemic inflammatory changes and increased oxidative stress in rural Indian women cooking with biomass fuels. In: *Toxicology and applied pharmacology* 261 (3), S. 255–262. DOI: 10.1016/j.taap.2012.04.004.

Engel-Cox, Jill; Kim Oanh, Nguyen Thi; van Donkelaar, Aaron; Martin, Randall V.; Zell, Erica (2013): Toward the next generation of air quality monitoring. Particulate Matter. In: *Atmospheric Environment* 80 (17), S. 584–590. DOI: 10.1016/j.atmosenv.2013.08.016.

European Environmental Agency (2016): Air quality in Europe - 2016 report.

Fang, S. C.; Eisen, E. A.; Cavallari, J. M.; Mittleman, M. A.; Christiani, D. C. (2010): Circulating adhesion molecules after short-term exposure to particulate matter among welders. In: *Occupational and environmental medicine* 67 (1), S. 11–16. DOI: 10.1136/oem.2008.043794.

Forns, Joan; Dadvand, Payam; Esnaola, Mikel; Alvarez-Pedrerol, Mar; López-Vicente, Mònica; Garcia-Esteban, Raquel et al. (2017): Longitudinal association between air pollution exposure at

school and cognitive development in school children over a period of 3.5 years. In: *Environmental research* 159, S. 416–421. DOI: 10.1016/j.envres.2017.08.031.

Franklin, Barry A.; Brook, Robert; Arden Pope, C. (2015): Air Pollution and Cardiovascular Disease. In: *Current Problems in Cardiology* 40 (5), S. 207–238. DOI: 10.1016/j.cpcardiol.2015.01.003.

Fujii, T.; Hayashi, S.; Hogg, J. C.; Vincent, R.; van Eeden, S. F. (2001): Particulate matter induces cytokine expression in human bronchial epithelial cells. In: *American journal of respiratory cell and molecular biology* 25 (3), S. 265–271. DOI: 10.1165/ajrcmb.25.3.4445.

González Ortiz, Alberto; Guerreiro, Cristina; Soares, Joana (2020): Air quality in Europe. 2020 report. Luxembourg: Publications Office of the European Union (EEA report, No 09/2020).

Gould, J. M.; Weiser, J. N. (2001): Expression of C-reactive protein in the human respiratory tract. In: *Infection and immunity* 69 (3), S. 1747–1754. DOI: 10.1128/IAI.69.3.1747-1754.2001.

Graham, D. E.; Koren, H. S. (1990): Biomarkers of inflammation in ozone-exposed humans. Comparison of the nasal and bronchoalveolar lavage. In: *The American review of respiratory disease* 142 (1), S. 152–156. DOI: 10.1164/ajrccm/142.1.152.

Griffith, Jason W.; Sokol, Caroline L.; Luster, Andrew D. (2014): Chemokines and chemokine receptors. Positioning cells for host defense and immunity. In: *Annual review of immunology* 32, S. 659–702. DOI: 10.1146/annurev-immunol-032713-120145.

Habre, Rima; Zhou, Hui; Eckel, Sandrah P.; Enebish, Temuulen; Fruin, Scott; Bastain, Theresa et al. (2018): Short-term effects of airport-associated ultrafine particle exposure on lung function and inflammation in adults with asthma. In: *Environment international* 118, S. 48–59. DOI: 10.1016/j.envint.2018.05.031.

Hackett, Tillie-Louise; Singhera, Gurpreet K.; Shaheen, Furquan; Hayden, Patrick; Jackson, George R.; Hegele, Richard G. et al. (2011): Intrinsic phenotypic differences of asthmatic epithelium and its inflammatory responses to respiratory syncytial virus and air pollution. In: *American journal of respiratory cell and molecular biology* 45 (5), S. 1090–1100. DOI: 10.1165/rcmb.2011-0031OC.

Hajat, Anjum; Allison, Matthew; Diez-Roux, Ana V.; Jenny, Nancy Swords; Jorgensen, Neal W.; Szpiro, Adam A. et al. (2015): Long-term exposure to air pollution and markers of inflammation, coagulation, and endothelial activation. A repeat-measures analysis in the Multi-Ethnic Study of Atherosclerosis (MESA). In: *Epidemiology (Cambridge, Mass.)* 26 (3), S. 310–320. DOI: 10.1097/EDE.0000000000000267.

He, Congrong; Morawska, Lidia; Taplin, Len (2007): Particle emission characteristics of office printers. In: *Environmental science & technology* 41 (17), S. 6039–6045. DOI: 10.1021/es063049z.

HEI Panel on the Health Effects of Traffic-Related Air Pollution (2010): Traffic-Related Air Pollution: A Critical Review of the Literature on Emissions, Exposure, and Health Effects. HEI Special Report 17.

HEI Review Panel on Ultrafine Particles (2013): Understanding the Health Effects of Ambient Ultrafine Particles. HEI Perspectives 3. Hg. v. Health Effects Institute, Boston, MA.

Hellack, Bryan; Soppa, Vanessa, Quass, Ulrich; Kaminski, Heinz; Neumeyer, Andrea; Buschka, Anna; Albrecht, Catrin et al. (2014): Effekte von Partikeln aus Innenraum-Aktivitäten (EPIA) -

(Untersuchungen zur Freisetzung feiner und ultrafeiner Partikel aus Quellen im Innenraum: chemisch-physikalische Charakterisierung der Partikel und Studien zur gesundheitlichen Wirkung). Institut für Energie- und Umwelttechnik e. V. (IUTA), Leibniz-Institut für umweltmedizinische Forschung gGmbH (371162205).

Henriquez, Kelsey M.; Hayney, Mary S.; Xie, Yaoguo; Zhang, Zhengjun; Barrett, Bruce (2015): Association of interleukin-8 and neutrophils with nasal symptom severity during acute respiratory infection. In: *Journal of medical virology* 87 (2), S. 330–337. DOI: 10.1002/jmv.24042.

Hirasawa, Yukei; Shirasu, Mika; Okamoto, Masako; Touhara, Kazushige (2019): Subjective unpleasantness of malodors induces a stress response. In: *Psychoneuroendocrinology* 106, S. 206–215. DOI: 10.1016/j.psyneuen.2019.03.018.

Hoffmann, Barbara; Moebus, Susanne; Dragano, Nico; Stang, Andreas; Möhlenkamp, Stefan; Schmermund, Axel et al. (2009): Chronic residential exposure to particulate matter air pollution and systemic inflammatory markers. In: *Environmental health perspectives* 117 (8), S. 1302–1308. DOI: 10.1289/ehp.0800362.

Hua, Susan (2013): Targeting sites of inflammation. Intercellular adhesion molecule-1 as a target for novel inflammatory therapies. In: *Frontiers in pharmacology* 4, S. 127. DOI: 10.3389/fphar.2013.00127.

Hvidtfeldt, Ulla Arthur; Severi, Gianluca; Andersen, Zorana Jovanovic; Atkinson, Richard; Bauwelinck, Mariska; Bellander, Tom et al. (2021): Long-term low-level ambient air pollution exposure and risk of lung cancer - A pooled analysis of 7 European cohorts. In: *Environment international* 146, S. 106249. DOI: 10.1016/j.envint.2020.106249.

Isaxon, C.; Gudmundsson, A.; Nordin, E. Z.; Lönnblad, L.; Dahl, A.; Wieslander, G. et al. (2015): Contribution of indoor-generated particles to residential exposure. In: *Atmospheric Environment* 106 (18), S. 458–466. DOI: 10.1016/j.atmosenv.2014.07.053.

Jung, Da-Jung; Cha, Jun-Youl; Kim, Sung-Eun; Ko, Il-Gyu; Jee, Yong-Seok (2013): Effects of Ylang-Ylang aroma on blood pressure and heart rate in healthy men. In: *Journal of exercise rehabilitation* 9 (2), S. 250–255. DOI: 10.12965/jer.130007.

Kim, Ki-Hyun; Kabir, Ehsanul; Kabir, Shamin (2015): A review on the human health impact of airborne particulate matter. In: *Environment international* 74, S. 136–143. DOI: 10.1016/j.envint.2014.10.005.

Kim, Kyung Eun; Cho, Daeho; Park, Hyun Jeong (2016): Air pollution and skin diseases. Adverse effects of airborne particulate matter on various skin diseases. In: *Life sciences* 152, S. 126–134. DOI: 10.1016/j.lfs.2016.03.039.

Klepeis, N. E.; Nelson, W. C.; Ott, W. R.; Robinson, J. P.; Tsang, A. M.; Switzer, P. et al. (2001): The National Human Activity Pattern Survey (NHAPS). A resource for assessing exposure to environmental pollutants. In: *Journal of exposure analysis and environmental epidemiology* 11 (3), S. 231–252. DOI: 10.1038/sj.jea.7500165.

Lanzinger, Stefanie; Schneider, Alexandra; Breitner, Susanne; Stafoggia, Massimo; Erzen, Ivan; Dostal, Miroslav et al. (2016): Associations between ultrafine and fine particles and mortality in five central European cities - Results from the UFIREG study. In: *Environment international* 88, S. 44–52. DOI: 10.1016/j.envint.2015.12.006.

Lelieveld, Jos; Klingmüller, Klaus; Pozzer, Andrea; Pöschl, Ulrich; Fnais, Mohammed; Daiber, Andreas; Münzel, Thomas (2019): Cardiovascular disease burden from ambient air pollution in Europe reassessed using novel hazard ratio functions. In: *European heart journal* 40 (20), S. 1590–1596. DOI: 10.1093/eurheartj/ehz135.

Li, Ning; Georas, Steve; Alexis, Neil; Fritz, Patricia; Xia, Tian; Williams, Marc A. et al. (2016): A work group report on ultrafine particles (American Academy of Allergy, Asthma & Immunology). Why ambient ultrafine and engineered nanoparticles should receive special attention for possible adverse health outcomes in human subjects. In: *The Journal of allergy and clinical immunology* 138 (2), S. 386–396. DOI: 10.1016/j.jaci.2016.02.023.

Li, Yanli; Rittenhouse-Olson, Kate; Scheider, William L.; Mu, Lina (2012): Effect of particulate matter air pollution on C-reactive protein. A review of epidemiologic studies. In: *Reviews on environmental health* 27 (2-3), S. 133–149. DOI: 10.1515/reveh-2012-0012.

Lidia Morawska, Aneta Wierzbicka, Giorgio Buonanno, Josef Cyrys, Jüergen Schnelle-Kreis, Michal Kowalski, Michael Riediker, Wolfram Birmili, Xavier Querol, Annette Peters, Alexandra Schneider, Enembe Okokon, Evangelia Samoli, Massimo Stafoggia (2019): Ambient ultrafine particles: evidence for policy makers. White Paper. Prepared by the "thinking outside the box team".

Liu, Cong; Chen, Renjie; Sera, Francesco; Vicedo-Cabrera, Ana M.; Guo, Yuming; Tong, Shilu et al. (2019a): Ambient Particulate Air Pollution and Daily Mortality in 652 Cities. In: *The New England journal of medicine* 381 (8), S. 705–715. DOI: 10.1056/NEJMoa1817364.

Liu, Feifei; Chen, Gongbo; Huo, Wenqian; Wang, Chongjian; Liu, Suyang; Li, Na et al. (2019b): Associations between long-term exposure to ambient air pollution and risk of type 2 diabetes mellitus. A systematic review and meta-analysis. In: *Environmental pollution (Barking, Essex : 1987)* 252 (Pt B), S. 1235–1245. DOI: 10.1016/j.envpol.2019.06.033.

Magalhaes, Sandra; Baumgartner, Jill; Weichenthal, Scott (2018): Impacts of exposure to black carbon, elemental carbon, and ultrafine particles from indoor and outdoor sources on blood pressure in adults. A review of epidemiological evidence. In: *Environmental research* 161, S. 345–353. DOI: 10.1016/j.envres.2017.11.030.

Mannucci, Pier Mannuccio; Harari, Sergio; Martinelli, Ida; Franchini, Massimo (2015): Effects on health of air pollution. A narrative review. In: *Intern Emerg Med* 10 (6), S. 657–662. DOI: 10.1007/s11739-015-1276-7.

Mirowsky, Jaime; Gordon, Terry (2015): Noninvasive effects measurements for air pollution human studies. Methods, analysis, and implications. In: *Journal of exposure science & environmental epidemiology* 25 (4), S. 354–380. DOI: 10.1038/jes.2014.93.

Morawska, L.; Ayoko, G. A.; Bae, G. N.; Buonanno, G.; Chao, C. Y. H.; Clifford, S. et al. (2017): Airborne particles in indoor environment of homes, schools, offices and aged care facilities. The main routes of exposure. In: *Environment international* 108, S. 75–83. DOI: 10.1016/j.envint.2017.07.025.

Morawska, L.; Ristovski, Z.; Jayaratne, E. R.; Keogh, D. U.; Ling, X. (2008): Ambient nano and ultrafine particles from motor vehicle emissions. Characteristics, ambient processing and implications on human exposure. In: *Atmospheric Environment* 42 (35), S. 8113–8138. DOI: 10.1016/j.atmosenv.2008.07.050.

Mukaida, Naofumi (2003): Pathophysiological roles of interleukin-8/CXCL8 in pulmonary diseases. In: *American journal of physiology. Lung cellular and molecular physiology* 284 (4), L566-77. DOI: 10.1152/ajplung.00233.2002.

Nemmar, Abderrahim; Holme, Jørn A.; Rosas, Irma; Schwarze, Per E.; Alfaro-Moreno, Ernesto (2013): Recent advances in particulate matter and nanoparticle toxicology. A review of the in vivo and in vitro studies. In: *BioMed research international* 2013, S. 279371. DOI: 10.1155/2013/279371.

Oberdörster, Günter; Oberdörster, Eva; Oberdörster, Jan (2005): Nanotoxicology. An emerging discipline evolving from studies of ultrafine particles. In: *Environmental health perspectives* 113 (7), S. 823–839. DOI: 10.1289/ehp.7339.

Ohlwein, Simone; Kappeler, Ron; Kutlar Joss, Meltem; Künzli, Nino; Hoffmann, Barbara (2019): Health effects of ultrafine particles. A systematic literature review update of epidemiological evidence. In: *International journal of public health* 64 (4), S. 547–559. DOI: 10.1007/s00038-019-01202-7.

Olsen, Yulia; Karottki, Dorina Gabriela; Jensen, Ditte Marie; Bekö, Gabriel; Kjeldsen, Birthe Uldahl; Clausen, Geo et al. (2014): Vascular and lung function related to ultrafine and fine particles exposure assessed by personal and indoor monitoring. A cross-sectional study. In: *Environmental health : a global access science source* 13, S. 112. DOI: 10.1186/1476-069X-13-112.

Orellano, Pablo; Reynoso, Julieta; Quaranta, Nancy; Bardach, Ariel; Ciapponi, Agustin (2020): Short-term exposure to particulate matter (PM10 and PM2.5), nitrogen dioxide (NO2), and ozone (O3) and all-cause and cause-specific mortality. Systematic review and meta-analysis. In: *Environment international* 142, S. 105876. DOI: 10.1016/j.envint.2020.105876.

Pepys, Mark B.; Hirschfield, Gideon M. (2003): C-reactive protein. A critical update. In: *The Journal of clinical investigation* 111 (12), S. 1805–1812. DOI: 10.1172/JCI18921.

Polidori, Andrea; Turpin, Barbara; Meng, Qing Yu; Lee, Jong Hoon; Weisel, Clifford; Morandi, Maria et al. (2006): Fine organic particulate matter dominates indoor-generated PM2.5 in RIOPA homes. In: *Journal of exposure science & environmental epidemiology* 16 (4), S. 321–331. DOI: 10.1038/sj.jes.7500476.

Pope, C. Arden; Burnett, Richard T.; Thun, Michael J.; Calle, Eugenia E.; Krewski, Daniel; Ito, Kazuhiko; Thurston, George D. (2002): Lung cancer, cardiopulmonary mortality, and long-term exposure to fine particulate air pollution. In: *JAMA* 287 (9), S. 1132–1141. DOI: 10.1001/jama.287.9.1132.

Pope, C. Arden; Coleman, Nathan; Pond, Zachari A.; Burnett, Richard T. (2020): Fine particulate air pollution and human mortality. 25+ years of cohort studies. In: *Environmental research* 183, S. 108924. DOI: 10.1016/j.envres.2019.108924.

Pope, C. Arden; Dockery, Douglas W. (2006): Health effects of fine particulate air pollution. Lines that connect. In: *Journal of the Air & Waste Management Association (1995)* 56 (6), S. 709–742. DOI: 10.1080/10473289.2006.10464485.

Ramos, Theresa N.; Bullard, Daniel C.; Barnum, Scott R. (2014): ICAM-1. Isoforms and phenotypes. In: *Journal of immunology (Baltimore, Md. : 1950)* 192 (10), S. 4469–4474. DOI: 10.4049/jimmunol.1400135.

Rückerl, Regina; Greven, Sonja; Ljungman, Petter; Aalto, Pasi; Antoniades, Charalambos; Bellander, Tom et al. (2007): Air pollution and inflammation (interleukin-6, C-reactive protein, fibrinogen) in myocardial infarction survivors. In: *Environmental health perspectives* 115 (7), S. 1072–1080. DOI: 10.1289/ehp.10021.

Rückerl, Regina; Schneider, Alexandra; Breitner, Susanne; Cyrys, Josef; Peters, Annette (2011): Health effects of particulate air pollution. A review of epidemiological evidence. In: *Inhalation toxicology* 23 (10), S. 555–592. DOI: 10.3109/08958378.2011.593587.

Scarpa, M. C.; Kulkarni, N.; Maestrelli, P. (2014): The role of non-invasive biomarkers in detecting acute respiratory effects of traffic-related air pollution. In: *Clinical and experimental allergy : journal of the British Society for Allergy and Clinical Immunology* 44 (9), S. 1100–1118. DOI: 10.1111/cea.12373.

Shah, Anoop S. V.; Lee, Kuan Ken; McAllister, David A.; Hunter, Amanda; Nair, Harish; Whiteley, William et al. (2015): Short term exposure to air pollution and stroke. Systematic review and meta-analysis. In: *BMJ (Clinical research ed.)* 350, h1295. DOI: 10.1136/bmj.h1295.

Shah, Prakesh S.; Balkhair, Taiba (2011): Air pollution and birth outcomes. A systematic review. In: *Environment international* 37 (2), S. 498–516. DOI: 10.1016/j.envint.2010.10.009.

Sigsgaard, T.; Bonefeld-Jørgensen, E. C.; Kjaergaard, S. K.; Mamas, S.; Pedersen, O. F. (2000): Cytokine release from the nasal mucosa and whole blood after experimental exposures to organic dusts. In: *The European respiratory journal* 16 (1), S. 140–145. DOI: 10.1034/j.1399-3003.2000.16a25.x.

Sithu, Srinivas D.; English, William R.; Olson, Paul; Krubasik, Davia; Baker, Andrew H.; Murphy, Gillian; D'Souza, Stanley E. (2007): Membrane-type 1-matrix metalloproteinase regulates intracellular adhesion molecule-1 (ICAM-1)-mediated monocyte transmigration. In: *The Journal of biological chemistry* 282 (34), S. 25010–25019. DOI: 10.1074/jbc.M611273200.

Soppa, Vanessa J.; Schins, Roel P. F.; Hennig, Frauke; Hellack, Bryan; Quass, Ulrich; Kaminski, Heinz et al. (2014): Respiratory effects of fine and ultrafine particles from indoor sources--a randomized sham-controlled exposure study of healthy volunteers. In: *International journal of environmental research and public health* 11 (7), S. 6871–6889. DOI: 10.3390/ijerph110706871.

Sørensen, Mette; Schins, Roel P. F.; Hertel, Ole; Loft, Steffen (2005): Transition metals in personal samples of PM2.5 and oxidative stress in human volunteers. In: *Cancer epidemiology, biomarkers & prevention : a publication of the American Association for Cancer Research, cosponsored by the American Society of Preventive Oncology* 14 (5), S. 1340–1343. DOI: 10.1158/1055-9965.EPI-04-0899.

Steptoe, Andrew; Hamer, Mark; Chida, Yoichi (2007): The effects of acute psychological stress on circulating inflammatory factors in humans. A review and meta-analysis. In: *Brain, behavior, and immunity* 21 (7), S. 901–912. DOI: 10.1016/j.bbi.2007.03.011.

Stone, Vicki; Miller, Mark R.; Clift, Martin J. D.; Elder, Alison; Mills, Nicholas L.; Møller, Peter et al. (2017): Nanomaterials Versus Ambient Ultrafine Particles. An Opportunity to Exchange Toxicology Knowledge. In: *Environmental health perspectives* 125 (10), S. 106002. DOI: 10.1289/EHP424.

Trial, JoAnn; Potempa, Lawrence A.; Entman, Mark (2016): The role of C-reactive protein in innate and acquired inflammation: new perspectives. In: *Inflammation and cell signaling* (3).

Vinzents, Peter S.; Møller, Peter; Sørensen, Mette; Knudsen, Lisbeth E.; Hertel, Ole; Jensen, Finn Palmgren et al. (2005): Personal exposure to ultrafine particles and oxidative DNA damage. In: *Environmental health perspectives* 113 (11), S. 1485–1490. DOI: 10.1289/ehp.7562.

Wallace, L. A.; Ott, W. R.; Weschler, C. J. (2015): Ultrafine particles from electric appliances and cooking pans. Experiments suggesting desorption/nucleation of sorbed organics as the primary source. In: *Indoor air* 25 (5), S. 536–546. DOI: 10.1111/ina.12163.

Wallace, Lance (2006): Indoor Sources of Ultrafine and Accumulation Mode Particles. Size Distributions, Size-Resolved Concentrations, and Source Strengths. In: *Aerosol Science and Technology* 40 (5), S. 348–360. DOI: 10.1080/02786820600612250.

Wallace, Lance; Ott, Wayne (2011): Personal exposure to ultrafine particles. In: *Journal of exposure science & environmental epidemiology* 21 (1), S. 20–30. DOI: 10.1038/jes.2009.59.

Waring, M. S. (2014): Secondary organic aerosol in residences. Predicting its fraction of fine particle mass and determinants of formation strength. In: *Indoor air* 24 (4), S. 376–389. DOI: 10.1111/ina.12092.

WHO Regional Office for Europe (2013): Review of evidence on health aspects of air pollution – REVIHAAP Project. Technical Report [Internet]. Hg. v. WHO Regional Office for Europe und 2013.

Witkowska, Anna Maria; Borawska, Maria Halina (2004): Soluble intercellular adhesion molecule-1 (sICAM-1). An overview. In: *European cytokine network* 15 (2), S. 91–98.

World Health Organisation (2015): WHO guidelinesfor indoor air quality. Household fuel combustion.

Wu, Shaowei; Deng, Furong; Wei, Hongying; Huang, Jing; Wang, Hongyi; Shima, Masayuki et al. (2012): Chemical constituents of ambient particulate air pollution and biomarkers of inflammation, coagulation and homocysteine in healthy adults. A prospective panel study. In: *Particle and fibre toxicology* 9, S. 49. DOI: 10.1186/1743-8977-9-49.

Xie, Yan; Bowe, Benjamin; Mokdad, Ali H.; Xian, Hong; Yan, Yan; Li, Tingting et al. (2018): Analysis of the Global Burden of Disease study highlights the global, regional, and national trends of chronic kidney disease epidemiology from 1990 to 2016. In: *Kidney international* 94 (3), S. 567–581. DOI: 10.1016/j.kint.2018.04.011.

Yang, Bo-Yi; Fan, Shujun; Thiering, Elisabeth; Seissler, Jochen; Nowak, Dennis; Dong, Guang-Hui; Heinrich, Joachim (2020): Ambient air pollution and diabetes. A systematic review and meta-analysis. In: *Environmental research* 180, S. 108817. DOI: 10.1016/j.envres.2019.108817.

Yitshak-Sade, Maayan; Kloog, Itai; Zanobetti, Antonella; Schwartz, Joel D. (2019): Estimating the causal effect of annual PM2.5 exposure on mortality rates in the Northeastern and mid-Atlantic states. In: *Environmental epidemiology (Philadelphia, Pa.)* 3 (4), e052. DOI: 10.1097/EE9.0000000000000052.

Yoshimura, T.; Matsushima, K.; Tanaka, S.; Robinson, E. A.; Appella, E.; Oppenheim, J. J.; Leonard, E. J. (1987): Purification of a human monocyte-derived neutrophil chemotactic factor that has peptide sequence similarity to other host defense cytokines. In: *Proceedings of the*

National Academy of Sciences of the United States of America 84 (24), S. 9233–9237. DOI: 10.1073/pnas.84.24.9233.

Danksagung

An dieser Stelle möchte ich allen Personen danken, die mich bei der Anfertigung dieser Dissertationsschrift unterstützt haben.

Mein besonderer Dank gilt Prof. Dr. med. Barbara Hoffmann und PD Dr. Roel Schins für die hervorragende und geduldige persönliche Betreuung bei der Planung, Durchführung und Gestaltung der gesamten Arbeit.

Darüber hinaus möchte ich mich bei Dr. Frauke Hennig, Anna Buschka und Dr. Vanessa Soppa bedanken für ihre Hilfe bei der statistischen Ausarbeitung und allen größeren und kleineren Datenfragen.

Ebenfalls bedanke ich mich bei Dr. Waluree Thongkam und Dr. Catrin Albrecht für ihre Einarbeitung in die Labortätigkeit und deren aktive Begleitung.

Außerdem danke ich meinen Eltern, die mir - wann immer möglich - eine große Unterstützung waren und mir halfen, den Blick zu fokussieren. Zuletzt danke ich Charlotte für Motivation auf der Zielgeraden und Emilia für ihre endlose Geduld während unzähliger Stunden Schreibtischarbeit.